SIMULATION PACKAGE SYSTEM DESIGN TO ANALYSIS AND CONTROL A DISTILLATION COLUMN USING FREQUENCY RESPONSE METHOD

A Thesis
Submitted to the College of Engineering of
Al-Nahrain University
In Partial Fulfillment of the Requirements
for the Degree of Master of Science in
Chemical Engineering

by

YOSSOR RIADH ABDUL–MAJEED AL-ANI

(B.Sc. in Chemical Engineering 2001)

Ramadan	1425
November	2004

CERTIFICATION

We certify that this thesis entitled **"Simulation Package System Design to Analysis and Control a Distillation Column using Frequency Response Method"** was prepared by **Yossor Riadh Abdul-Majeed Al-Ani**, under our supervision at AL-Nahrain University, College of Engineering, in partial fulfillment of the requirements for the degree of Master of Science in Chemical Engineering.

Signature:

Dr. Naseer A. Al-Haboby

Date: 3 / 1 /2005

Signature:

Prof. Dr. Qasim J. Slaiman

Head of Chemical Engineering Department

Date: 3 / 1 /2005

CERTIFICATE

We certify, as an examining committee, that we have read the thesis titled "**Simulation Package System Design to Analysis and Control a Distillation Column using Frequency Response Method** " and examined the student **YOSSOR RIADH ABDUL-MAJEED AL-ANI** and found that the thesis meets the standard for the degree of Master of Science in Chemical Engineering.

Signature: *Naseer Al-Haboby*

Dr. Naseer A. Al–Haboby

(Supervisor)

Date : 3 / 1 /2005

Signature:

Ass. Prof. Dr. Mohammed Z. Al–Faiz

(Member)

Date : 3 / 1 /2005

Signature: *M.I. Abdul Wahab*

Dr. Majid I. Abdul–Wahab

(Member)

Date : 3 / 1 / 2005

Signature: *Nada*

Prof. Dr. Nada B. Nakkash

(Chairman)

Date : 3 / 1 / 2005

Approval of the College of Engineering

Signature:

Prof. Dr. Fawzi M. AL–Naima

Dean of the College of Engineering

Date: 18 / 1 / 2005

ABSTRACT

Because of the practical importance of analyzing and controlling the systems arises the need to study the frequency response analysis for any system of several industrial plants.

The frequency response used for the studies of dynamic characteristics of chemical processes and control loops in the present work. The process control implemented for different control strategies and compare between them by using frequency response techniques.

Frequency response methods also give transient response information. By defining such frequency response quantities as gain margin and phase margin, the transient response can be analyzed.

Special software was constructed and designed for the purpose of analyzing the systems using Bode plots technique to determine the characteristics, which also used as interface control to perform the transient response; this system was given the abbreviation *IFRA* (*Interface for Frequency Response Analysis*).

In this work, using VISUAL BASIC$_{6.0}$ and MATLAB$_{6.5}$ programs to studying and analyze the system by Bode plots, which is represents a method to form the frequency response, which is used to analyze the system and to determine its characteristics such as stability or steady-state error characteristics.

In this work we presents dynamic analysis of the distillation column, which is Multi-input Multi-output (*MIMO*) system by using different control strategies such as feedback loops with *P, PI, PID*-controller or decoupling also with different controllers. Also, using one closed-loop with different controllers and the other loop is open.

Other analysis tools relate the closed-loop frequency response such as peak and bandwidth to the transient response. In additional methods, using graphic aid in order to obtain the closed-loop frequency response from the open-loop frequency response. By superimposing the open-loop frequency response over the Nichols chart, to obtain the closed-loop frequency response and then analyze for transient response.

Also we describe the effect for step changes in the manipulated variables on the response of the system.

In this work, we use the relative gain array method to find the interaction between loops and then using the decouplers to eliminate this interacting, and compare the system with and without time delay and knowing its characteristics.

List of contents

Chapter One-Introduction

Chapter Two- Frequency Response Analysis and Dynamic Behavior for Distillations column

Chapter Three-Computer Simulation

Chapter Four-Results and Discussion

Chapter Five-Conclusions and Recommendations

Appendices

NOMENCLATURE

Symbol	Definition	Units
A	State space matrix in Eq. A.18	-
B	State space matrix in Eq. A.18	-
B_m	Bottoms product molar flow rates	mol/s
C	State space matrix in Eq. A.19	-
D	Transfer function of decoupler	-
D_m	Distillate molar flow rates	mol/s
e_{SS}	Steady state error	-
F	Feed stream	mol/s
f_i	Steady state equation for component balance on stage i	-
$G(jw)$	Open-loop Transfer function	-
$\left\| G(jw) \right\|$	Magnitude of the open loop system	-
$\angle G(jw)$	Phase angle of the open-loop system	degree
G_C	Transfer function of controller	-
G_m	Gain margin	-
j	Complex variable	-
K	Steady-state gain	-
k_a	Acceleration constant	-
K_C	Controller gain	-
K_i	Equilibrium constant	-
k_p	Position constant in equation 2.4	-
K_u	Ultimate gain	-
k_v	Velocity constant	-
L	Reflux flow	mol/s

Li	Liquid molar flow rate from stage i	mol/s
L_R	Liquid flow in rectifying section	mol/s
L_S	Liquid flow in stripping section	mol/s
m	Manipulated variable	-
M	Magnitude of the closed loop system	-
M_B	Bottoms molar holdup	mol
M_D	Overhead receiver molar holdup	mol
M_i	Liquid molar holdup on stage i	mol
M_T	Feed tray molar holdup	mol
$\%OS$	Percent over shoot	-
P_m	Phase margin	degree
P_u	Ultimate period	s
$Q(s)$	Characteristic equation of the system	-
q_F	Quality feed stream	-
s	Laplace form	-
t	Time	s
$T(jw)$	Closed-Loop Transfer function	-
t_d	Time delay	s
T_p	Peak Time	s
T_s	Settling Time	s
u	Input variables	-
V	Vapor flow rate	mol/s
V_i	Vapor molar flow rate from stage i	mol/s
V_R	Vapor flow in rectifying section	mol/s
V_S	Vapor flow in stripping section	mol/s
w	Angular frequency	rad/s
w_{BW}	Band width of closed-loop frequency	rad/s

	response	
w_{fm}	Gain Crossover frequency	rad/s
w_{Gm}	Phase crossover frequency	rad/s
x	Controlled variable	-
x	State space variables in equation A-18	-
x_B	Bottom composition	-
$x_{B,sp}$	Desired set point of the bottom composition	-
x_D	Distillate composition	-
$x_{D,Sp}$	Desired set point of the overhead composition	-
x_F	Feed composition	-
x_i	Liquid composition from stage i	-
y	Output variables	-
y_i	Vapor composition from stage i	-

GREEK LETTERS

Symbol	Definition	Units
α	Relative volatility	-
β_{ij}	ijth element in the relative gain array	-
θ_C	Controller output	-
τ	Time constant	s
τ_D	Derivative time	s
τ_I	Reset time	s

ρ_F	Density of fluid	kg/m^3
ρ_w	Density of metal in wall	kg/m^3
ξ	Damping Ratio	-

Subscripts

Symbol	Definition
a	Lead approximation
i	Number of component
j	Number of component
k	Constant
p	Lag approximation
P	Peak value
min	Minimum value
NF	Number of the feed stage
Ns	Number of stages

Glossary

Symbol	Definition
A	Amplitude of the input signal
ADC	Analog to Digital Converter
$AE's$	Algebraic equations
AR	Amplitude Ratio
CC	Cohen-Coon
DAC	Digital to Analog Converter
IC	Integral Circuit
$IFRA$	Interface for Frequency Response Analysis

MIMO	Multi-Input/Multi-Output
N	Number of controllers in multivariable systems
ODE's	Ordinary Differential Equations
P	Proportional controller
PC	Personal Computer
PI	Proportional-Integral controller
PID	Proportional-Integral-Derivative controller
RAM	Read Access Memory
RGA	Relative Gain Array
SISO	Single-Input/Single-Output
ZN	Zeigler-Nichols

INTRODUCTION

Frequency response of a system is defined as the steady–state response of the system to a sinusoidal input signal. The sinusoid is a unique input signal, and the resulting output signal for a linear system, as well as signals throughout the system, is sinusoidal in the steady–state; it differs from the input wave form only in amplitude and phase angle. In linear time–invariant systems, only the amplitude and phase angle may change as a result of a change in frequency. So, frequency response is an important tool for linear systems and cannot directly be used in nonlinear systems. In general, if a system is nonlinear or time varying, the response to sinusoids will not necessarily be sinusoids.

1.1 FREQUENCY RESPONSE METHODS

Frequency response methods were developed by the Nyquist [1] and Bode [2]. This method is the most conventional methods available to control engineer for analysis and design of control. [3]

Pollard [4] described the frequency response method which can be applied experimentally to existing systems by a use of a suitable sine wave generator to inject a sinusoidal signal into either open or closed-loop, and in this way the frequency response characteristics of the complete system or of the elements of a system can be obtained when the transfer functions are not known.

The advantages that they generally possess which make them very practical are the following [5, 6]:

1- The frequency response methods can be worked on limited amount of experimental data.

2- The frequency response methods cope easily with on-line tuning requirements.

3- The frequency response method is ready availability of sinusoid test signals for various ranges of frequencies and amplitudes. Thus the experimental determination of the frequency response of a system is easily a completed and is the most reliable and uncomplicated method for the experimental analysis of a system. Often as we shall find, the unknown transfer function of system can be deduced from the experimentally determined frequency response of a system.

4- The frequency response method is that the transfer functions describing the sinusoidal steady–state behavior of a system can be obtained by replacing *s* with *jw* in the system transfer function *G(s)*. The transfer function representing the sinusoidal steady–state behavior of a system is then a function of a complex variable *jw* and is itself a complex function *G(jw)* that possesses a magnitude and phase angle. The magnitude and phase angle of *G(jw)* are readily represented by graphical plots that provide significant insight into the analysis and design of control systems.

The basic disadvantages of the frequency response method for the analysis and design are the indirect link between the frequency and the time domain, except for case second order system. [3]

Frequency response data are complex numbers, by varying the input frequency over a range, to obtain a group of frequency response data, these data can be manipulated and displayed in a variety of ways, as explained briefly in the following and expanded upon in detail elsewhere in this work.

1. Linear frequency response plots. Two plots: one of magnitude of *G(jw)* and another of phase angle of *G(jw)* with the horizontal axis in both plots is angular frequency *w* with linear scaling, as figure 1.1 [7]
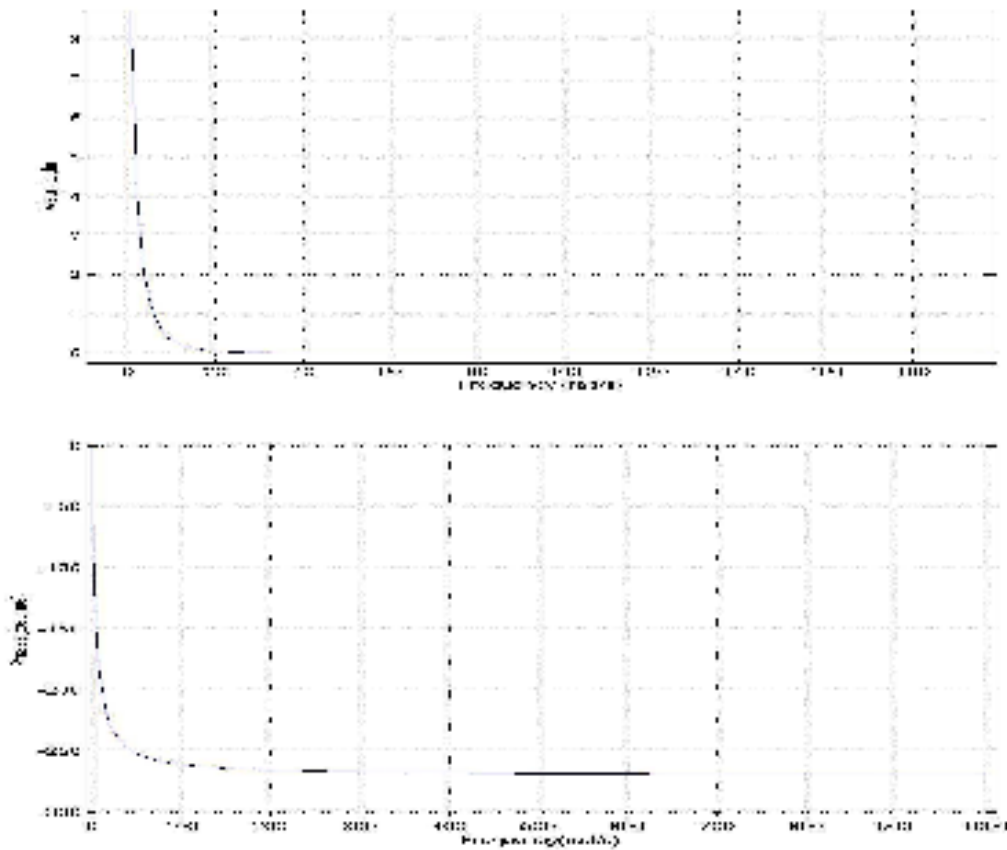
Figure 1.1 *Linear frequency response plots*

3

2. Linear frequency response plots versus logarithm (w) . Two plots: similar to the preceding case, but the horizontal axis are logarithmically scaled (also known as semi-log plots) this allows a larger frequency scale to be used, as figure 1.2 [7]
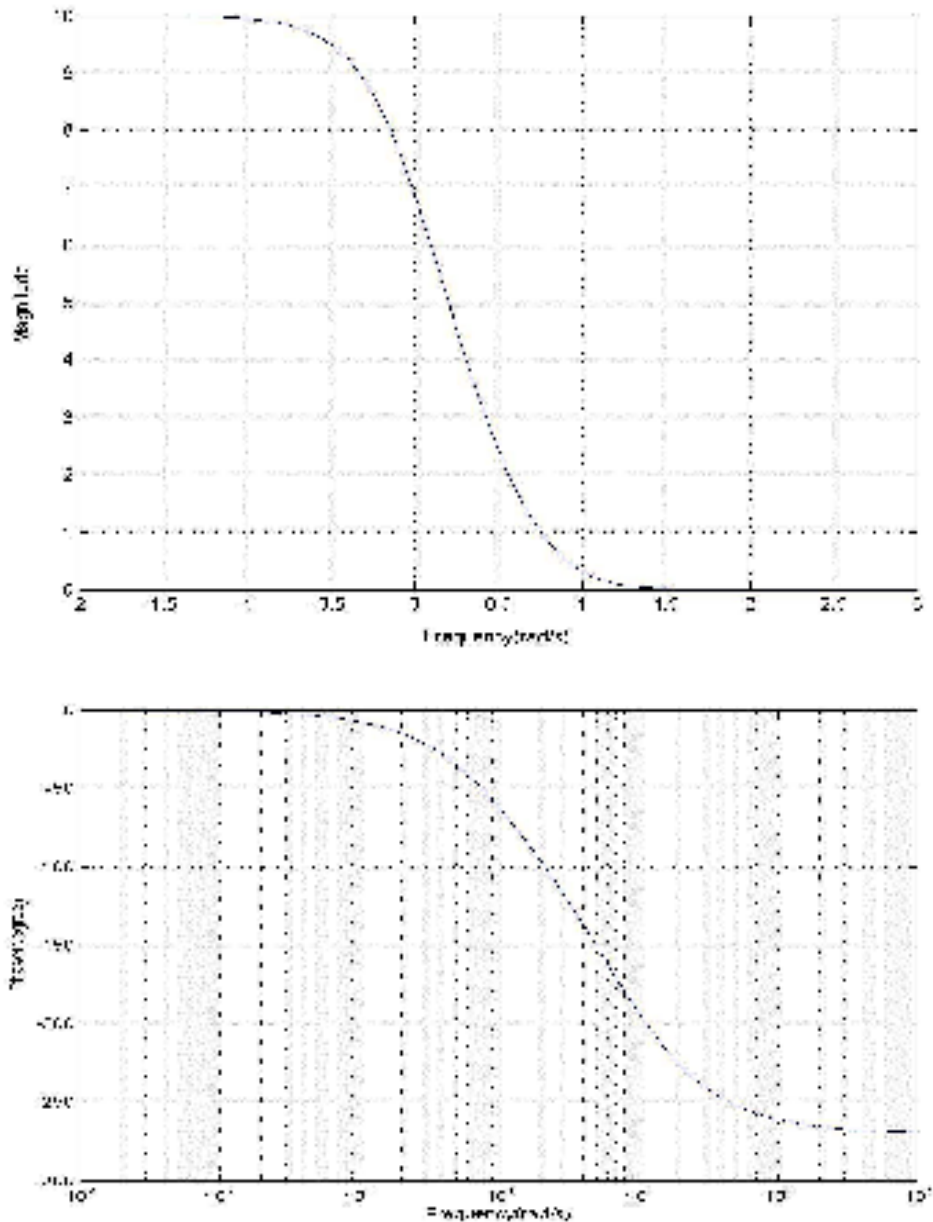
Figure 1.2 *Linear frequency response plots versus logarithm (w)*

*3. **Bode plots.*** Two plots**:** the magnitude of *G(jw)* is in decibels; phase is in degrees. The horizontal axes are logarithm of angular frequency. Bode plots are most frequently used in control systems analysis and design, figure 1.3 **[8]**
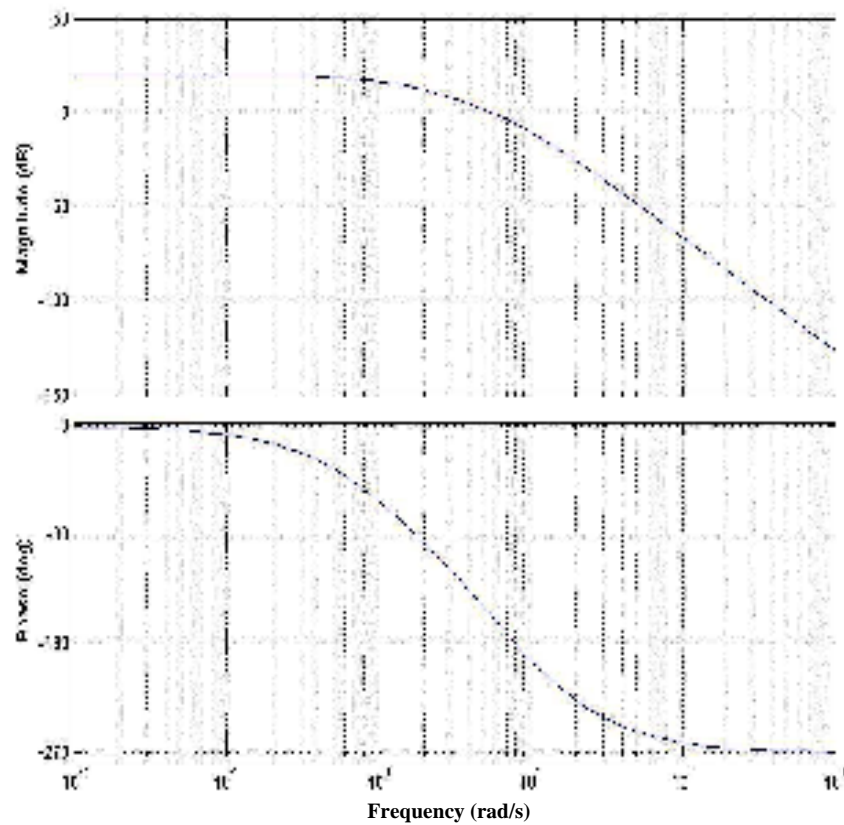
Figure 1.3 *Bode plots*

4. Polar (Nyquist) plot. This is a plot of the imaginary versus the real part of $G(jw)$, or plot of $|G(jw)|$ versus $\angle G(jw)$; this is effectively a plot of the function $G(jw)$ in the complex plane, figure 1.4 [4]
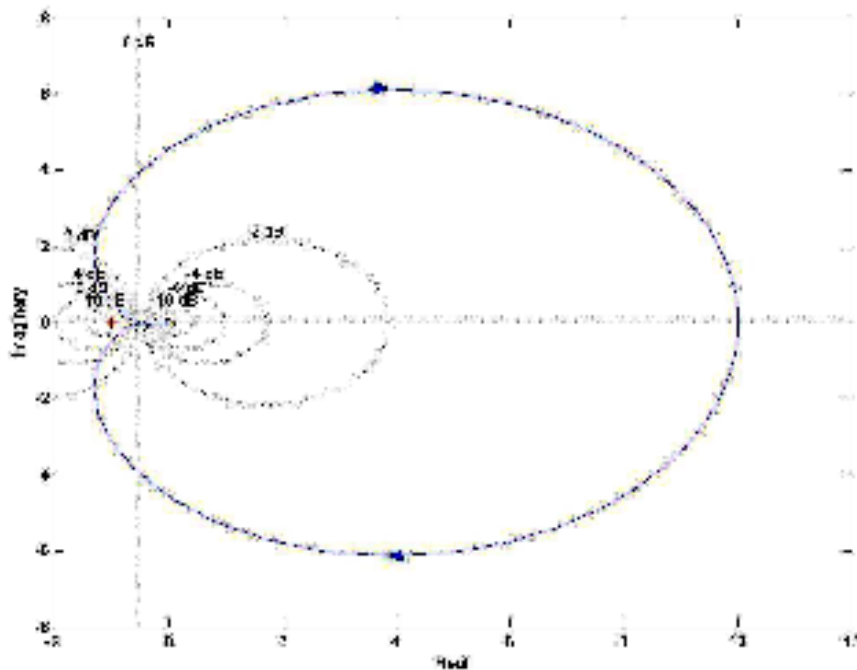
Figure 1.4 *Polar (Nyquist) plot*

5. Nichols plot. A Nichols plot is the plot of the magnitude in (dB) versus the phase in degrees, figure 1.5 [7]
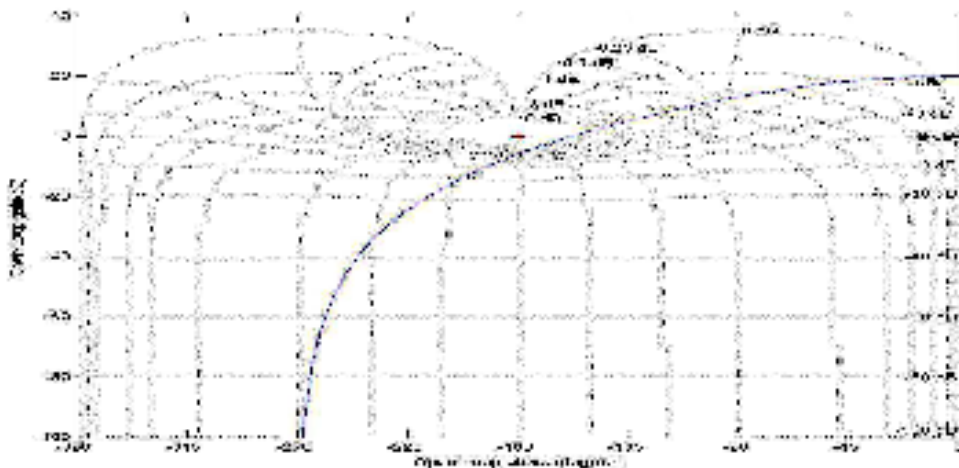
Figure 1.5 *Nichols plot*

6

6. Rutherford-Aikman plot. It is an inversion of the Bode plot, log *(1/AR)* being plotted against the logarithm of the angular frequency, and also phase lag versus logarithm of the angular frequency, figure 1.6 [4]
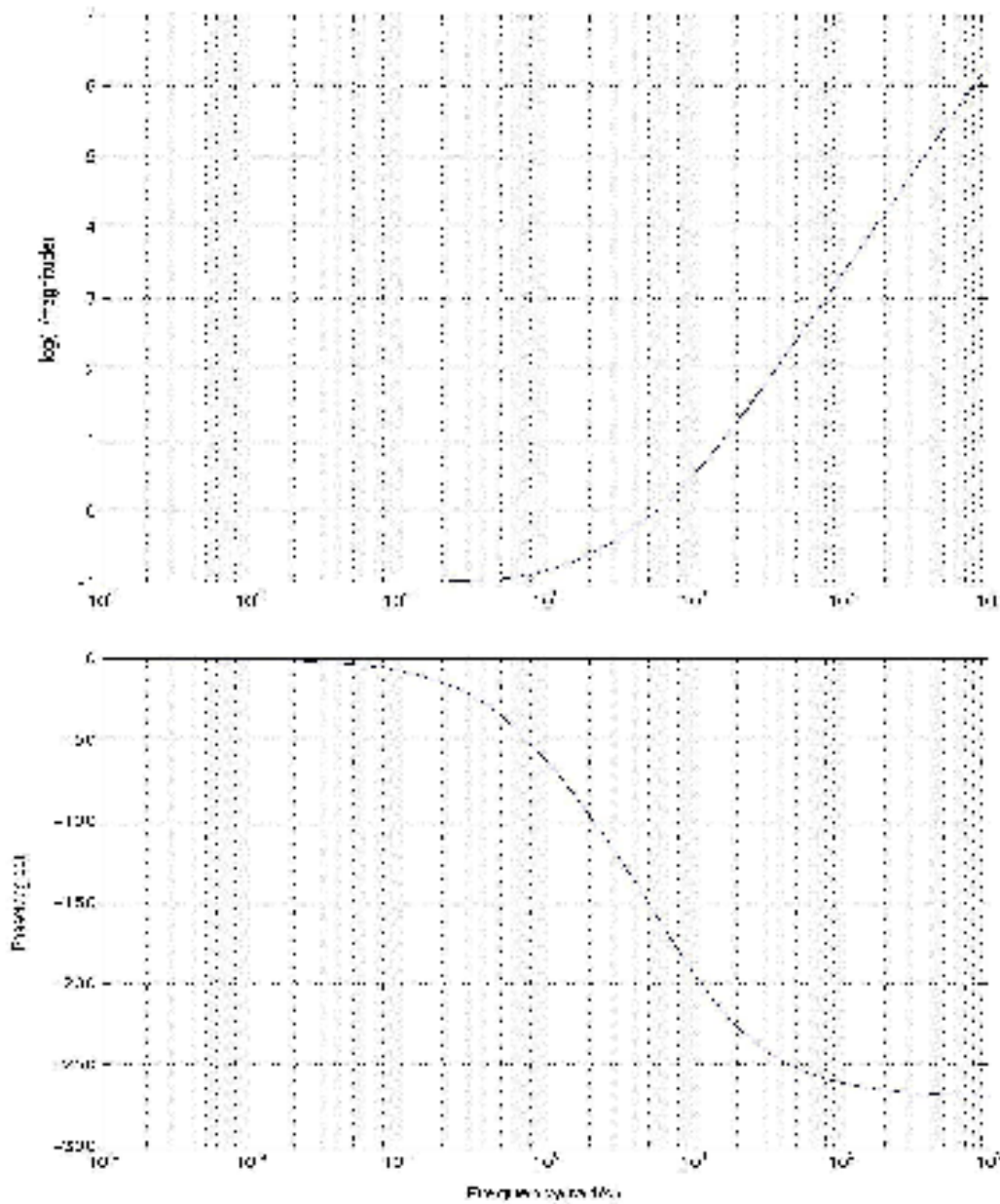
Figure 1.6 *Rutherford-Aikman plot*

7. *The inverse Nyquist plot.* It is the polar plot of $1/(G(jw))$ versus $\angle G(jw)$, figure 1.7 [4]
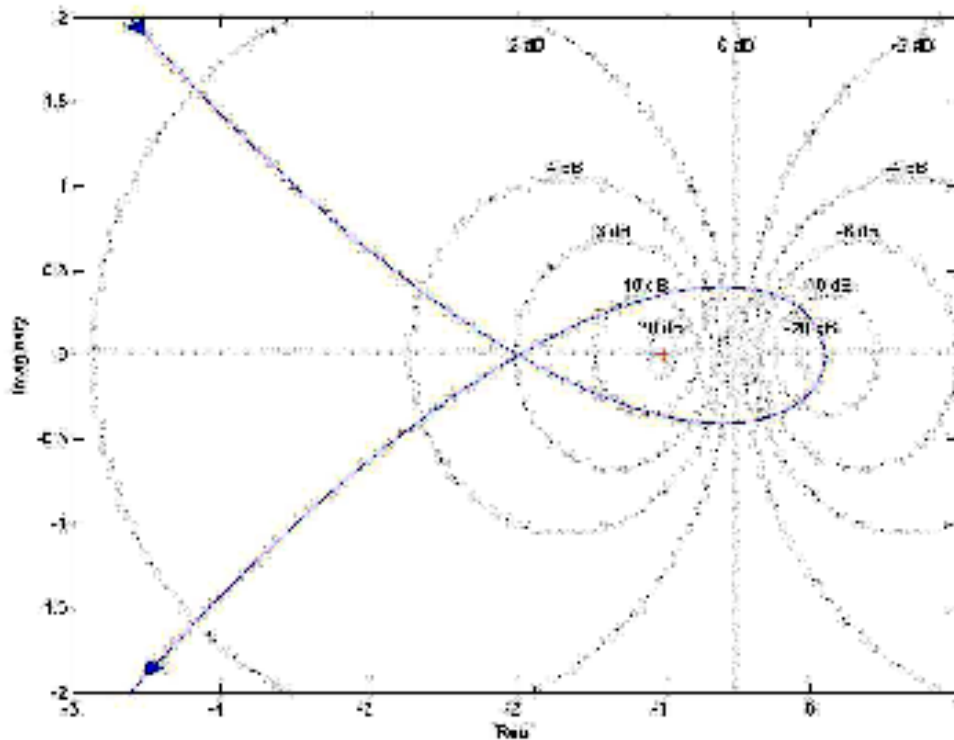
Figure 1.7 *The inverse Nyquist plot*

1.2 <u>PROCESS CONTROL</u>

The conventional method of process control is to use feedback control loops with controllers. The control action depends upon the control modes present and at what parameters values of the modes are set. [9]

Feedback system gives satisfactory control for a wide range of processes and principles involves the use of controlled variable to maintain it at a desired value.

Other control technique involves decoupling control, is applied to multivariable processes, where there is interaction between control loops.

This technique eliminates the effect of this interaction by designing suitable decouplers for the loops. It requires a wide knowledge of the dynamic behavior of the controlled variables for change in disturbance and in the manipulated variables. [10]

1.3 DISTILLATION COLUMN CONTROL

Distillation column is a multi-input/multi-output (*MIMO*) process which is more difficult to analysis and operate than single-input/single-output (*SISO*) process.

A typical simple distillation column separates a mixture of chemical components into two product streams, the lighter components at the top and the heavier components at the bottom. This separation depends upon the number of trays in the column, the reflux ratio, the relative volatilities and the way the feed is split between overhead and bottom products.

For an existing operating column where the number of trays is fixed and the pressure is constant so that the relative volatilities are fixed, the product composition can be controlled by only two variables [10]:

1. Reflux flow rate.
2. Vapor flow rate.

1.4 COMPUTER ANALYSIS OF CONTROL SYSTEMS

A computer model of a system in mathematical form suitable for demonstrating the system behavior may be utilized to investigate various designs of a planned system without actually building the system itself [11].

Assuming that the model and the simulation are reliably accurate, computer simulation has the following advantages [12]:

1- System performance can be observed under all conceivable conditions.

2- Decisions concerning future system presently in a conceptual stage can be examined.

3- Trials of systems under test can be accomplished in a much reduced period of time.

4- Simulation results can be obtained at lower cost than real experimentation.

5- Computer modeling and simulation is often the only feasible safe technique to analyze and evaluate a system.

1.5 COMPUTER AND SOFTWARE S

Digital computers have a major influence on our lives and the development of computers is the most important technological advance over the past 40 years.

Mathematical modeling and simulation are important and useful areas of computer application. In the mid 1970s engineers in industry were skeptical of simulation as a valid way to solve manufacturing problems; few people then believed accurate predictions could be obtained from mathematical models. However, today the prevailing view in industry is that it is much less expensive and more reproducible to run simulation experiments than it is to perform repeated experiments involving actual equipment. The confidence level in what can be done with simulation has risen considerably, and this is having a profound influence on the practice of process engineering. [13]

One of the key elements of planning a VISUAL BBASIC$_{6.0}$ application is deciding what the user sees-in other words, designing the screen.

Programs in conventional programming languages run from the top to the bottom. For folder programming languages, execution starts and moves with the flow of the program to different parts as needed.

A VISUAL BASIC$_{6.0}$ program works completely differently. The core of a programmer thinks should happen, the user is in control. Most of the programming instruction in VISUAL BASIC$_{6.0}$ that tell your program how to respond to events. Essentially anything executable in a VISUAL BASIC$_{6.0}$ program is either in an event procedure or is used by an event procedure to help the procedure carry out its job. [14]

1.6 <u>AIM OF THE WORK</u>

1. To build simulation package for process control (top and /or bottom compositions of a binary distillation column)

2. To analyze the studied system and plot its Bode plot from which the process stability and steady state error can be determine.

3. To design the required controller (*P, PI, PID*) to improve process response according to the demand requirements.

DISTILLATION COLUMN AND
FREQUENCY RESPONS ANALYSIS

2.1 FREQUUENCY RESPONSE METHOD

Frequency response method such as Bode techniques have been successfully applied to the analysis and design of single control systems. In recent years there has also been a great amount of work in order to extend these methods to include multivariable systems. [3]

2.1.1 *Advantages of working with frequency response in terms of Bode plots include [5]:*

1. Bode plots of systems in series simply add..
2. A much wider range of the behavior of the system can be displayed; i.e., both low–and high–frequency behaviors can be displayed in one plot.
3. Bode plot can be determined experimentally.

2.1.2 *Stability, gain margin, and phase margin via Bode plots*

The gain margin is found by using the phase plot to find the frequency, w_{Gm}, where the phase angle is 180°. At this frequency look at the magnitude plot to determine the gain margin, G_m, which is the gain required raising the magnitude curve to 0 dB. The phase margin is found by using the magnitude curve to find the frequency, w_{Pm}, where the gain is 0 dB. On the phase curve at that frequency, the phase margin, P_m, is the difference between the phase value and 180°.

A criterion for stability for a closed–loop system in Bode plots can thus be based on the open–loop frequency response characteristics, that the system

will be unstable if the magnitude ratio exceeds unity at the phase lag is 180°. [5]

2.2 <u>DYNAMIC BEHAIVIOR FOR DISTILLATION COLUMN</u>

Distillation columns were the subject of many dynamic and control studies because of their unique and challenging control problems. These systems have many troublesome features from a control standpoint: slow dynamic response, high order behavior, significant dead times, nonlinearity, and multivariable interaction. The stable and reliable performance of one or more distillation columns is imperative for safe and economic operation of many plants.

This chapter reviews the literature and studies that deal with control aspects and includes the dynamic simulation of the distillation control, types of controllers.

2.2.1 <u>DYNAMIC SIMULATION OF DISTILLATION COLUMN</u>

The dynamic and steady state simulation models of distillation columns consist of a system of equations based on mass and energy balances around each plate of the column.

Typically for the dynamic problems, these balances lead to system of ordinary differential equations (*ODE's*) or to mixed system of equations (*ODE's* and Algebraic Equations *(AE's))*. [10]

There are many studies on computer applications to distillation calculations. This is superficially due to the repetitive nature of these calculations, which render them suitable for solution by computer.

Most of the earlier studies; Lapidus and Amundson [15], Rose and Jahnson [16], Armstrong and Wood [17], dealt with only one section of the

column, and the problem was more difficult when both the stripping and enriching sections were considered.

Morris and Sevreck [18] developed a simulator for multicomponent distillation which had a highly modular structure and an explicit integration scheme.

Thomas [19] reviewed the digital dynamic solution of distillation processes, and presented a new approach which allows for consideration of the effect of varying vapor holdups. It was found that calculation of the instantaneous calculation of the instantaneous component boil-off rates was reduced to the problem of solving a set of linear simultaneous equations of the same orders as the number of components present.

Berber [20] developed a simulation program to predict the dynamic behavior of a theoretical distillation column fractionating a three component feed mixture. Berber and Ates [21] used a dynamic mathematical model based on the previous study [20], to predict the transient response of a continuous stage wise distillation column.

Chimowitz et al. [22], presented an algorithm using local thermodynamic and physical property models in dynamic simulation of multicomponent distillation column. The dynamic models used were relatively simple, but provided a good description of the dynamics of many distillation processes. The local model concept, however, could be interfaced with any dynamic model of distillation, regardless of its complexity. The use of the local model significantly speeds-up execution time, often by a factor of (5-10) when compared to algorithms that use rigorous thermodynamic evolutions. For applications where speed is important, like on-line control, it should prove to be a valuable result.

Gani et al. [23] presented a generalized model for the dynamic simulation of distillation columns. The successful application of the model to

solve different type of test problems demonstrated its wide applicability and flexibility. The good matching of the industrial data showed that the model was reliable and could be used for the study of industrial processes. Evan where the industrial data were not available, the results obtained when analyzed qualitatively, seemed to be varying reasonable.

Ranzi et al. [24] presented a general program for dynamic simulation of multicomponent distillation columns.

Ranzi et al. [25] analyzed and discussed the role of energy balances in simulating the transient behavior of multicomponent distillation columns. A few examples were considered to show how big discrepancies could be observed as a result of neglecting the time derivative of the energy balance hold-ups. Comparisons were presented to show the possible important benefits related to a simultaneous solution of the whole system of algebraic and differential equations. The results showed that the enthalpy balance equations should be taken into account.

2.2.2 <u>CONTROL STRATEGIES OF DISTILLATION COLUMN</u>

Distillation column is a Multi-Input/Multi-Output (*MIMO*) process which is more difficult to analysis and operates than Single-Input/Single-Output (*SISO*) process.

Many techniques were used to control distillation column. In this work the feedback and decoupling controller will be illustrated and discussed.

2.2.2.1 <u>Feedback Controller</u>

Feedback control is achievement and maintenance of a desired condition by using an actual value of this condition and comparing it with a reference value, then using the difference between these two values to eliminate any difference between them.

Hu and Fredramirez [26] applied control theory for distillation column control. Both linear and non-linear distillation models were developed and tested. They achieved a good result by using an optimal multivariable Proportional integral (*PI*) controller for systems with unmeasurable disturbances. When the disturbances were measurable, an optimal multivariable proportional controller with error coordination was recommended. Their results showed that due to the non-linear behavior of the system the multivariable proportional controller algorithm forced the top and bottom compositions near the original steady-state with some offset (0.06 % maximum error).

A simple practical approaches to the problem of finding reasonable *PI*-controller settings of the *N* single-input single-output controllers in a Nth order typical industrial multivariable process was presented by Luyben [27]. The procedure was straight-forward extension of the familiar Nyquist method and required only nominal computing power. The method was tested on ten multivariable distillation column examples taken from the literature. The resulting settings gave reasonable and stable responses.

Al-Elg and Palazoglu [28] developed a rigorous dynamic model of a high purity double effect distillation column to study loop interaction as well as the impact of modeling errors on the effectiveness *PI* controller. Their results indicated the severity of interactions and control performance degradation associated with high purity specifications.

Anderson [29] used a frequency domain approach to compare the nominal performance and robustness of dual-composition distillation column control tuned according to Ziegler-Nichols (*ZN*) and Biggest Log Modulus Tuning (*BLT*) described by Luyben [27] for three binary distillation columns. The scope of their work was to examine whether *ZN* and *BLT* designs yield

satisfactory control of distillation columns. Further, *PI* controllers were tuned according to a proposed multivariable frequency domain method.

2.2.2.2 <u>Decoupling Control</u>

Being the major energy consumers in a chemical plant [30], distillation columns offer most challenging design and control problems. In order to save energy, dual composition control has been proposed and its merits have been extensively studied by Luyben [31] and Shinsky [32]. However, control of both top and bottom compositions usually results in undesirable interaction among the control loops. To be able to cope with such interactions, a lot of research effort has been devoted to decoupling control (Luyben [33], Wood and Berry [34], Ryskamp [35], Waller [36], Schwanke [37], Shinsky [30], Jafary and McAvoy [38], McAvoy [39], Weischedel and McAvoy [40] Fagervik [41]). Because of the simplicity and transparency of the design procedure decoupling is the most popular control strategy in distillation however the need for accurate models to active decoupling limits the success of the method. [11]

Luyben [33] presented a quantitative study of two types of decoupling elements to achieve a non-interacting feedback control of overhead and bottom compositions in binary distillation, ideal and simplified decoupling. It was concluded that in ideal decoupling, leading to unstable feedback loops, while simplified decoupling was effective and stable and appeared to be easily implemented with commercial control instrumentation.

Weischedel and McAvoy [40] studied the two variables controls using the reflux and boil up as manipulated variables to control both top and bottom compositions. They concluded that complete decoupling was not feasible for many (high purity) columns due to sensitivity to model error.

Frey et al. [42] examined the control variable pairing by using the relative gain array. Their results indicated that decoupling of the column was possible by proper selection and pairing of the manipulated and control variables. It was shown that the column decoupled at steady-state compositions independently to design parameters.

Arkun and Morgan [43] gave numerical robustness analysis for low purity and high purity columns with no decoupling, simplified decoupling and ideal decoupling control schemes.

2.3 DESCRIPTION OF THE DISTILLATION COLUMN USED IN THIS WORK

The process under consideration is a binary distillation column, which separates a mixture for example methanol and ethanol.

This column was originally modeled by Waschedel and McAvoy [40]. It represents a benchmark that has been studied by a number of researches for the purpose of controller analysis and design. It is referred to as dual-composition control. A schematic of the process can be found in figure 3.1.
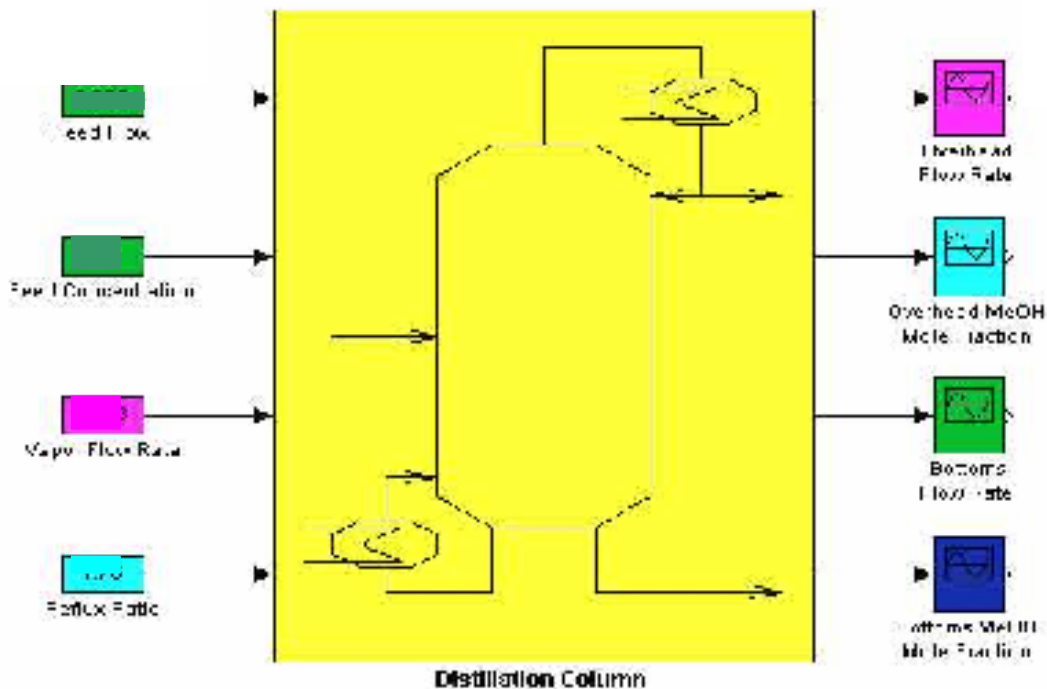
Figure *The distillation column with it's inputs and outputs.*

The column is modeled with component mass balances and energy balances which results in coupled nonlinear differential and algebraic equations. The column model has four inputs and four outputs as listed in table 2.1. [40]

Table 2.1 The inputs and outputs of the distillation column

INPUTS	OUTPUTS
Reflux flow rate	Overhead MeOH composition
Vapor flow rate	Overhead flow rate
Feed MeOH composition	Bottom MeOH composition
Feed flow rate	Bottom flow rate

Also the column has the following manipulated and controlled variables shown in table 2.2. [40]

Table 2.2 The manipulated and controlled variables of the distillation column

MAINPULATED VARIABLES	CONTROLED VARIABLES
Reflux flow rate	Overhead MeOH composition
Vapor flow rate	Bottom MeOH composition

The system also has the following load (or disturbance) variables:

LOAD VARIABLES
Feed flow rate
Feed MeOH composition

The column important parameters are given in table 2.3. [40]

Table 2.3 Parameters for distillation column studied ($q_F=1; x_f= 0.5$)

Component methanol-ethanol Approx.	1.65
Product split	0.01-0.99
No. of trays	27
Reflux ratio	$1.5*L_{min}$

The column specifications are given in table 2.4. [40]

Table 2.4 Column specifications

Diameter	1.8 ft
Weir height	2.0 in
Weir length	1.26 ft
Tray area	2.32 ft^2
Pressure drop per plate	0.0085 atm.
Reboiler holdup	10 times average tray holdup
Condenser holdup	10 times average tray holdup

2.4 DESCRIPTION OF THE COMPUTER CONTROL DEVICES

The computer control system requires a Personal Computer (*PC*) and an interface unit, which consists of an Analog to Digital Converter (*ADC*) and Digital to Analog Converter (*DAC*). These units are shown in figure 2.2. [5]

2.4.1 The Interface Unit

The interface unit receives an analog signal and converts it to a digital signal through an *ADC* then sends it to the computer. The output signal from the computer is loaded to the *DAC*, which converts it to an analog signal. Then this signal can be applied to the control element. [5]

2.4.1.1 *Input Interfacing*

Most *ADC*'s are available in the form of Integrated Circuits (*IC*). It was connected to the measuring device via an amplifier to receive a suitable input signal.

The overhead and bottom composition were measured using the measuring devices which was connected to the *ADC* by means of an amplifier to make the signal larger before it was sent to the *ADC*, figure 2.2. [5]

2.4.1.2 *Output Interfacing*

A Digital to Analog Converter (*DAC*) accepts digital information and transforms it to an analog voltage. The digital information is in the form of a binary number with some fixed number of digits. Especially when used in connection with a computer, this binary number is called a binary word or computer word. The *DAC* converts a digital word into an analog voltage, figure 2.2. [5]

(a)

(b)
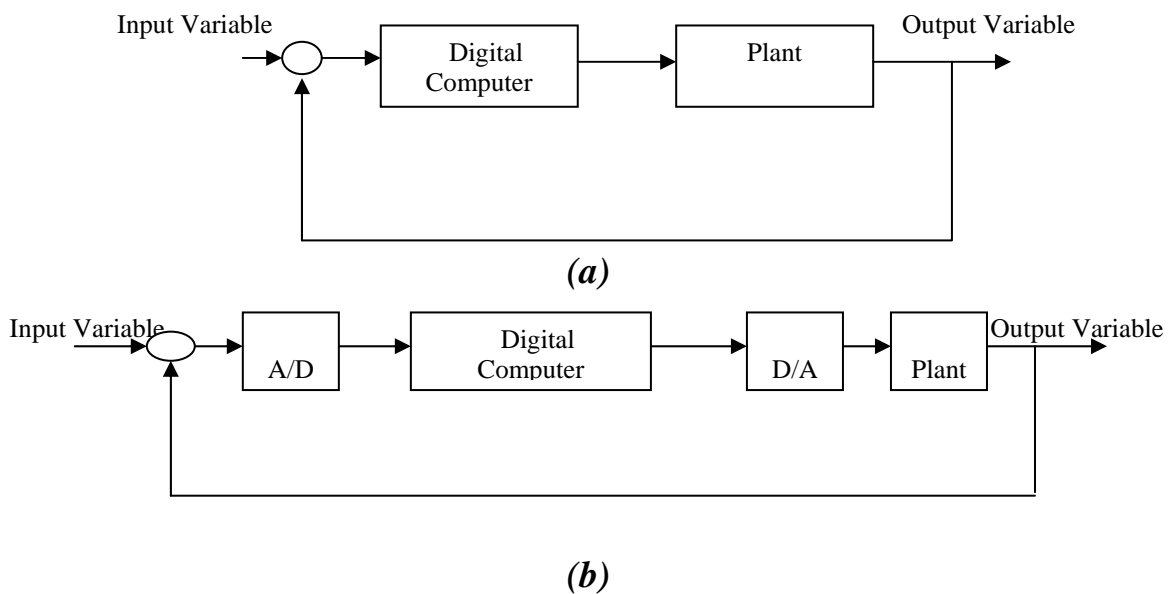
Figure 2.2 *(a) Placement of the digital computer within the loop.*
        (b) Detailed block diagram showing placement of A/D and D/A converters.

2.5 OBTAINING TRANSFER FUNCTION EXPERIMANTALLY

The analytical determination for the system's transfer function is difficult. The individual component values may not be known, or the internal configuration of the system may not be accessible. In such cases, the frequency response of the system, from input to output, can be obtained experimentally and using the frequency response to determine the transfer functions. To obtain frequency response plot experimentally, by using a sinusoidal force or signal generator at the input of the system and measure the output steady-state sinusoidal amplitude and phase angle. Repeating this process at a number of frequencies yields data for a frequency response plot. [5]

Bode plots are a convenient presentation of the frequency response data for the purpose of estimating the transfer function. These plots allow parts of the transfer function to be determined and extracted, leading the way to further refinements to find the remaining parts of the transfer function. [44]

2.6 THE TRANSFER FUNCTION MODELS

In this work the transfer function models for the column by step forcing the manipulative variables in the nonlinear column simulation. Both positive and negative steps were made. An alternative industrial approach would be to step force the actual column and record the overhead composition x_D and bottom composition x_B responses. The gains in the transfer functions were not fitted but were determined from the difference between the initial and final compositions. In choosing which transfer function model to use, it was desired to have a model with the smallest number of fitted parameters which adequately represented the column dynamics.

In arriving at final transfer function models for the column, the average of the gains was used. The transfer function models for the column are given below, [40]

$$\begin{bmatrix} x_D(s) \\ x_B(s) \end{bmatrix} = \begin{bmatrix} \dfrac{0.471\, e^{-1.0s}}{(30.7s+1)(30.7s+1)} & \dfrac{-0.495\, e^{-2.0s}}{(28.5s+1)(28.5s+1)} \\ \dfrac{0.749\, e^{-1.7s}}{(57.0s+1)(57.0s+1)} & \dfrac{-0.832\, e^{-1.0s}}{(50.5s+1)(50.5s+1)} \end{bmatrix} \begin{bmatrix} L(s) \\ V(s) \end{bmatrix} \qquad (2.1)$$

For this column, a step change of 1% was made in the manipulated variables. The time constants and dead times for each transfer function were similar regardless of whether a positive or negative step made. The gains for positive and negative step changes for distillation column are given in [40].

2.7 THEORITICAL ASPECTS FOR FINDING THE TRANSFER FUNCTION

The theoretical model of various process units is derived by using the fundamental principles of conservation of mass, energy and momentum:

Input - Output = Accumulation.

In steady state condition, the accumulation is equal to zero. For dynamic simulation, the accumulation term to the mass balance must be added. In practice, application of this procedure introduces additional complexity into the system equation, so it is some times necessary to make simplifying assumptions of the dynamic behavior. [45]

Then the mathematical model and theoretical aspects was found below:

2.7.1 *Process Assumptions*

The following assumptions are made to drive the mathematical model [45].

1. The feed is saturated liquid.

2. Equimolal overflow.

3. Constant molar hold up in the distillate receiver.

4. Constant liquid phase molar holdup.

5. Constant relative volatility.

6. Vapor holdup is negligible compared with liquid holdup.

7. Perfect mixing on each plate.

8. The overhead vapor is totally condensed in the condenser.

9. Column pressure is constant.

10. Plate efficiency is 100%.

11. Thermal dynamic of reboiler and condenser are negligible.

2.7.2 *Dynamic Material Balances*
2.7.2.a *All Stages expect feed, condenser, and reboiler*

The component balance for the liquid phase of a typical stage as shown in figure 2.3
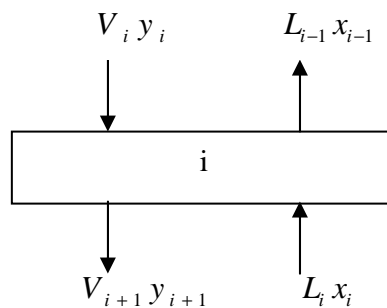
Figure 2.3 *Stage i*

$$M_i \frac{\partial}{\partial t} X_i = L_{i-1} X_{i-1} + V_{i+1} Y_{i+1} - L_i X_i - V_i Y_i \qquad \dots (2.2)$$

where M_i *is* the liquid molar holdup on stage i.

For this distillation model, the common assumptions is equimolal overflow then for any stage accept the feed stage, the vapor flow rate from one stage is equal to the vapor molar flow rate of the stage below.

$$V_i = V_{i+1} \qquad\qquad \text{… (2.3)}$$

and that the liquid leaving the stage is equal to the liquid flowing from one stage above:

$$L_i = L_{i-1} \qquad\qquad \text{… (2.4)}$$

2.7.2.b *Feed stage*

If the feed is a saturated liquid, then $q_F = 1$. The vapor molar flow rate leaving the feed stage is (NF = number of the feed stage)

$$V_{NF} = V_{NF+1} + F(1 - q_F) \qquad\qquad \text{… (2.5)}$$

Where q_F represent the quality of the feed stream.

Similarly, the liquid molar flow rate of the stream leaving the feed stage is:

$$L_{NF} = L_{NF-1} + F q_F \qquad\qquad \text{… (2.6)}$$

2.7.2.c *Condenser*

A total condenser removes energy from the overhead vapor, resulting in a saturated liquid. Assuming a constant molar holdup in the distillate receiver, the total input flow rate from the distillate receiver (reflux + distillate flows) is equal to the flow rate of the vapor from the top tray:

$$L + D_m = V_2 \qquad\qquad \text{… (2.7)}$$

Where L and D_m represent the reflux and distillate molar flow rates, respectively.

2.7.2.d *Reboiler*

A total material balance around the reboiler yields:

$$B = L_{NS-1} - V \qquad\qquad \text{… (2.8)}$$

Where V is the reboiler molar flow rate and B is the bottoms product molar flow rate.

2.7.2.e *Summary of the modeling equations*

The rectifying section liquid molar flow rates are:

$$L_R = L \hspace{4cm} \text{... (2.9)}$$

The stripping section liquid molar flow rates are:

$$L_S = L_R + Fq_F \hspace{3cm} \text{... (2.10)}$$

The stripping section vapor molar flow rates are:

$$V_S = V \hspace{4cm} \text{... (2.11)}$$

The rectifying section vapor molar flow rates are:

$$V_R = V_S + F(1 - q_F) \hspace{3cm} \text{... (2.12)}$$

In the following, assuming a constant liquid phase molar holdup $\left(\dfrac{dM_i}{dt} = 0 \right)$.

The overhead receiver component balance is:

$$\frac{dx_i}{dt} = \frac{1}{M_D} \left[V_R(y_2 - x_1) \right] \hspace{2cm} \text{... (2.13)}$$

The rectifying section component balance is (from $i=2$ to NF-1):

$$\frac{dx_i}{dt} = \frac{1}{M_T} \left[L_R x_{i-1} + V_R y_{i+1} - L_R x_i - V_R y_i \right] \hspace{1cm} \text{... (2.14)}$$

The feed stage balance is:

$$\frac{dx_{NF}}{dt} = \frac{1}{M_T} \left[L_R x_{NF-1} + V_S y_{NF+1} + F z_F - L_S x_{NF} - V_R y_{NF} \right] \hspace{0.5cm} \text{... (2.15)}$$

The striping section component balance is (from $i=NF+1$ to NS-1):

$$\frac{dx_i}{dt} = \frac{1}{M_T} \left[L_S x_{i-1} + V_S y_{i+1} - L_S x_i - V_S y_i \right] \hspace{1cm} \text{... (2.16)}$$

And the reboiler component balance is:

$$\frac{dx_{NS}}{dt} = \frac{1}{M_B} \left[L_S x_{NS-1} - B x_{NS} - V_S y_{NS} \right] \qquad \text{... (2.17)}$$

Equilibrium relationship

It is assumed that the vapor leaving a stage is in equilibrium with the liquid on the stage. The relationship between the liquid and vapor phase concentrations on a particular stage can be calculated using the constant relative volatility expression:

$$y_i = \frac{\alpha x_i}{1 + (\alpha - 1) x_i} \qquad \text{... (2.18)}$$

2.7.3 <u>State-Space Linear Method for Distillation Models</u>

Linear state-space models are useful for stability analysis and control system analysis and design. Here we develop models of the form:

$$\&= A x' + B u' \qquad \text{... (2.19)}$$

$$y' = C x' \qquad \text{... (2.20)}$$

Where ´ is used to represent the deviation variables $x' = x - x_S$, $u' = u - u_S$ (the subscript s indicates the steady-state values). Defining

$$K_i = \frac{\partial y_i}{\partial x_i} = \frac{\alpha}{(1 + (\alpha - 1) x_i)^2} \qquad \text{... (2.21)}$$

and linearizing the dynamic equations (from *(2.13)* to *(2.17)*) and evaluates the parameters (*A*, *B*, and *C*) of equations *(2.19)* and *(2.20)*. Such as below:

2.7.4 <u>State-Space Equations for Distillation Columns [52]</u>

After linearizing the dynamic equations *(2.13)* to *(2.17)* can be estimated the equation below:

$$A_{1,1} = \frac{\partial f_1}{\partial x_1} = -\frac{V_R}{M_D} \qquad \qquad \dots (2.22)$$

$$A_{1,2} = \frac{\partial f_1}{\partial x_2} = \frac{V_R K_2}{M_D} \qquad \qquad \dots (2.23)$$

For i=2 to *NF*-1:

$$A_{i,i-1} = \frac{\partial f_i}{\partial x_{i-1}} = \frac{L_R}{M_T} \qquad \qquad \dots (2.24)$$

$$A_{i,i} = \frac{\partial f_i}{\partial x_i} = -\left(\frac{L_R + V_R K_i}{M_T} \right) \qquad \qquad \dots (2.25)$$

$$A_{i,i+1} = \frac{\partial f_i}{\partial x_{i+1}} = \frac{V_R K_{i+1}}{M_T} \qquad \qquad \dots (2.26)$$

For the feed stage:

$$A_{NF,NF-1} = \frac{\partial f_{NF}}{\partial x_{NF-1}} = \frac{L_R}{M_T} \qquad \qquad \dots (2.27)$$

$$A_{NF,NF} = \frac{\partial f_{NF}}{\partial x_{NF}} = -\left(\frac{L_S + V_R K_i}{M_T} \right) \qquad \qquad \dots (2.28)$$

$$A_{NF,NF+1} = \frac{\partial f_{NF}}{\partial x_{NF+1}} = \frac{V_S K_{NF+1}}{M_T} \qquad \qquad \dots (2.29)$$

For $i = NF+1$ to *NS*-1:

$$A_{i,i-1} = \frac{\partial f_i}{\partial x_{i-1}} = \frac{L_S}{M_T} \qquad \qquad \dots (2.30)$$

$$A_{i,i} = \frac{\partial f_i}{\partial x_i} = -\left(\frac{L_S + V_S K_i}{M_T} \right) \qquad \qquad \dots (2.31)$$

$$A_{i,i+1} = \frac{\partial f_i}{\partial x_{i+1}} = \frac{V_S K_{i+1}}{M_T} \qquad \qquad \dots (2.32)$$

and for the reboiler (stage *NS*):

$$A_{NS,NS-1} = \frac{\partial f_i}{\partial x_{i-1}} = \frac{L_S}{M_B} \qquad \qquad \dots (2.33)$$

$$A_{NS,NS} = \frac{\partial f_i}{\partial x_i} = -\left(\frac{B + V_S K_{NS}}{M_B} \right) \qquad \qquad \dots (2.34)$$

Now, for the derivatives with respect to the inputs; $u_1 = L_R = L_1$ and $u_2 = V_S = V$

$$B_{1,1} = \frac{\partial f_1}{\partial u_1} = 0 \qquad\qquad B_{1,2} = \frac{\partial f_1}{\partial u_2} = 0 \qquad\qquad \text{... (2.35)}$$

For $i = 1$ to NS-1:

$$B_{i,1} = \frac{\partial f_1}{\partial u_1} = \frac{x_{i-1} - x_i}{M_T} \qquad\qquad B_{i,2} = \frac{\partial f_1}{\partial u_2} = \frac{y_{i+1} - y_i}{M_T} \qquad\qquad \text{... (2.36)}$$

and for the bottom stage:

$$B_{NS,1} = \frac{\partial f_1}{\partial u_1} = \frac{x_{i-1} - x_i}{M_{NS}} \qquad\qquad B_{NS,2} = \frac{\partial f_1}{\partial u_2} = \frac{x_{NS} - y_{NS}}{M_{NS}} \qquad\qquad \text{... (2.37)}$$

If the output variables are the overhead and bottoms compositions, then:

$C_{1.1} = 1$, while $C_{1,i} = 0$ for i 1   ... (2.38)

$C_{2.NS} = 1$, while $C_{2,i} = 0$ for i NS   ... (2.39)

2.7.5 <u>Transforming the State-Spase Linear Models to Transfer Function Form</u>

After estimate the parameters of equations *(2.19)* and *(2.20)* we can transforming the state-spase linear models to transfer function form by:

$$G(s) = C(sI - A)^{-1} B \qquad\qquad\qquad \text{... (2.40)}$$

2.8 <u>THE CONTROL STRATEGIES</u>

In this work using different control strategies to showing its effect on the system. Feedback control in general is the achievements and maintained of desired condition by using an actual value of this condition and comparing it to a reference value (set point), and using the differences between those to eliminate any difference between them. Most controllers use negative feedback which a measured process output (controlled variable) is subtracted from a desired value (set point) to generate an error signal. The controller recognizes the error signal and manipulates a process input (control element)

to reduce the error [46]. The most important types of industrial feedback controllers; include *P, PI,* and *PID*-controller. In frequency response there will be G_c's which are add to the transfer function G of a system to get the total open-loop transfer function of a system. [47]

2.8.1 *Proportional controller (P)*

The output of a proportional controller changes only if the errors signal changes. Since a manipulated variable requires a new control value position, the controller must end up with a new error signal. This means that the proportional controller usually gives a steady state error or offset. [46]

The transfer function of a *P*-controller is

$$G_c = K_c \qquad \qquad \qquad \text{… (2.41)}$$

In frequency response, a proportional controller merely multiplies the magnitude of system at every frequency by a constant K_c on a Bode plot, this means a proportional controller raises the log magnitude curve by *20 log (K_c)* decibels but has no effect on the phase angle curve. [47]

2.8.2 *Proportional-Integral controller (PI)*

Most control loops use (*PI*) controller. The integral action eliminates steady state error. The smaller the integral time $_I$, the faster the error is reduced, but the system becomes more under-damped as $_I$ is reduced, end if it is made too small loop becomes unstable. [46]

The transfer function of a *PI*-controller is

$$G_C = K_c(1 + \frac{1}{\tau_I s}) = K_c(\frac{\tau_I s + 1}{\tau_I s}) \qquad \qquad \text{… (2.42)}$$

in Bode plot, at low frequencies a *PI*-controller amplifies magnitude and contributes -90º of phase angle lag. This loss of phase angle is undesirable from a dynamic standpoint since it moves the system to unstability. [47]

2.8.3 *Proportional-Integral-Derivative controller (PID)*

PID controllers are used in loops where tight dynamic response is important. The derivative action helps to compensate for lags in the loop. [46]

A *PID* controller is usually satisfactory for about 80% of all control applications [48].

The transfer function of a *PID*-controller is

$$G_C = K_C(1 + \tau_D s + \frac{1}{\tau_I s}) \, [47] \qquad \qquad \text{... (2.43)}$$

2.9 *RELATIVE GAIN ARRAY METHOD [RGA]*

Undoubtedly the most discussed method for studying interaction is the *RGA*. It was proposed by Bristol [49]. Shinskey [50] and McAvoy [51] discussed this method and explain it. The *RGA* is a matrix of numbers. The ijth element in the array is called β_{ij}. It is the ratio of the steady state gain between the ith controlled variable and the ith manipulated variable when all other manipulated variables are constant, divided by the steady state gain between the same two variables when all other controlled variables are constant.

$$\beta_{ij} = \frac{\left[x_i / m_j\right]_{\overline{m}_k}}{\left[x_i / m_j\right]_{\overline{x}_k}} \qquad \qquad \text{... (2.44)}$$

when we have a 2*2 system with the steady state gains $K_{pij.}$

$$\begin{aligned} x_1 &= K_{p11}m_1 + K_{p12}m_2 \\ x_2 &= K_{p21}m_1 + K_{p22}m_2 \end{aligned} \qquad \qquad \text{... (2.45)}$$

for this system the gain between x_1 and m_1 when m_2 is constant is

$$\left[\frac{x_1}{m_1}\right]_{\overline{m}_2} = K_{p11} \qquad \qquad \text{... (2.46)}$$

the gain between x_1 and m_1 when x_2 is constant ($x_2 = 0$) is found from solving the equations

$$x_1 = K_{p11} m_1 + K_{p12} m_2 \qquad \qquad \ldots (2.47)$$

$$0 = K_{p21} m_1 + K_{p22} m_2 \qquad \qquad \ldots (2.48)$$

$$x_1 = K_{p11} m_1 + K_{p12} \left[\frac{-K_{p21} m_1}{K_{p22}} \right] \qquad \qquad \ldots (2.49)$$

$$x_1 = \left[\frac{K_{p11} K_{p22} - K_{12} K_{p21}}{K_{p22}} \right] m_1 \qquad \qquad \ldots (2.50)$$

$$\left[\frac{x_1}{m_1} \right]_{\bar{x}_2} = \left[\frac{K_{p11} K_{p22} - K_{12} K_{p21}}{K_{p22}} \right] \qquad \qquad \ldots (2.51)$$

therefore the β_{ij} term in the *RGA* is

$$\beta_{11} = \left[\frac{K_{p11} K_{p22} - K_{12} K_{p21}}{K_{p22}} \right] \qquad \qquad \ldots (2.52)$$

$$\beta_{11} = \left[\frac{1}{1 - \dfrac{K_{p12} K_{p21}}{K_{p11} K_{p22}}} \right] \qquad \qquad \ldots (2.53)$$

The elements in the *RGA* can be numbers that vary from very large negative values to very large positive values. There should be less interaction when *RGA* elements near 1. Numbers around 0.5 indicate interaction. Numbers that are very large indicate interaction. [47]

2.10 *DECOPLING CONTROL SCHEMES*

The decoupler is denoted by *D(s)* which isolate the individual single-input single-output control loops. The general design equation for the decoupler is

$$G(s)D(s) = M(s) \qquad \qquad \ldots (2.54)$$

Where *M(s)* is a diagonal matrix to be chosen by the designer. When M(s) is chosen to consist of the diagonal elements of G(s), table 2.6 summaries the transfer functions involved in decoupling control. [52]

Table 3-6: Transfer Function for Decoupling Control [52]

	$G_p(s)$	$M(s)$	$D(s)$	Decoupling single-input single-output loops
Ideal decoupling	$\begin{bmatrix} G_{11} & G_{12} \\ G_{21} & G_{22} \end{bmatrix}$	$\begin{bmatrix} G_{11} & 0 \\ 0 & G_{22} \end{bmatrix}$	$\begin{bmatrix} \dfrac{1}{1-\dfrac{G_{12}G_{21}}{G_{11}G_{22}}} & \dfrac{-G_{12}/G_{11}}{1-\dfrac{G_{12}G_{21}}{G_{11}G_{22}}} \\[4mm] \dfrac{-G_{21}/G_{22}}{1-\dfrac{G_{12}G_{21}}{G_{11}G_{22}}} & \dfrac{1}{1-\dfrac{G_{12}G_{21}}{G_{11}G_{22}}} \end{bmatrix}$	$\dfrac{y_1}{u_1}=G_{11}$ $\dfrac{y_2}{u_2}=G_{22}$
Simplified decoupling	$\begin{bmatrix} G_{11} & G_{12} \\ G_{22} & G_{22} \end{bmatrix}$	$\begin{bmatrix} G_{11}\left(1-\dfrac{G_{12}G_{21}}{G_{11}G_{22}}\right) & 0 \\[3mm] 0 & G_{22}\left(1-\dfrac{G_{12}G_{21}}{G_{11}G_{22}}\right) \end{bmatrix}$	$\begin{bmatrix} 1 & -G_{12}/G_{11} \\ -G_{21}/G_{22} & 1 \end{bmatrix}$	$\dfrac{y_1}{u_1}=G_{11}\left(1-\dfrac{G_{12}G_{21}}{G_{11}G_{22}}\right)$ $\dfrac{y_2}{u_2}=G_{22}\left(1-\dfrac{G_{12}G_{21}}{G_{11}G_{22}}\right)$
One-way decoupling	$\begin{bmatrix} G_{11} & G_{12} \\ G_{21} & G_{22} \end{bmatrix}$	$\begin{bmatrix} G_{11}\left(1-\dfrac{G_{12}G_{21}}{G_{11}G_{22}}\right) & G_{12} \\[3mm] 0 & G_{22} \end{bmatrix}$	$\begin{bmatrix} 1 & 0 \\ -G_{21}/G_{22} & 1 \end{bmatrix}$	$y_1=G_{11}\left(1-\dfrac{G_{12}G_{21}}{G_{11}G_{22}}\right)u_1+G_{12}u_2$ $\dfrac{y_2}{u_2}=G_{22}$

2.11 *THE CLOSED LOOP TRANSFER FUNCTION*

The closed-loop transfer function for unity feedback system can be derived as:

Typical open-loop transfer function is $\Rightarrow G(s) = \dfrac{1}{\tau^2 s^2 + 2\zeta\tau s}$ [3]   *… (2.55)*

Then the closed-loop transfer function $\Rightarrow T(s) = \dfrac{G(s)}{1 + G(s)}$ *… (2.56)*

$$T(s) = \frac{\dfrac{1}{\tau^2 s^2 + 2\zeta\tau s}}{1 + \dfrac{1}{\tau^2 s^2 + 2\zeta\tau s}} = \frac{1}{\tau^2 s^2 + 2\zeta\tau s + 1} \qquad \text{… (2.57)}$$

When $s = jw$ then

$$T(jw) = \frac{1}{(1 - w^2 \tau^2) + 2 jw\zeta\tau} \qquad \text{… (2.58)}$$

This may be converted to the polar form, hence, the magnitude of the closed-loop frequency response as

$$M = |T(jw)| = \frac{1}{\sqrt{(1 - \tau^2 w^2)^2 + 4\zeta^2 \tau^2 w^2}} \qquad \text{… (2.59)}$$

The full derivation of equation *(2.59)* is shown in appendix A-1.

2.12 *RELATION BETWEEN CLOSED-LOOP TRANSIENT AND CLOSED-LOOP FREQUENCY RESPONSE*

2.12.1 Damping Ratio and Closed-Loop Frequency Response [5]

From the closed-loop transfer function the relationship can be derived between the closed–loop transient response and the poles of the closed–loop transfer function [5]. First, by squaring the equation *(2.59)* then

$$M^2 = \frac{1}{(1 - \tau^2 w^2)^2 + 4\zeta^2 \tau^2 w^2} \qquad \text{… (2.60)}$$

After that differentiation with respect to w^2 and setting the derivative equal to zero yields the maximum value of M, M_P, where

$$M_P = \frac{1}{2\zeta\sqrt{(1-\zeta^2)}} \qquad \qquad \dots (2.61)$$

at a frequency, w_p

$$w_P = \frac{1}{\tau}\sqrt{(1-2\zeta^2)} \qquad \qquad \dots (2.62)$$

The full derivation of equation *(2.62)* is shown in appendix A-2.

The maximum value or the resonant peak magnitude of the closed-loop magnitude response is related to the damping ratio, . Since is related to percent overshoot.

$$\% OS = e^{-\left(\zeta\pi / \sqrt{1-\zeta^2}\right)} * 100 \ [3] \qquad \qquad \dots (2.63)$$

Then the maximum magnitude on the frequency response curve is directly related to the damping ratio and, hence, the percent overshoot. [5]

2.12.2 Response Speed and Closed-Loop Frequency Response

Another relation between closed-loop transient and closed-loop frequency response can be derived in this section. It is the relationship between response speed and closed loop frequency response which is used $M = \frac{1}{\sqrt{2}}$ to find the frequency for *M*, which is defined *the bandwidth for closed-loop frequency response.* [5]

$$M = \frac{1}{\sqrt{2}} = \frac{1}{\sqrt{(1-\tau^2 w^2)^2 + 4\zeta^2\tau^2 w^2}} \qquad \qquad \dots (2.64)$$

The result is

$$w_{BW} = \frac{1}{\tau}\sqrt{(1-2\zeta^2) + \sqrt{4\zeta^4 - 4\zeta^2 + 2}} \qquad \qquad \dots (2.65)$$

To relate w_{BW} to settling time must be substitute $\frac{1}{\tau} = \frac{4}{T_s\zeta}$ [5] into equation *(2.64)* and obtain

$$w_{BW} = \frac{4}{T_S \zeta} \sqrt{(1-2\zeta^2) + \sqrt{4\zeta^4 - 4\zeta^2 + 2}} \qquad \qquad \dots (2.66)$$

Similary, since $\dfrac{1}{\tau} = \dfrac{\pi}{T_P \sqrt{1-\zeta^2}}$ [5]

$$w_{BW} = \frac{\pi}{T_P \sqrt{1-\zeta^2}} \sqrt{(1-2\zeta^2) + \sqrt{4\zeta^4 - 4\zeta^2 + 2}} \qquad \qquad \dots (2.67)$$

The full derivation of equations *(2.65), (2.66)* and *(2.67)* is shown in appendix A-3.

2.13 *RELATION BETWEEN CLOSED- AND OPEN-LOOP FREQUENCY RESPONSE*

The Nichols chart contains curves of constant closed-loop magnitude and phase angle. By its chart can be found the phase margin, gain margin resonant peak magnitude, and bandwidth of the closed-loop system from the plot of the open-loop system.

This chart is quit useful for determining the closed-loop frequency response from that of the open-loop. If the open-loop frequency response curve is superimposed on the Nichols chart, the intersections of the open-loop frequency response curve give the values of the magnitude and phase angle of the closed-loop frequency response at each frequency point. [3]

2.14 *RELATION BETWEEN CLOSED-LOOP TRANSIENT AND OPEN-LOOP FREQUENCY RESPONSE*

2.14.1 Damping Ratio from Phase Margin

In order to derive the relationship between the phase margin and the damping ratio the frequency for $|G(jw) = 1|$ must be estimated. Hence

$$G(s) = \frac{1}{\tau^2 s^2 + 2\zeta \tau s} \qquad \qquad \dots (2.68)$$

In order to derive the relationship between the phase margin and the damping ratio the frequency for $|G(jw)=1|$ must be estimated. Hence

$$G(s) = \frac{1}{\tau^2 s^2 + 2\zeta\tau s} \qquad\qquad \text{... (2.68)}$$

$$|G(jw)| = \left|\frac{1}{-w^2\tau^2 + 2jw\zeta\tau}\right| = 1 \qquad\qquad \text{... (2.69)}$$

The frequency, w_1, which satisfied equation *(2.69)*, is

$$w_1 = \frac{1}{\tau}\sqrt{(-2\zeta^2) + \sqrt{1 + 4\zeta^4}} \qquad\qquad \text{... (2.70)}$$

The phase angle of *G(jw)* at this frequency is

$$\angle G(jw) = -Tan^{-1}\frac{-2\zeta w\tau}{-w^2\tau^2} \qquad\qquad \text{... (2.71)}$$

By substituting equation *(2.70)* into equation *(2.71)*

$$\angle G(jw) = -Tan^{-1}\frac{2\zeta}{\sqrt{(-2\zeta^2) + \sqrt{1 + 4\zeta^4}}} \qquad\qquad \text{... (2.72)}$$

The difference between the phase angle of equation *(2.72)* and 180˚ is the phase margin [3] thus

$$P_m = 180 - Tan^{-1}\frac{2\zeta}{1 - \sqrt{(-2\zeta^2) + \sqrt{1 + 4\zeta^4}}} \qquad\qquad \text{... (2.73)}$$

The full derivation of equation *(2.73)* is shown in appendix A-4.

2.14.2 Response Speed From Open-Loop Frequency Response

In this section, the closed-loop bandwidth is used to the desired settling time and peak time with the damping ratio and the closed-loop bandwidth can be estimated from the open-loop frequency response. From the Nichols chart in figure 1.5, described the relationship between the open-loop gain and the closed-loop gain. Then the closed-loop bandwidth, w_{BW} (i.e., the frequency at which the closed-loop magnitude response is –3 dB),equals the frequency at which the open-loop magnitude response is betwwen –6 and –7.5 dB if the

open-loop phase response is between -135º and -225º. After that, find settling time and peak time, by the equations described in section 2.3.2. [5]

2.15 <u>STEADY-STATE ERROR (Characteristics From Frequency Response)</u>

In this section shows how to use Bode diagram to find the values of the static error constants for equivalent unity feedback systems: k_P for a type 0 system, k_v for a type 1 system, and k_a for a type 2 system. The results will be obtained from unnormalized and unscaled Bode log-magnitude plots. [5]

2.15.1 <u>Position Constant (k_p)</u>

This is the same as the value of low-frequency axis. Thus for unnormalized and unscaled Bode log-magnitude plot, the low-frequency magnitude is 20*log (k_p) for a type 0 system. [5]

And the steady-state error is equal to

$$e_{ss} = \frac{1}{1 + k_P} \text{ [3]} \qquad \qquad \text{… (2.74)}$$

2.15.2 <u>Velocity Constant (k_v)</u>

Velocity constant k_v can be found by extending the initial –20dB/decade slop to the frequency axis on an unnormalized and unscaled Bode plot. The intersection with the frequency axis is k_v. [5]

And the steady-state error is equal to

$$e_{ss} = \frac{1}{k_V} \text{ [3]} \qquad \qquad \text{… (2.75)}$$

2.15.3 <u>Acceleration Constant (k_a)</u>

The initial –40/decade slop intersects the frequency axis at $\sqrt{k_a}$. Where K_a is the acceleration constant. And the steady state error is found from equation bellow: [5]

$$e_{ss} = \frac{1}{k_a} \ [3] \qquad\qquad\qquad\qquad\qquad \dots (2.76)$$

2.16 <u>SYSTEMS WITH TIME DELAY</u>

Time delay occurs in control systems when there is a delay between the commanded response and the start of the output response. During the time delay, nothing is occurring at the output. From this the time delay is not the same as the time it takes the controlled variable to changes. [5]

COMPUTER SIMULATION

3.1 <u>SOFTWARE PACKAGE IN Visual Basic$_{6.0}$ FOR COMPUTER SIMULATION</u>

Historically, simulation packages were classified to be of two major types, namely, simulation languages and application oriented simulators. Simulation languages were general in nature, and model development was done by writing code.

In selecting simulation software, one most consider what computer platform the software is available. For almost all softwares are available for Windows-based *PCs*. The amount of *RAM* required to run the software should also be consider, since some products require 64 MB or even 128 MB. One should also considered what operating systems are supported, such as Windows 98 or Windows XP. Standard reports should be provided for the estimated performance measures. For each performance measure (e.g., time in system for a factory), the average observed value, the minimum observed value, and the maximum observed values are usually given. The software should provide a variety of graphics. First it should be possible to make a histogram for a set of observed data. In time plot, one or more key system variables are plotted over the length of experiment. [53]

3.2 INTERFACE FOR FREQUENCY RSPONSE ANALYSIS (IFRA

IFRA is a general system designed to analyze the systems by frequency response method (Bode plots) under windows XP environment using a processor of 850 MHz and RAM 128 MB. This system could be used both in academic and industrial fields, and it consists of software package and also it can be worked with hardware interface for future work.

Software package (CD at the end of this thesis).

A program designed and performed totally by using (VISUAL BASIC$_{6.0}$ builder) and consists of the following features, figures 3.1.

Figure 3.1 *About IFRA*

3.2.1 Wave Form Page

From this page the user can estimate the transient response for any system by using the process simulator or using signal port or signal recorder figure 3.2.
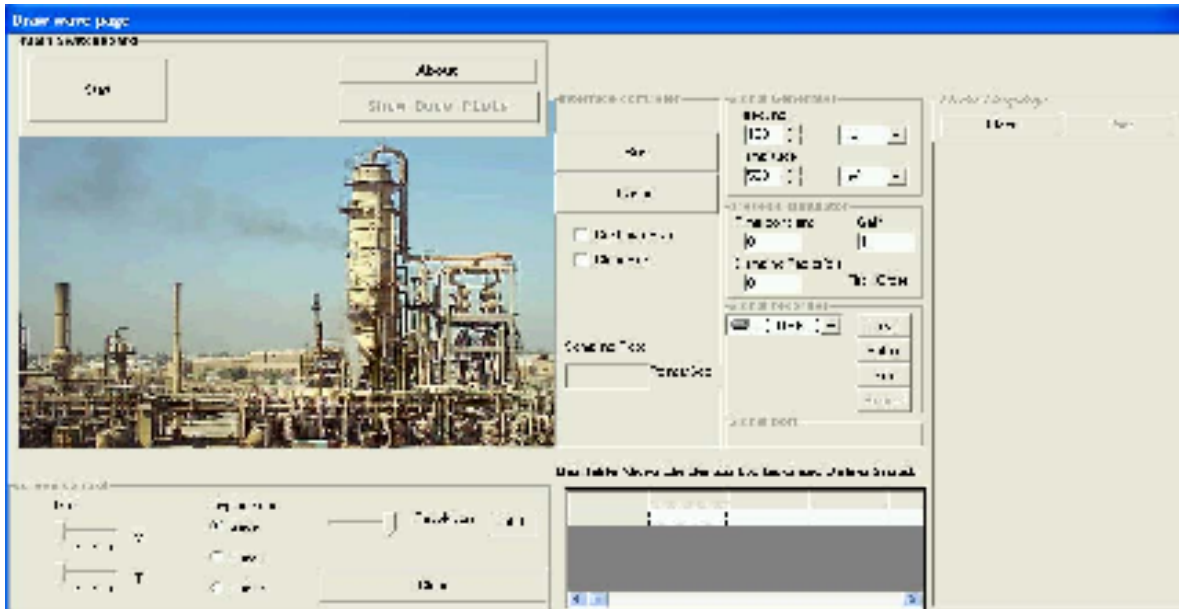
Figure 3.2 *Control panel of IFRA when it starts*

Firstly, click on the start button in order to activate the projects figure 3.3.
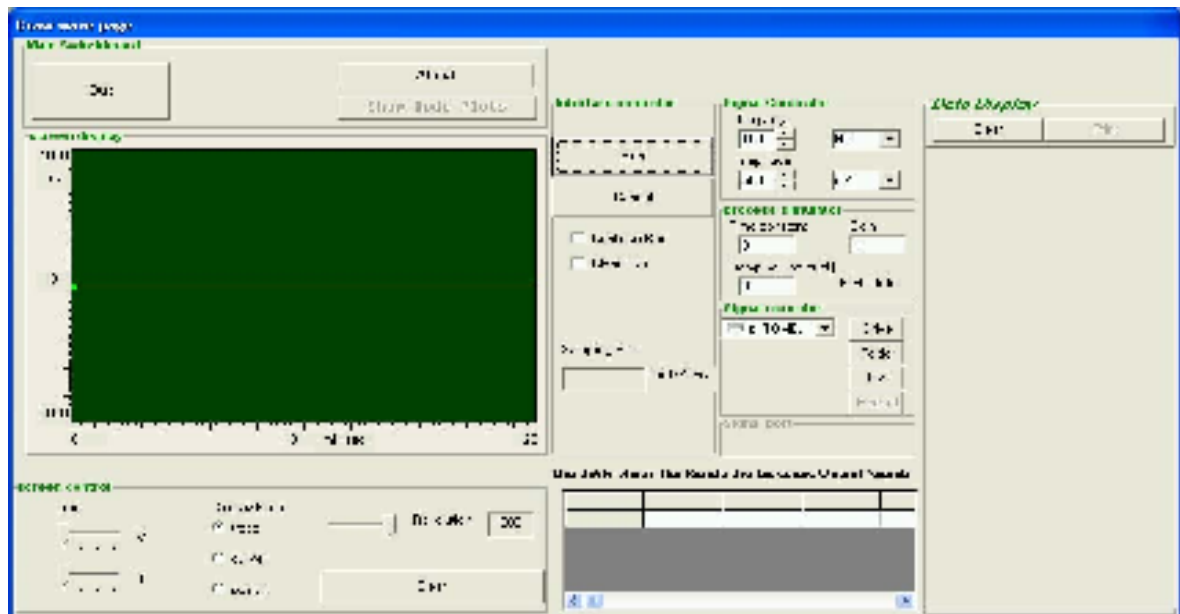
Figure 3.3 *Control panel of IFRA when the projects become activated*

To run the process simulator the user gives the value of time constant, damping factor, and gain for the system and also choosing amplitude with its unit and range of frequencies with its units, as shown in figure 3.4
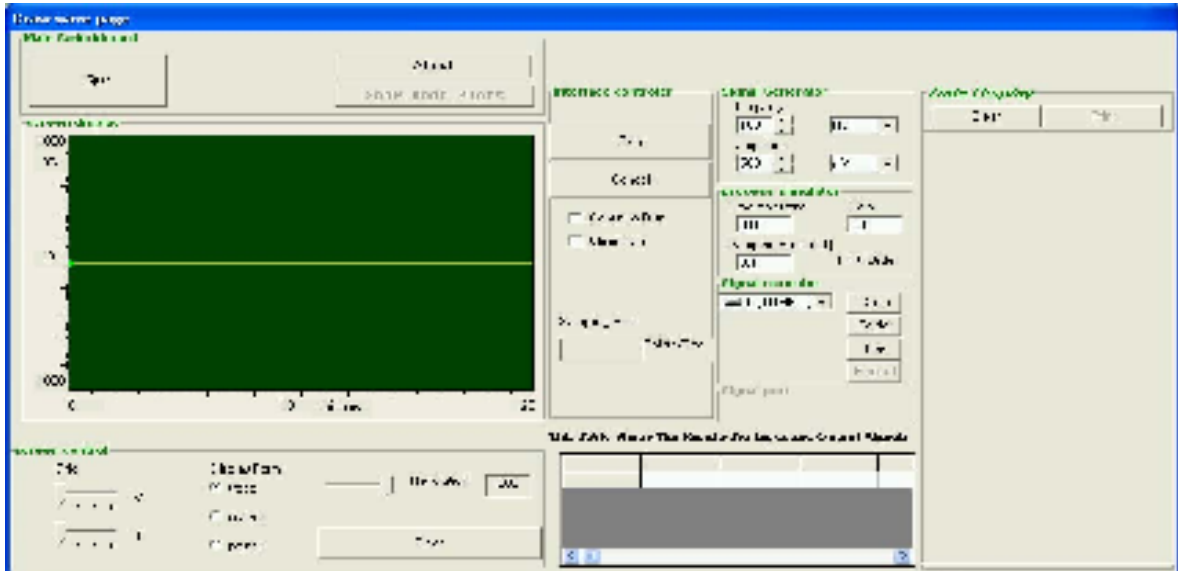
Figure 3.4 *Control panel of IFRA when using the process simulator*

Then the input and output signals for the giving system are analyzed and calculated after running this software, as shown in figure 3.5. We can notice input-output signals with time in the screen display area.
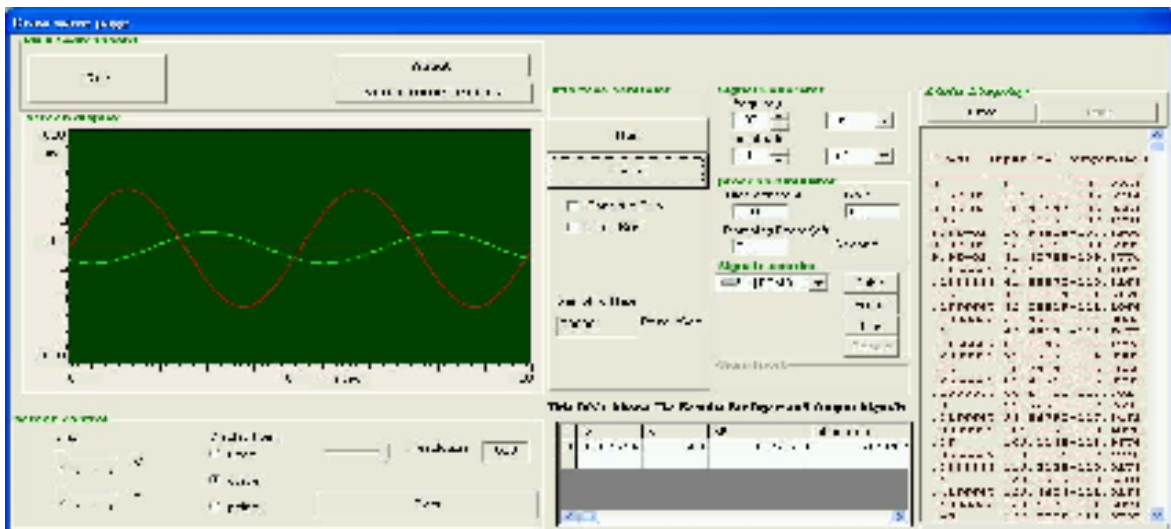
Figure 3.5 *Control panel of IFRA showing the signals interfacing graph (input signal (red curve) and output signal (green curve))*

Also, user can choose clear button to clear screen display after each run or continue to keep running or stop it by clicking cancel button as shown in figure 3.6
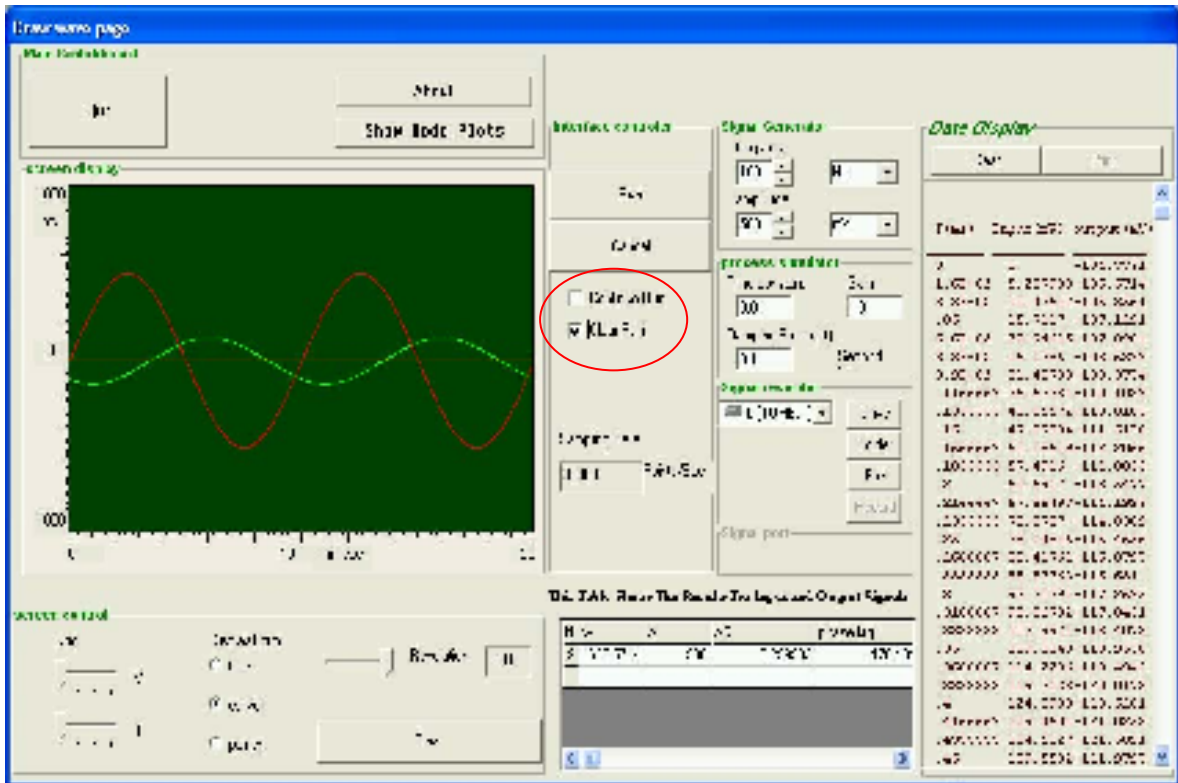
Figure 3.6 *Control panel of IFRA showing clear run button or continuo run button*

Also in this page, there is a table which records the amplitude ratio (*AR*), phase angle, angular frequency (*w*), and the amplitude of the input signal (*A*). There is another table in the data display area to describe the time in milli-second, input and output signals in milli-volt.

Screen display area gives the user ability to apply grid in x-axis and y-axis and modify plots in display form, trace, curve or point and we can control on the resolution of the plot. As shown in figure 3.7.
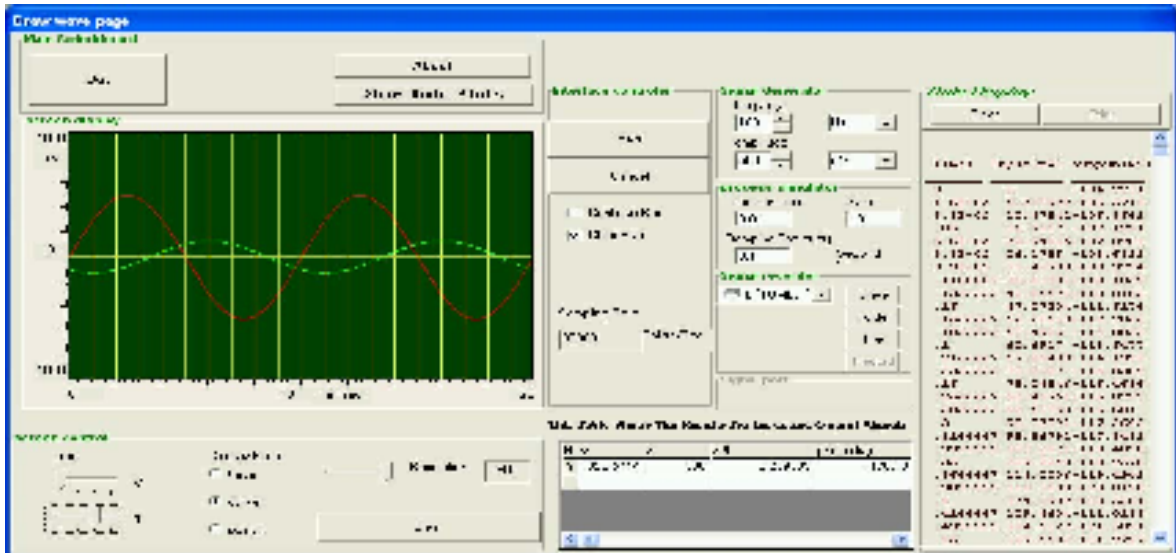
Figure 3.7 *The ability of the screen display area*

In draw wave form page, user can open data by using signal recorder from saved data in any drive, folder, or shred files to analyze the data, figure 3.8
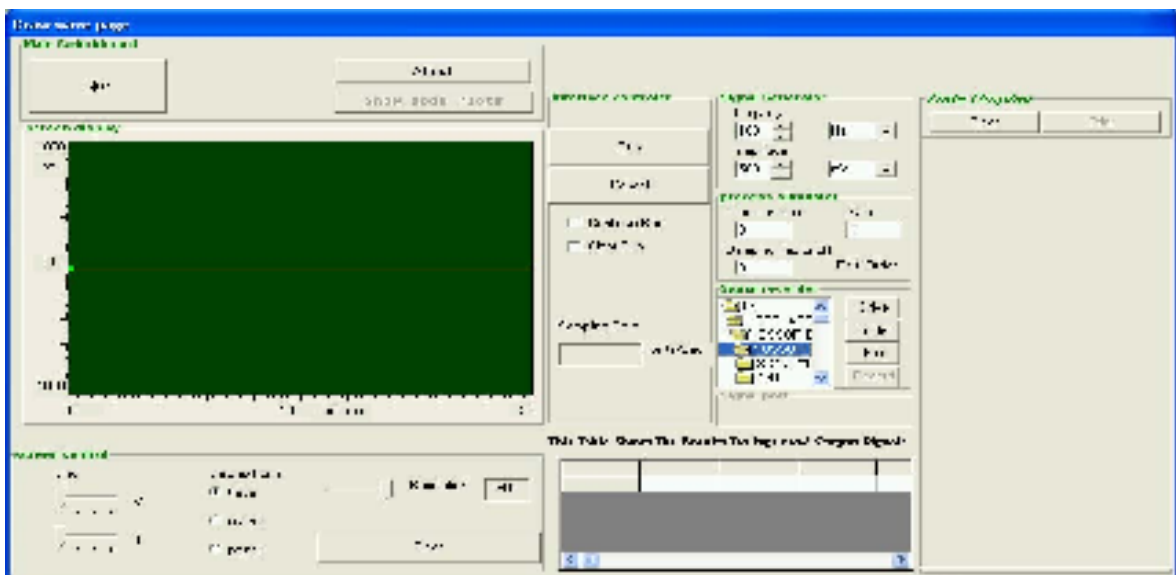
Figure 3.8 *Control panel of IFRA when using signal recorder*

3.2.2 Bode Diagrams Page

From this page the user can analyze the frequency response by using Bode diagrams. Also, user analyzes the system and calculates the stability of the system. As result of taking the data from the wave page and drawing Bode plots to analysis the system and determine its characteristics, such as type of the system, gain, time constant, corner frequency, slop, gain margin, and phase margin, as shown in figure 3.9.
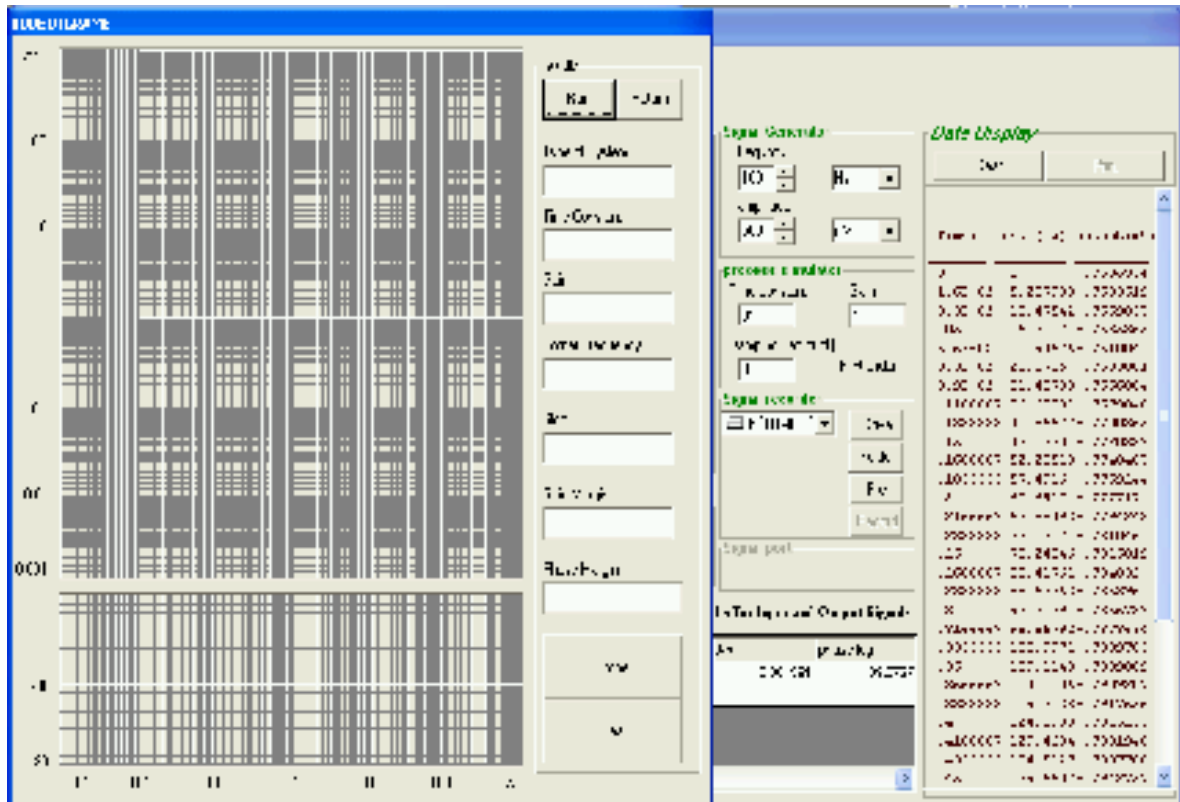
Figure 3.9 *Control panel of IFRA when it runs and going to the Bode diagrams*

Figure 3.10 shows attention window for incomplete entering data in wave form page such as running the program without entering value for the time constant.
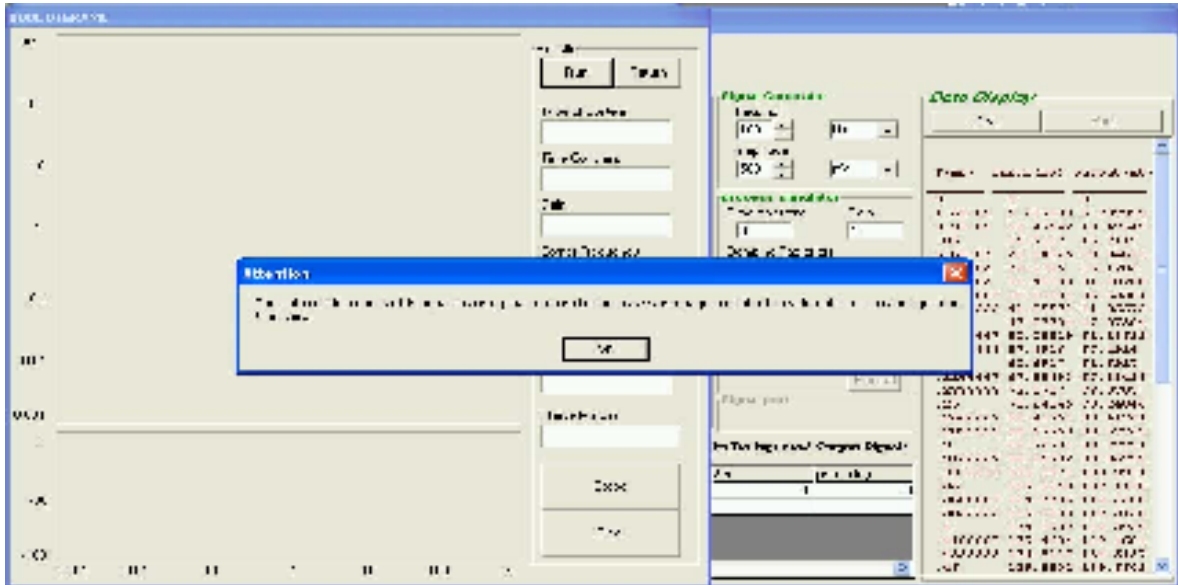
Figure 4.10 *Control panel of IFRA when it runs without giving the parameters of the system and going to the Bode plots page*

Figure 3.11 shows Bode diagrams for drawing system by input data of wave form page.
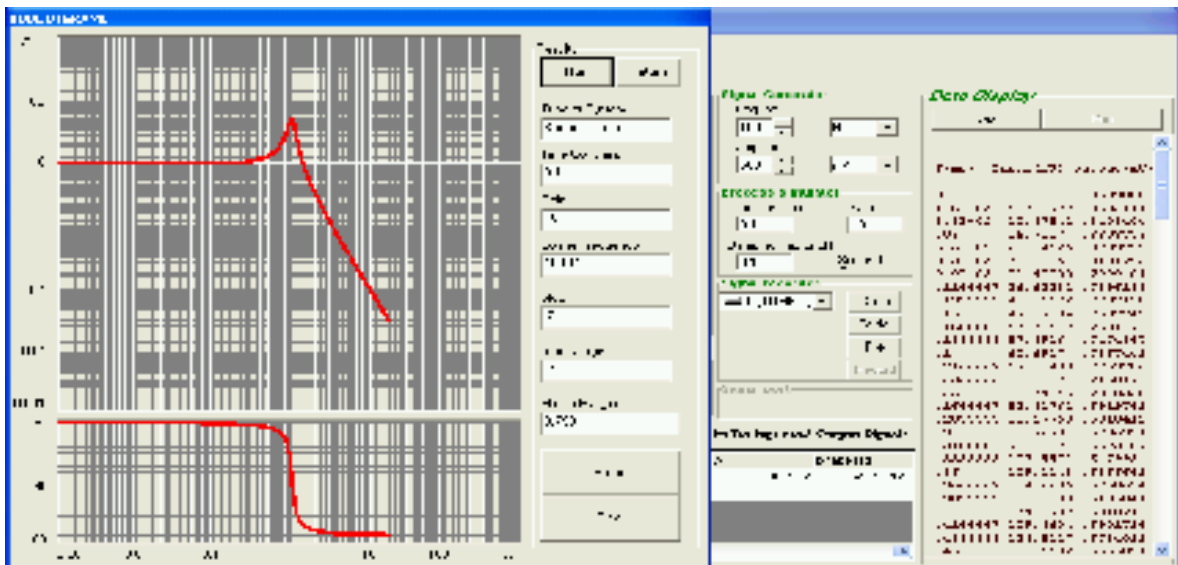
Figure 3.11 *Control panel of IFRA showing the Bode plots and the characteristics of the system*

3.3 <u>MATLAB SOFTWARE FOR COMPUTER SIMULATION</u>

In the very first version of MATLAB, written at the University of New Mexico and Stanford University in the late seventies, it was intended for use in courses in matrix theory, linear algebra, and numerical analysis. [54].

MATLAB has grown into the best platform available for several specialized scientific and technical visualization and simulations. The control system toolbox consists of functions specialized for system engineering in the matrix environment of the MATLAB. It is a collection of files containing algorithms to be used for modeling, analysis and design of continuous systems [55].

It has several toolboxes for simulating specialized problems in different areas in order to build a block diagram for any system we want to analysis and design, such as in figure 3.12

Simulink tool books for Matlab is use to simulate system by position the blocks, resize the blocks, label the blacks, specify block parameter, and interconnect blocks to form complete systems from which simulations can be run.

Simulink has block libraries from which subsystems, sources (i.e. transfer functions), and sink (i.e. scopes) can be copied. Subsystem blocks are a valuable for the represintig linear, nonlinear, and discrete systems. So the responses of distillation column were obtained using similar.
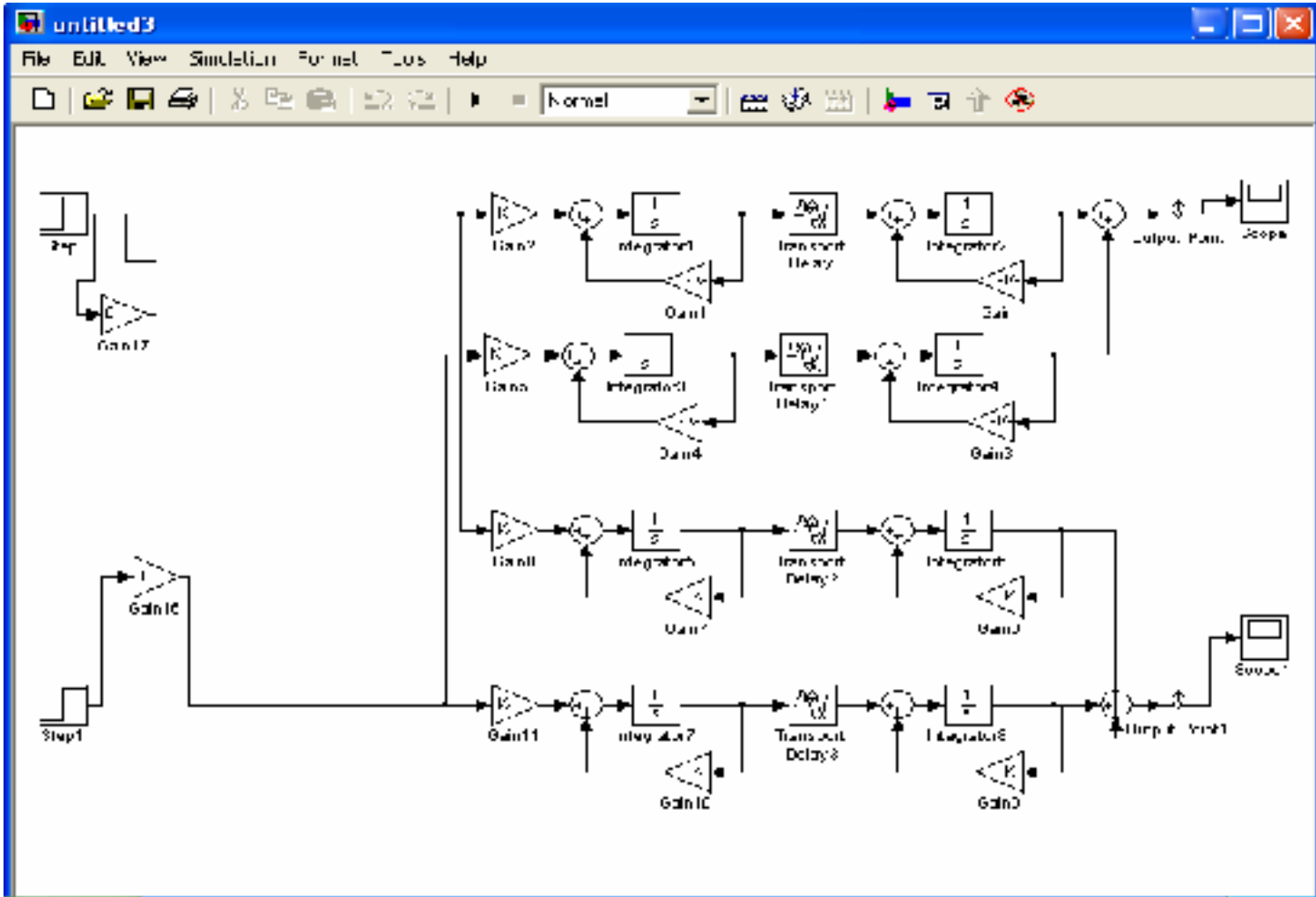
Figure 3.12 *Block diagram for distillation column by Simulink toolbox*

49

RESULTS AND DISCUSSION

4.1 FREQUENCY RESPONSE ANALYSIS

The frequency response of a control system presents a qualitative picture of the transient response, the correlation between frequency and transient responses is indirect, except for the case of the second-order system. In analyzing a closed-loop system, we adjust the frequency response characteristics of the open-loop transfer function by using analysis criteria in order to obtain acceptable transient response characteristics for the system.

If we have indicate the relative stability by frequency response method we must calculate the gain margin and phase margin for the control system when the loop is open

4.2 PHASE MARGIN AND GAIN MARGIN

The phase margin is the amount of additional phase angle at the gain crossover frequency required to bring the system to instability. The gain crossover frequency is the frequency at which the magnitude of the open-loop transfer function is unity. The phase margin is 180º plus the phase angle of the open-loop transfer function at the gain crossover frequency. For a minimum-phase system to be stable, the phase margin must be positive, while the gain margin is the reciprocal of the magnitude at the frequency at which the phase angle is -180º. The phase crossover frequency is the frequency at which the phase angle of the open-loop transfer function equals -180º gives the gain margin.

The gain margin expressed in decibels is positive if it is greater than unity and negative if it is smaller than unity. Thus a positive gain margin (in

decibels) means that the system is stable, and the negative gain margin (in disciples) means that the system is unstable.

4.3 FREQUENCY RESPONSE PLOTTING

In this work, frequency response plotting by Bode plots, which compute the magnitude and phase of the frequency response of linear models. The magnitude is plotted in decibels (dB), and the phase in degrees. Bode plots are used to analyze system properties such as the gain margin, phase margin, bandwidth, and stability.

4.4 DISTILLATION COLUMN ANALYZING

4.4.1 Describing the Block Diagram of the Distillation Column

We take a binary distillation column as a system, which was analyzed by frequency response methods and we find its stability. The column has two manipulated variables and two controlled variables, which are explained in table 2.2.

In this work, using the simulink and MATLAB$_{6.5}$ programs to show the composition response.

(*a*)

X_D X_D

Time (sec)   Time (sec)

(*b.1*)   (*b.2*)

X_B X_B

Time (sec)   Time (sec)
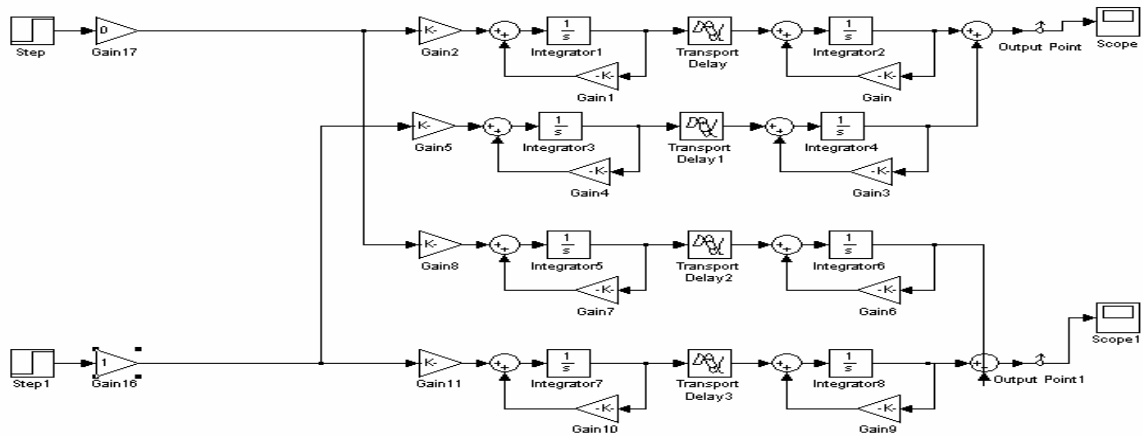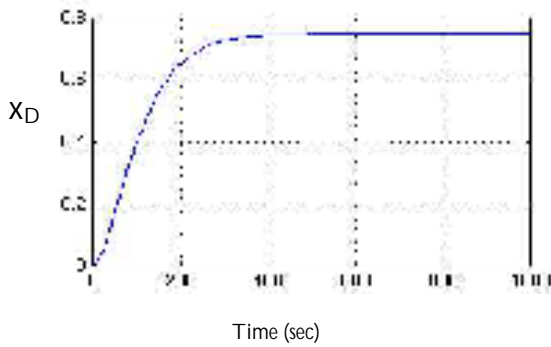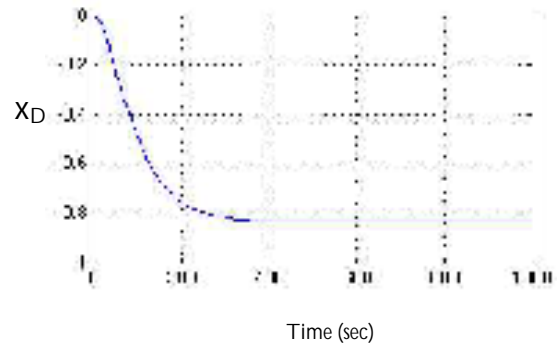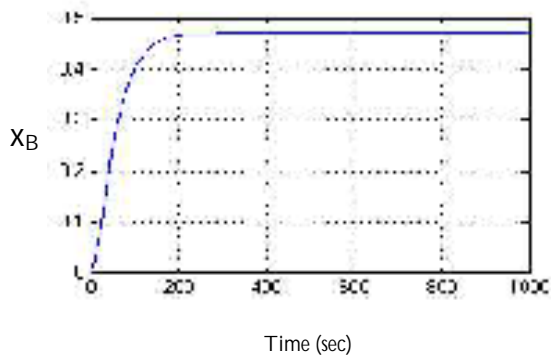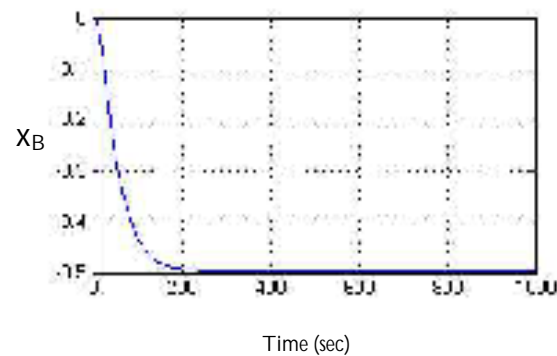
(*b.3*)   (*b.4*)

Figure 4.1   *(a)   Block diagram for open-loop process.*
(b)   The composition response for open-loop process.
(b.1) The change of x_D with the change of L
(b.2) The change of x_D with the change of V .
(b.3) The change of x_B with the change of L.
(b.4) The change of x_B with the change of V .

52
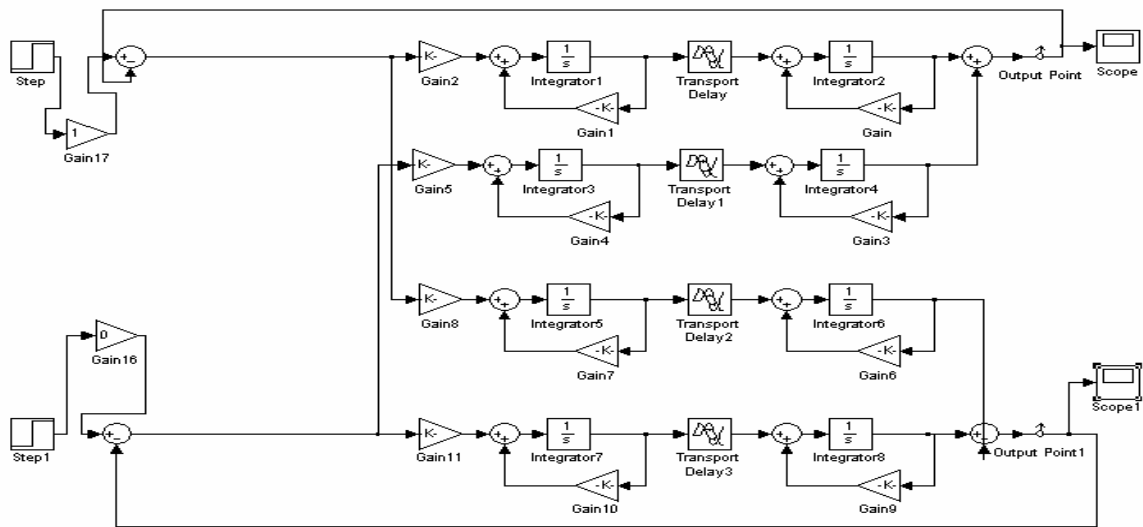
(*a*)
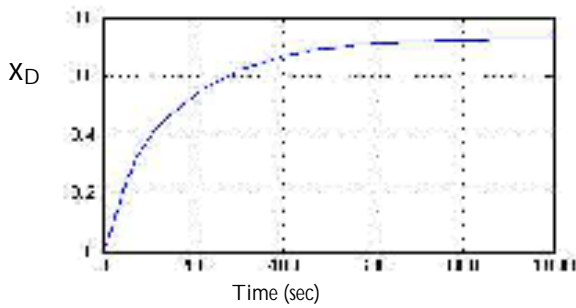
(*b.1*)
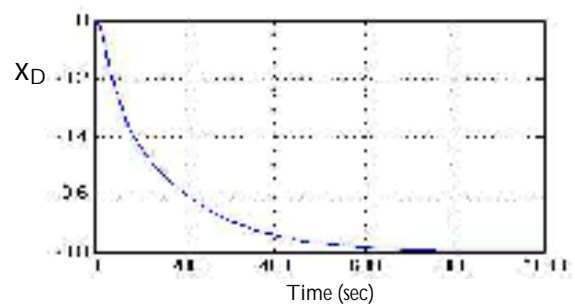
(*b.2*)
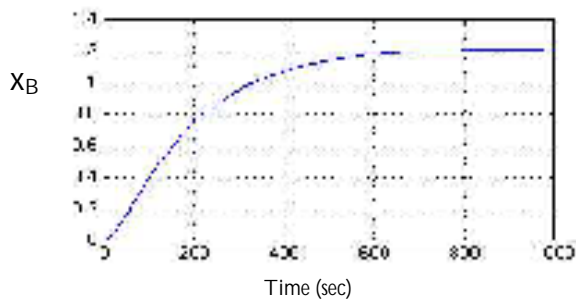
(*b.3*)
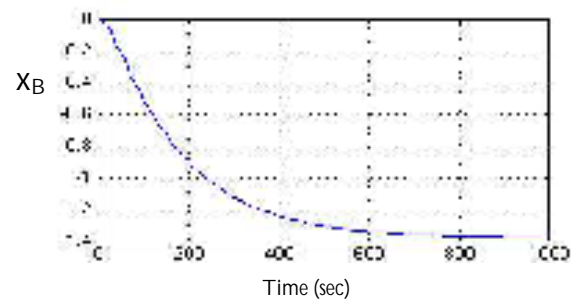
(*b.4*)

Figure 4.2   *(a)*   *Block diagram for closed-loop process.*
                   (b)   *The compositions response for closed-loop process.*
                             (b.1) The change of x_D with the change of L.
                             (b.2) The change of x_D with the change of V.
                             (b.3) The change of x_B with the change of L.
                             (b.4) The change of x_B with the change of V

From figures 4.1 and 4.2 the time response is seen, which shows the stability of the distillation column

4.4.2 Frequency Response Analysis for the Distillation Column

By using Bode plots we can estimate the frequency response of the open-loop system and its stability. As shown in the following figures 4.3, 4.4, 4.5, and 4.6
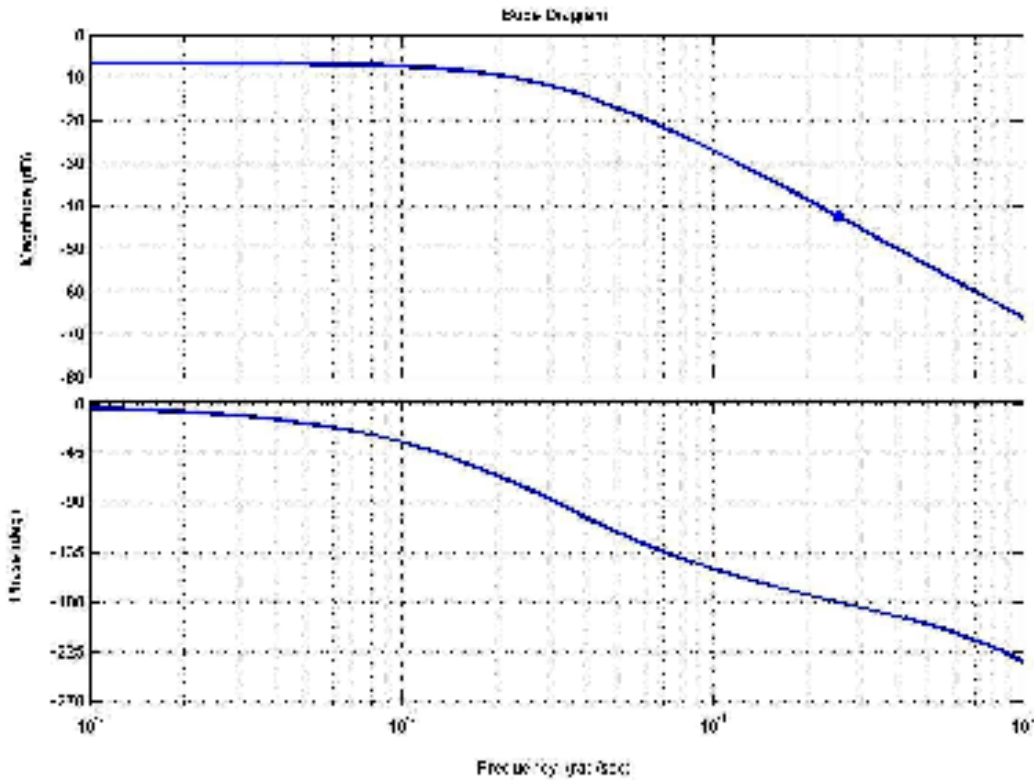
Figure 4.3 *The frequency response of overhead composition to reflux flow.*
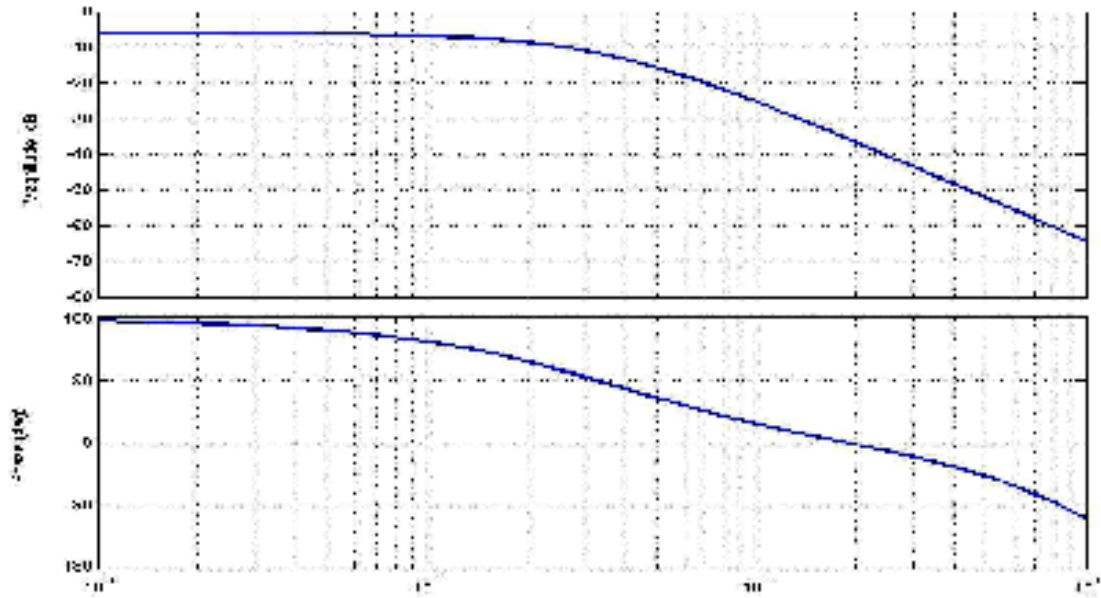
Figure 4.4 *The frequency response of overhead composition to vapor flow rate.*
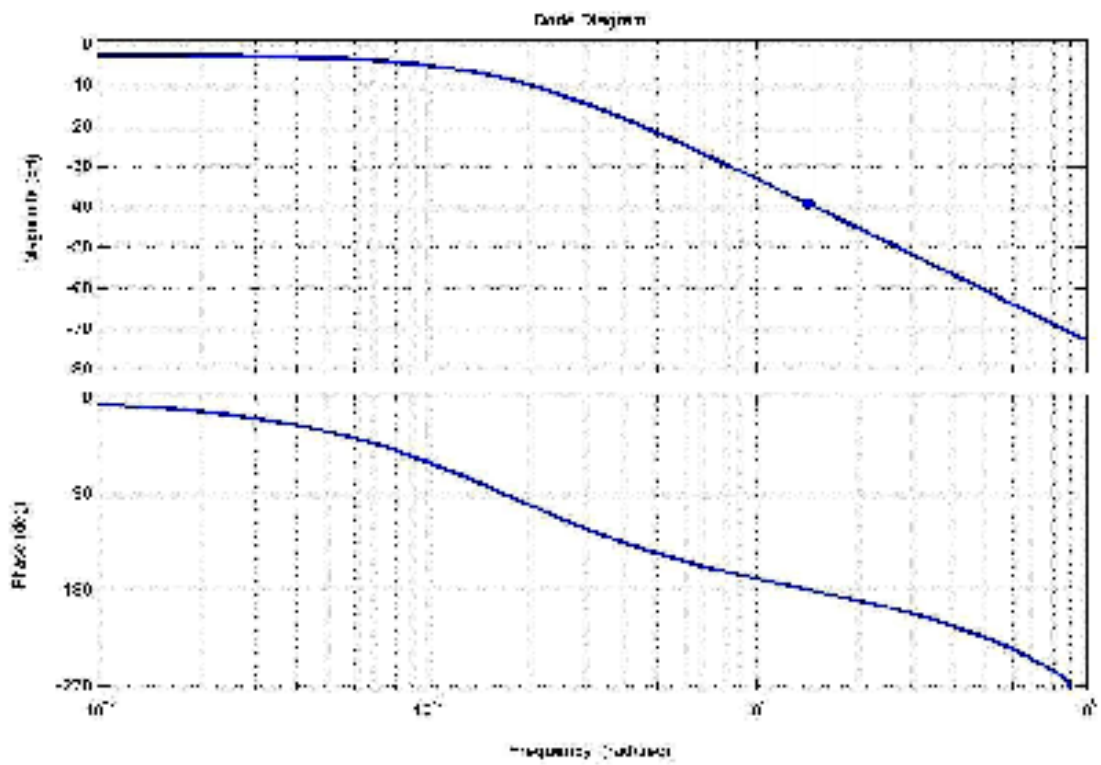
Figure 4.5 *The frequency response of bottom composition to reflux flow.*
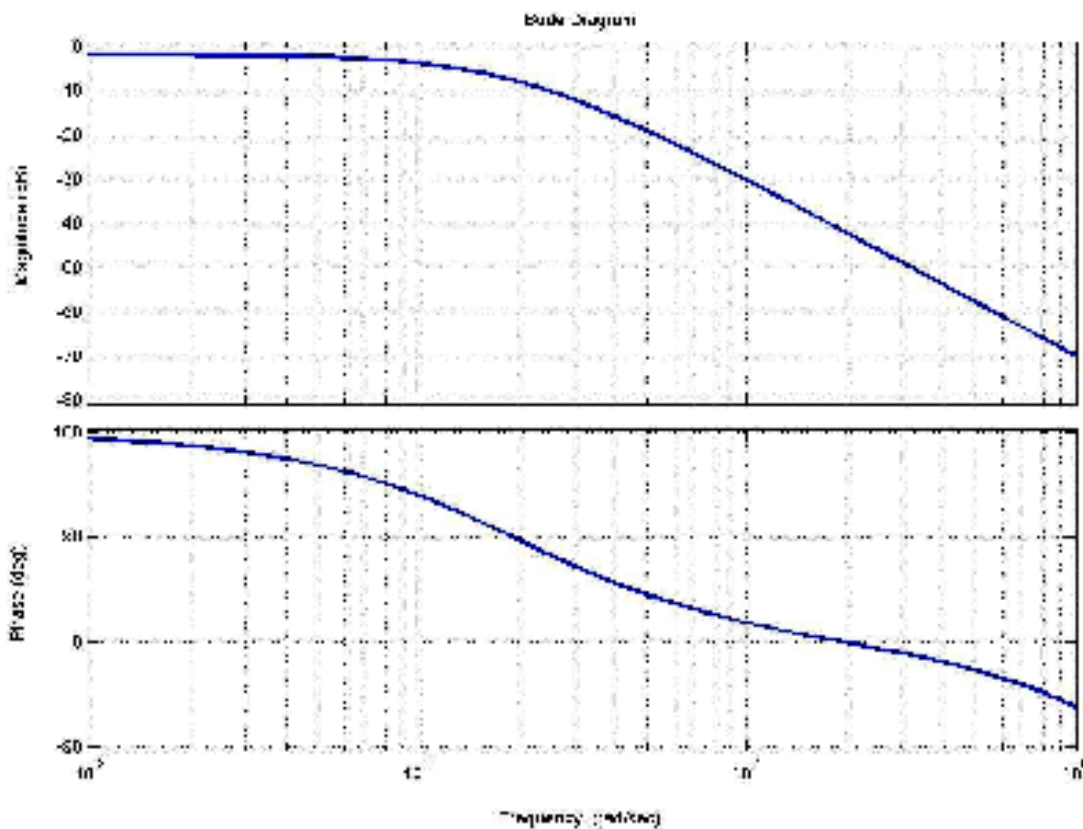
Figure 4.6 *The frequency response of bottom composition to vapor flow rate.*

The results of these figures shown in table 4.1

Table 4.1 *The characteristics of the system*

	Gain margin (dB)	Phase margin (degree)	Phase crossover frequency	Gain crossover frequency
Overhead composition to reflux flow	42.3	Inf.	0.2545	NaN
Overhead composition to vapor flow rate	6.1	Inf.	0	NaN
Bottom composition to reflux flow	39.1	Inf.	0.1433	NaN
Bottom composition to vapor flow rate	1.5	Inf.	0	NaN

Then these results show open-loop system is stable, when all gains margin and phases margin for the system are positive values.

From Wieschedel and McAvoy [40] the gains for both positive and negative step changes in reflux flow and vapor flow rate are given for distillation column, which are explained in table 4-2

Table 4-2 : *Gains of the system*

1% Increase in reflux flow and vapor flow rate

$$\begin{bmatrix} x_D(s) \\ x_B(s) \end{bmatrix} = \begin{bmatrix} 0.233 & -0.789 \\ 1.362 & -0.133 \end{bmatrix} \begin{bmatrix} L(s) \\ V(s) \end{bmatrix}$$

1% Decrease in reflux flow and vapor flow rate

$$\begin{bmatrix} x_D(s) \\ x_B(s) \end{bmatrix} = \begin{bmatrix} 0.719 & -0.200 \\ 0.136 & -1.53 \end{bmatrix} \begin{bmatrix} L(s) \\ V(s) \end{bmatrix}$$

From table 4-2 we can also estimate the frequency response of the system with these conditions and then estimate the effect of increase or decrease (in reflux flow and vapor flow rate) on the stability of the system.
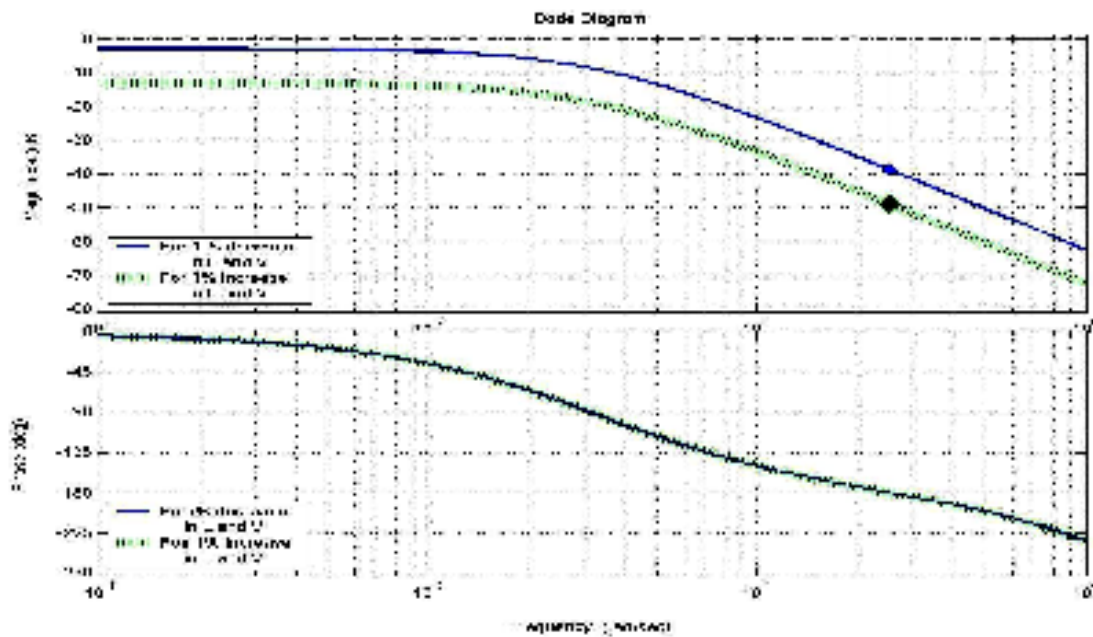
Figure 4.7 *The frequency response of overhead composition to reflux flow (for 1% decrease and increase in L and V).*
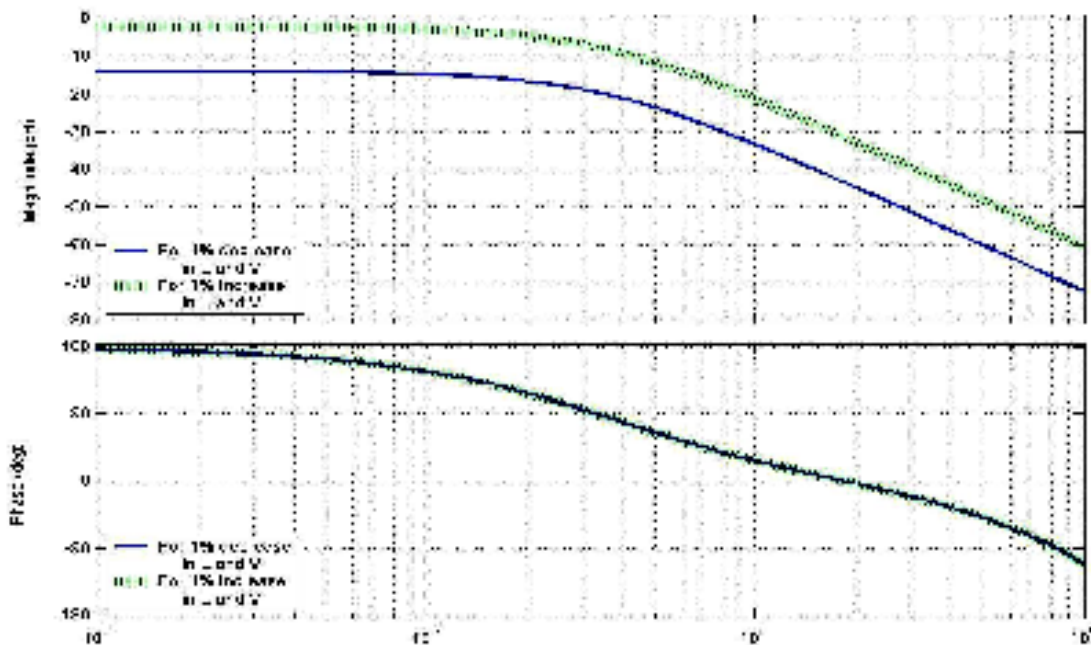
Figure 4.8 *The frequency response of overhead composition to vapor flow rate (for 1% decrease and increase in L and V)*
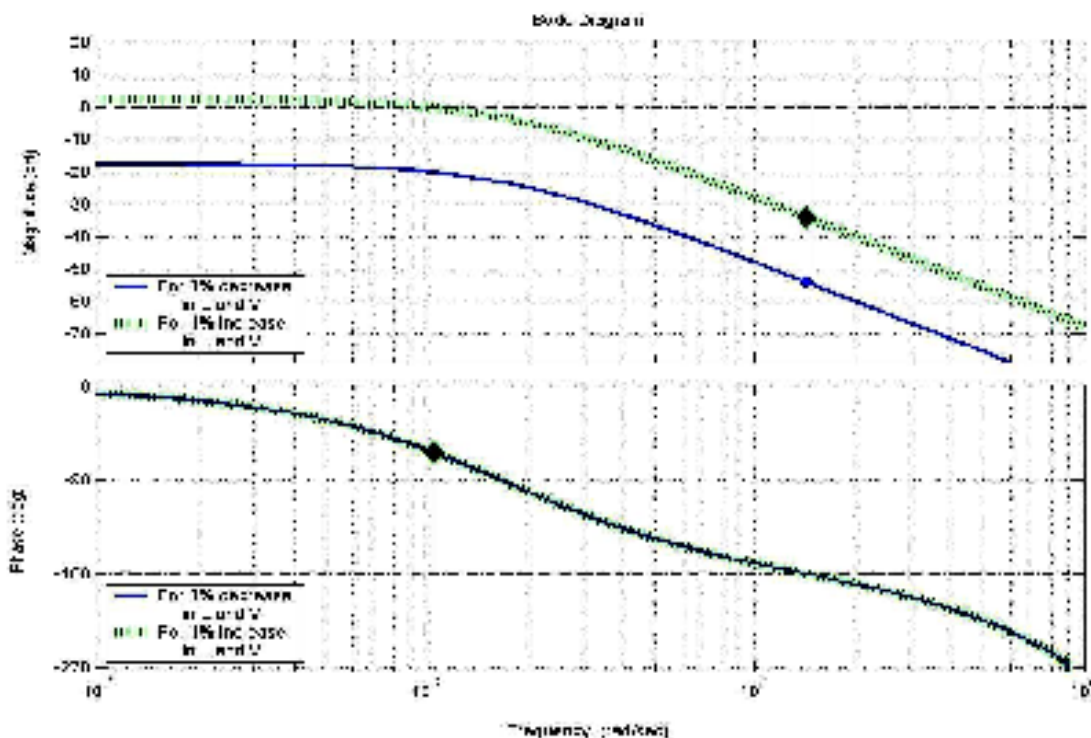
Figure 4.9 *The frequency response of bottom composition to reflux flow (for 1% decrease and increase in L and V).*
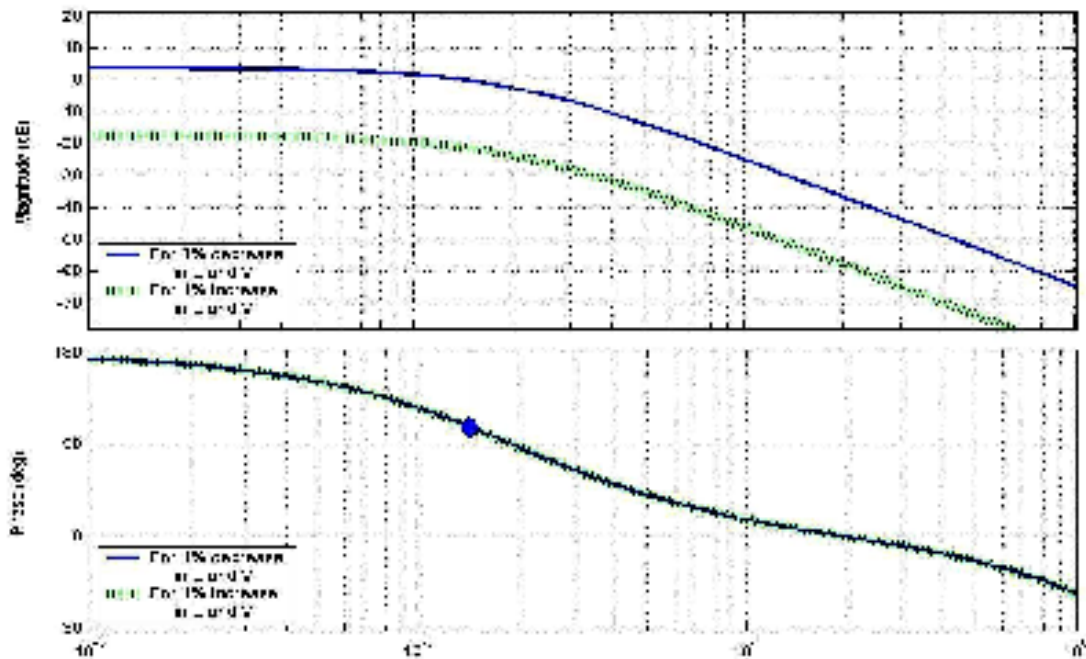
Figure 4.10 *The frequency response of bottom composition to vapor flow rate (for 1% decrease and increase in L and V).*

From figures 4.7, 4.8, 4.9, and 4.10 we note that, when 1% increase in manipulated variables the stability of the response for interaction parts between the two loops (overhead composition to vapor flow rate and bottom composition to reflux flow) is decreased while the stability of the other parts (overhead composition to reflux flow and bottom composition to vapor flow rate) are increased. And with 1% decrease in manipulated variables the stability of the response for interaction parts between the two loops (overhead composition to vapor flow rate and bottom composition to reflux flow) is increased but the stability of the other parts (overhead composition to reflux flow and bottom composition to vapor flow rate) is decreased. These results are the results of the presence of the coupling between loops for the system.

Table 4-3 *The characteristics of the system for 1% increase in reflux flow and vapor flow rate*

	Gain margin (dB)	Phase margin (degree)	Phase crossover frequency	Gain crossover frequency
Overhead composition to reflux flow	48.9	Inf.	0.2550	NaN
Overhead composition to vapor flow rate	2.1	Inf.	0	NaN
Bottom composition to reflux flow	33.9	117	0.1430	
Bottom composition to vapor flow rate	17.5	Inf.	0	NaN

All values of gain margin and phase margin have a positive value so that the overall system is stable.

Table 4-4 *The characteristics of the system for 1% decrease in reflux flow and vapor flow rate*

	Gain Margin (dB)	Phase Margin (degree)	Phase crossover frequency	Gain crossover frequency
Overhead composition to reflux flow	38.7	Inf.	0.2550	NaN
Overhead composition to vapor flow rate	13.9	Inf.	0	NaN
Bottom composition to reflux flow	53.9	Inf.	0.1430	NaN
Bottom composition to vapor flow rate	-3.7	Inf.	0	NaN

In table 4-4 we notice that the gain margin of bottom composition to vapor flow rate have a negative value then the overall system is unstable.

4.5 DISTILLATION COLUMN WITH CLOSED-LOOP FEEDBACK AND CONTROLLERS

In this section we must calculate:

1. The interaction among the loops of a *MIMO* process.

2. The relative gain array.

3. The analysis systems with non-interacting loops.

4.5.1 Interaction of Control Loops

The input-output relationships are given by

$$x_D(s) = G_{11}(s)\, L + G_{12}(s)\, V \qquad \qquad \dots (4.1)$$

$$x_B(s) = G_{21}(s)\, L + G_{22}(s)\, V \qquad \qquad \dots (4.2)$$

$G_{11}(s)$, $G_{12}(s)$, $G_{21}(s)$, and $G_{22}(s)$ are the four-transfer function relating the two outputs to the two inputs. Equation *(4.1)* and *(4.2)* indicate that a change in *L* and *V* will have effect on both outputs.

If G_{C1} and G_{C2} are the transfer functions of the two controllers in the system, the values of the manipulations are given by

$$L(s) = G_{C1}(x_{D,sp}(s) - x_D(s)) \qquad \qquad \dots (4.3)$$

$$V(s) = G_{C2}(x_{B,sp}(s) - x_B(s)) \qquad \qquad \dots (4.4)$$
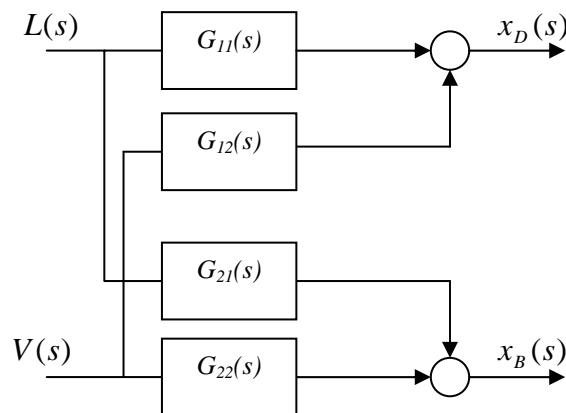
Figure 4.11 *Block diagram of process with two controlled variables and manipulated variables.*

The nature of interaction between two loops and how it arises can be explained by a study of the effects of input changes on the outputs when

1. One loop closed.

2. Both loops closed.

4.5.1.Case I *One loop closed*

Closed loop1 and open loop2 are shown in figure 4.12.a, by assume $V=$ constant [i.e, $V(s) = 0$], and make a change in the setpoint $x_{D,sp}$. Substituting equation *(4.3)* into equations *(4.1)* and *(4.2)*.

$$x_D(s) = \frac{G_{11} G_{C1}}{1 + G_{11} G_{C1}} x_{D,sp}(s) \qquad \qquad \dots (4.5)$$

$$x_B(s) = \frac{G_{21} G_{C1}}{1 + G_{11} G_{C1}} x_{D,sp}(s) \qquad \qquad \dots (4.6)$$

It is clear that any change in the setpoint $x_{D,sp}$ will affect both the behavior of the controlled outputs x_D, and the uncontrolled output x_B. Similar conclusions are drawn if loop1 is open and loop2 is closed.
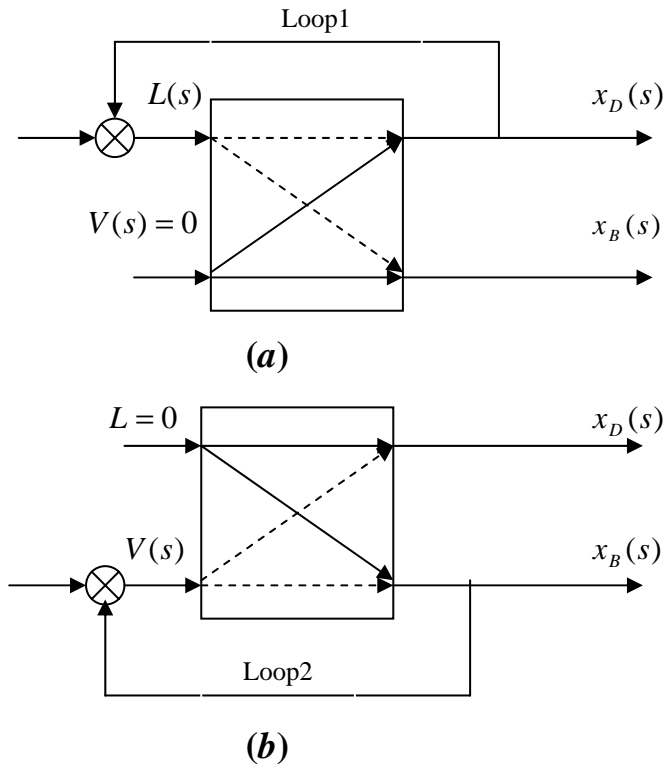
Figure 4.12   *(a) Closed Loop1.*
                  (b) Closed Loop2.

The stability of the system can be determined by frequency response analysis as follows:

4.5.1.Case I.a *Closed loop1 and open loop2 (without controller)*

The characteristic equation of this system is $1+G_{11}=0$ from equations *(4.5)* and *(4.6)*.
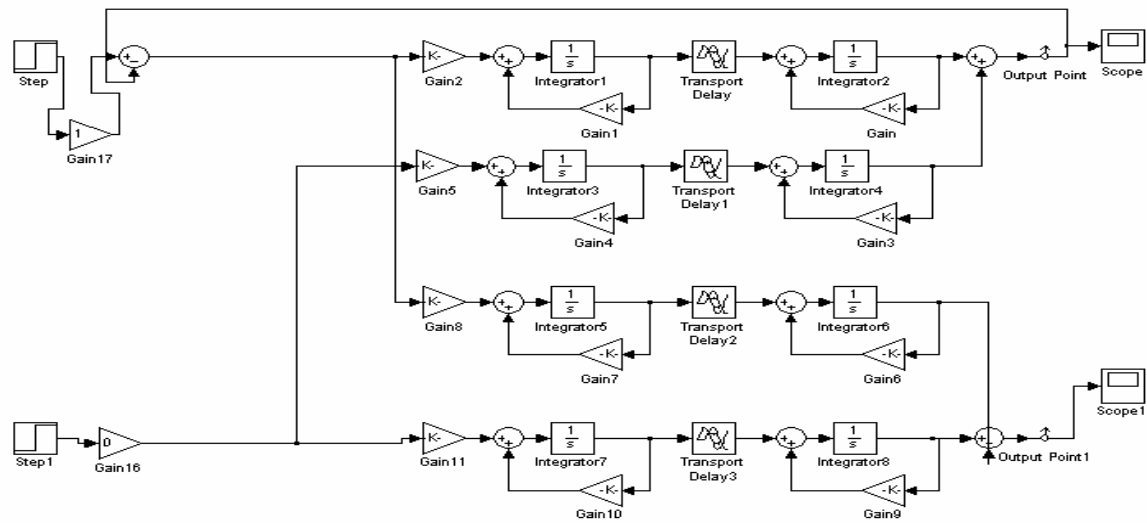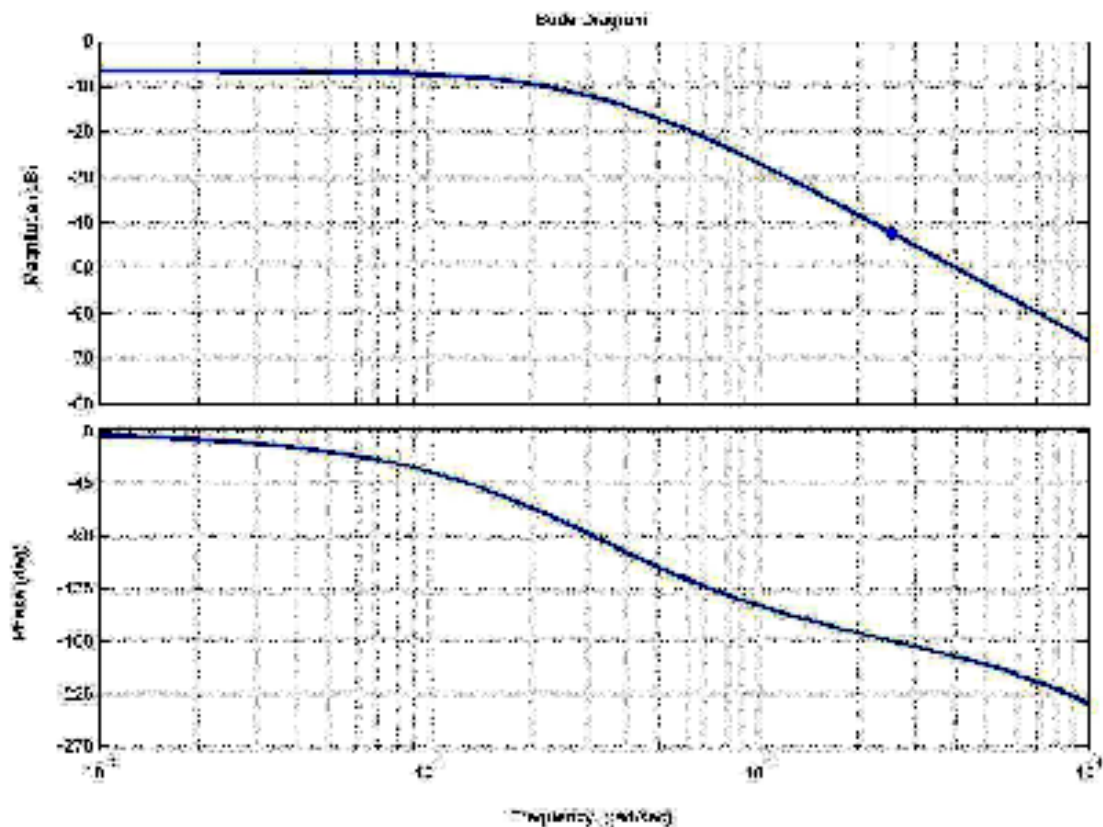

(*a*)
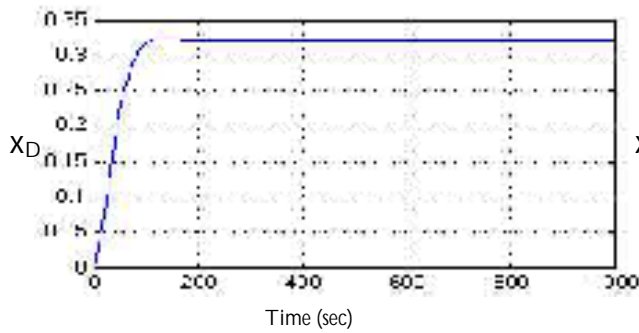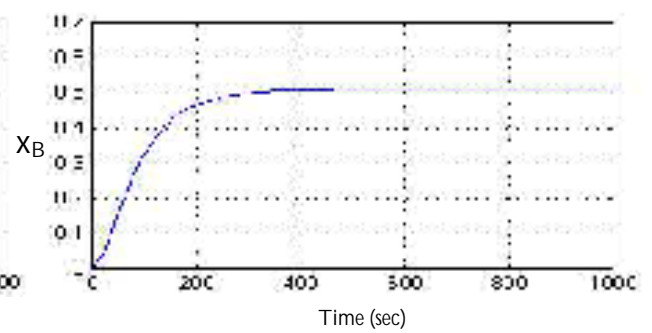
(*b.1*)   **(*b.2*)**

Figure 4.13   *(a)*   **Block diagram for closed-loop1**
                 (b)   **The composition response for closed-loop1 process**
                        (b.1) The change of x_D with the change of L.
                        (b.2) The change of x_B with the change of L.

Figure 4.14 *The frequency response of the open-loop system if the system has closed-loop1.*

From figure 4.14 gain margin is equal to 42.4 dB which is positive value at angular frequency equal to 0.255 rad/s and phase margin is equal to infinity value because the magnitude curve never reaches to 0 dB at any angular frequency value, which is positive value, then from these results the system is stable

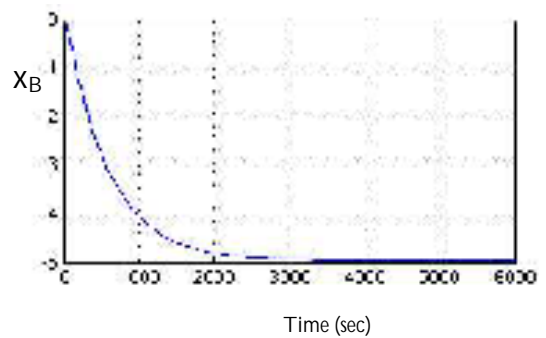**4.5.1.Case I.b** *Closed loop2 and open loop1 (without controller)*

In order to derive the characteristics equation we must follow the same procedure to derive equations *(4.5)* and *(4.6)* then the characteristics equation of this system is *1+G$_{22}$=0*

(a)

Time (sec)

(b.1)

Time (sec)
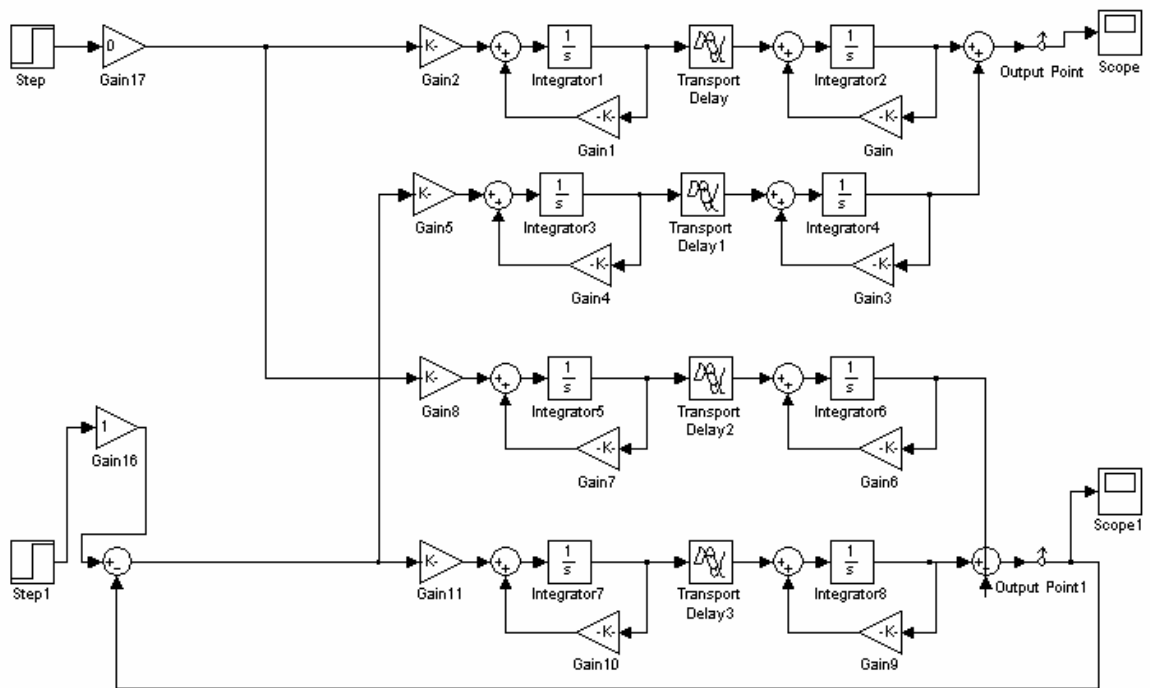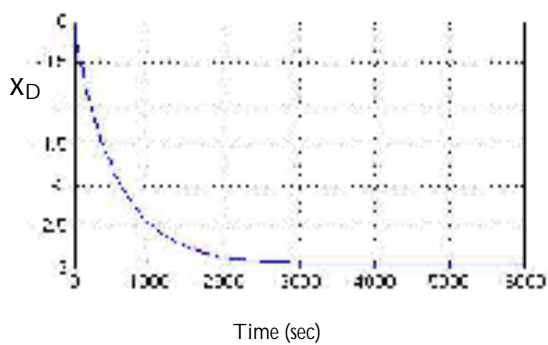
(b.2)

Figure 4.15 *(a)* **Block diagram for closed-loop2**
(b) **The composition response for closed-loop2 process**
(b.1) **The change of x_D with the change of V .**
(b.2) **The change of x_B with the change of V .**
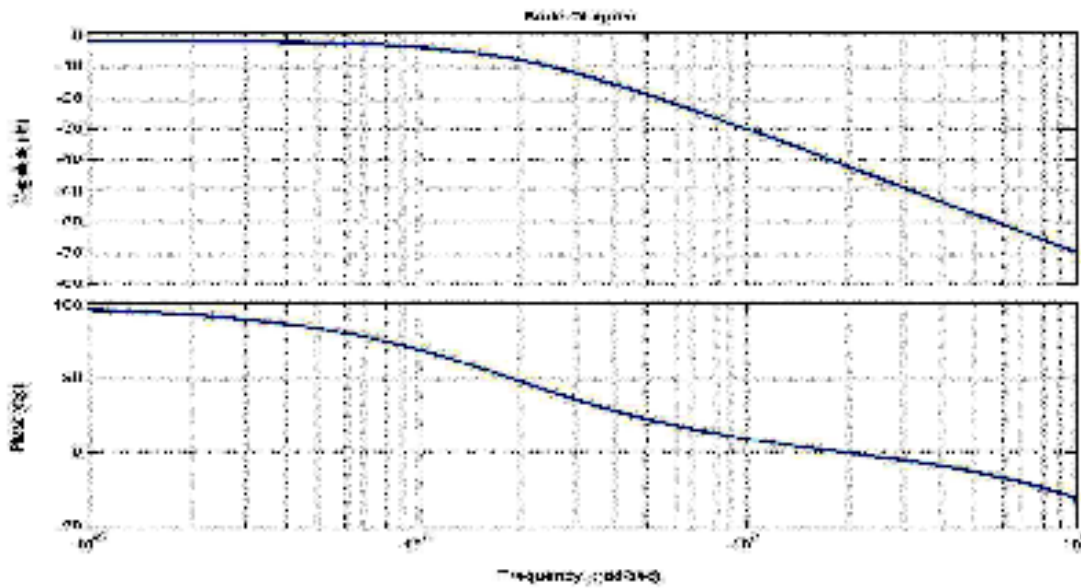
Figure 4.16 *The frequency response of the open-loop system if the system has closed-loop2.*

From figure 4.16 gain margin is equal to 1.6 dB which is positive value at angular frequency equal to 0 rad/s when the phase curve started from 180 and phase margin is equal to infinity value because of the magnitude curve never reaches to 0 dB at any angular frequency curve, which is positive value, Then from these results the system is stable

4.5.1.Case I.c *Closed loop1 with feedback controllers G_{CI} and open loop2*

Feedback controllers *P*, *PI* and *PID* are used in order to find its effect on the system. The controller parameters (K_C, $_I$, $_D$) are obtained by using computer simulation program for the two methods which are Zeigler-Nichols method and Cohn-Coon method, the results of these parameters are shown in table 4-5

66

Table 4-5 *Computed parameters for G_{C1} depending on open-loop frequency response*

Method	P-Controller	PI-Controller		PID-Controller		
	K_C	K_C	$_I(s)$	K_C	$_I(s)$	$_D(s)$
Ziegler-Nichols	65.888	59.300	20.574	79.067	12.344	3.086
Cohen-Coon	65.889	58.839	3.118	87.438	2.427	0.361

Ziegler–Nichols method and Cohen-Coon method are discussed in appendix B.1. Comparing the Ziegler–Nichols (*ZN*) to the Cohen-Coon (*CC*) setting we observe that:-

1- The proportional gains are little larger for the *CC* settings.

2- The reset and rate time constant are higher for the *ZN*.

The characteristics equation of this system is $1+G_{C1}G_{11}=0$ from equations *(4.5)* and *(4.6)*
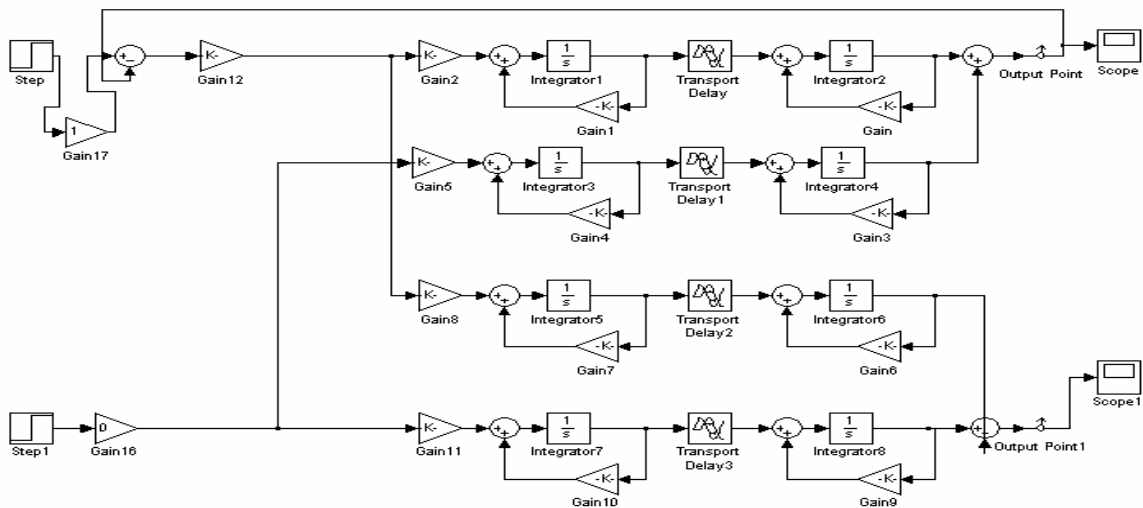
Figure 4.17 *Block diagram for closed-loop1 with P-Controller*
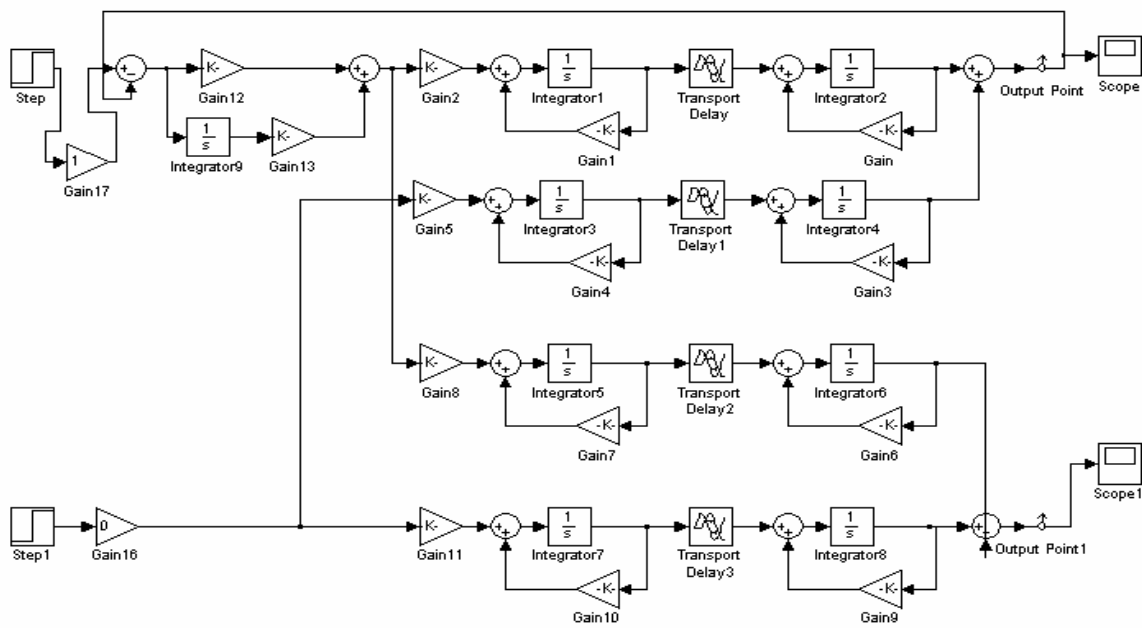
Figure 4.18 *Block diagram for closed-loop1 with PI-Controller*
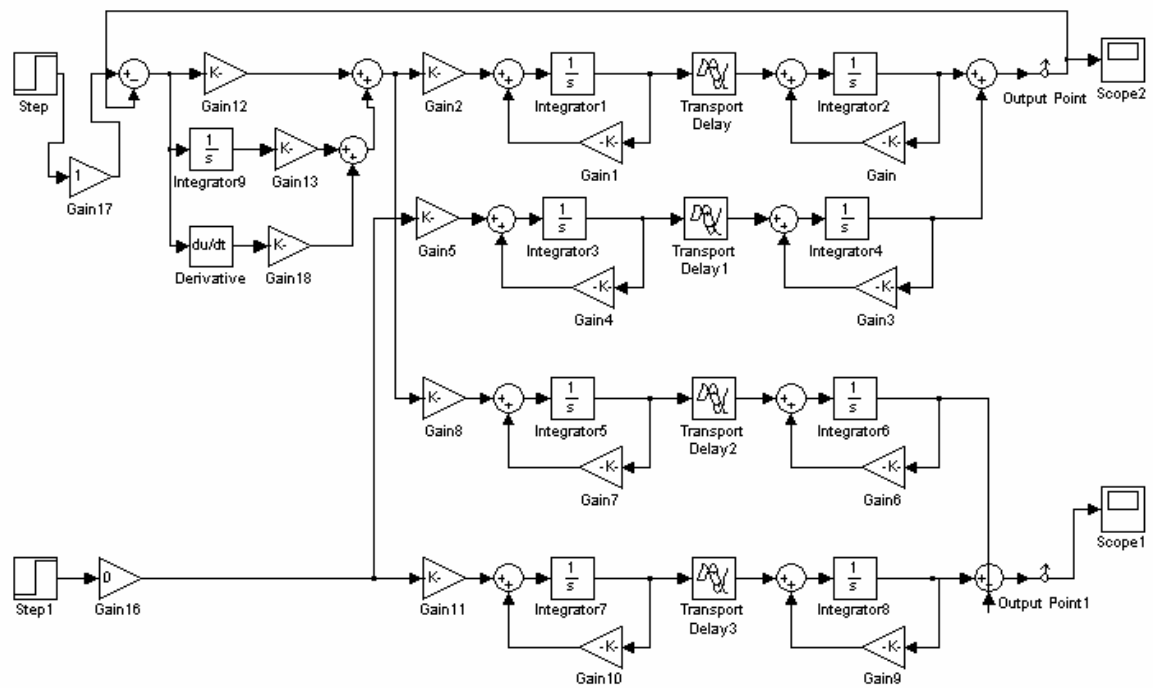
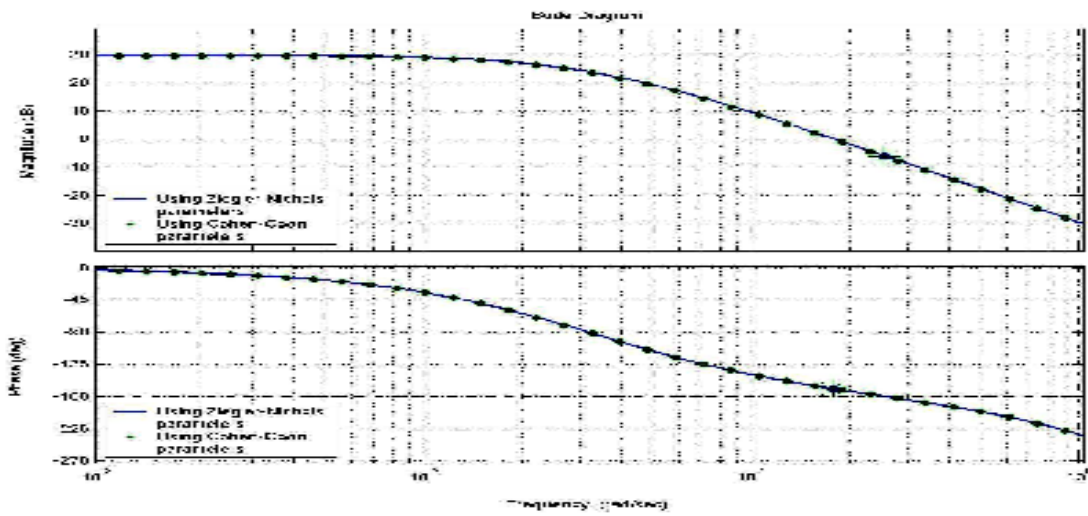**Figure 4.19** *Block diagram for closed-loop1 with PID-Controller*

Figure 4.20 *Tthe frequency response of the open-loop1 system with P-controller*
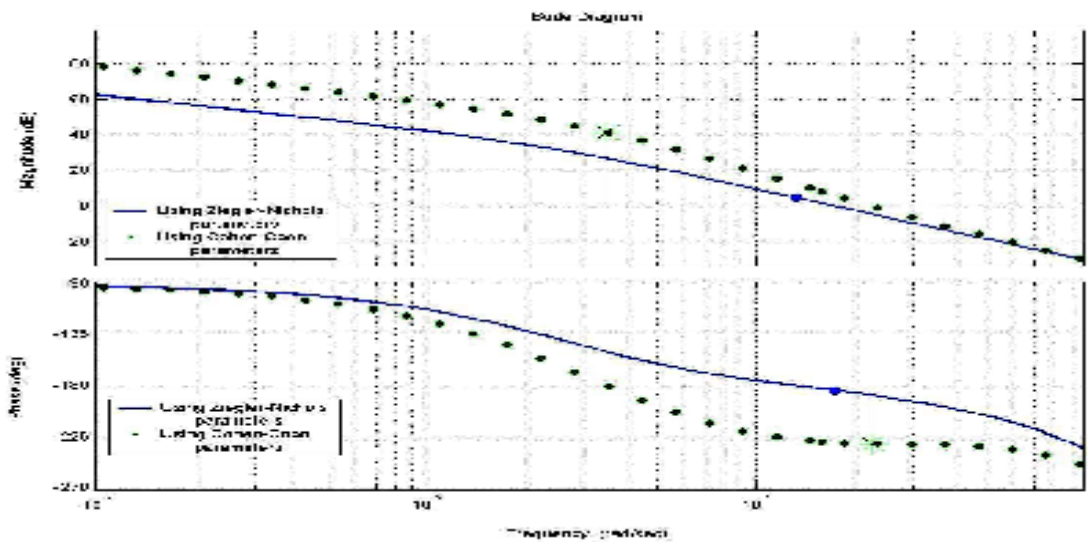

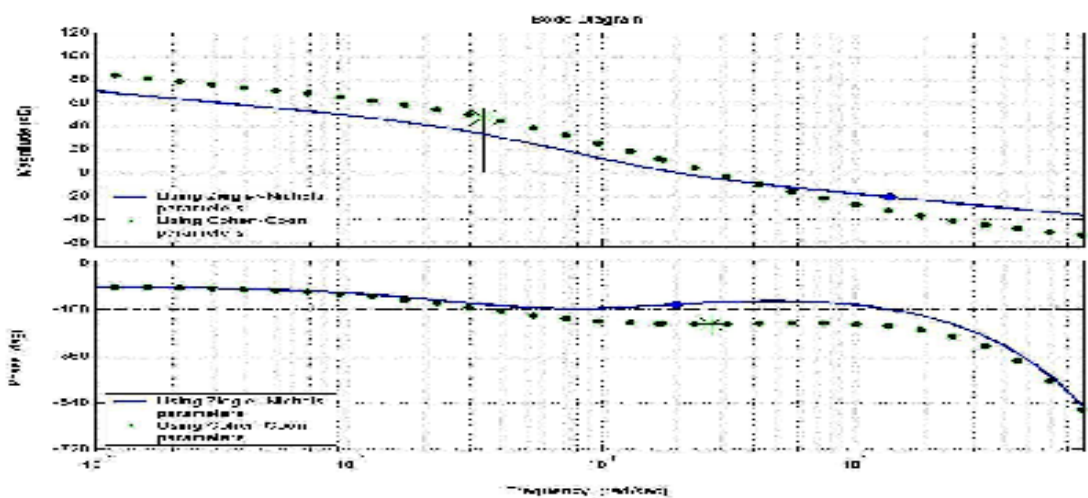**Figure 4.21** *The frequency response of the open-loop1 system with PI-controller*

Figure 4.22 *The frequency response of the open-loop1 system with PID-controller*

From figures 4.17 to 4.22 and also from table 4-6 we note that if using the *ZN* setting for *P*-controller the system is stable, for *PI*-controller the response of the system becomes faster but is unstable, and for *PID*-controller the system is more stable and its response becomes faster. But in using the *CC* setting for *P*-controller the system is stable but for *PI* and *PID*-controller the response of the system becomes unstable.

Table 4-6 *Gain margin and phase margin if loop1 is closed with feedback controller*

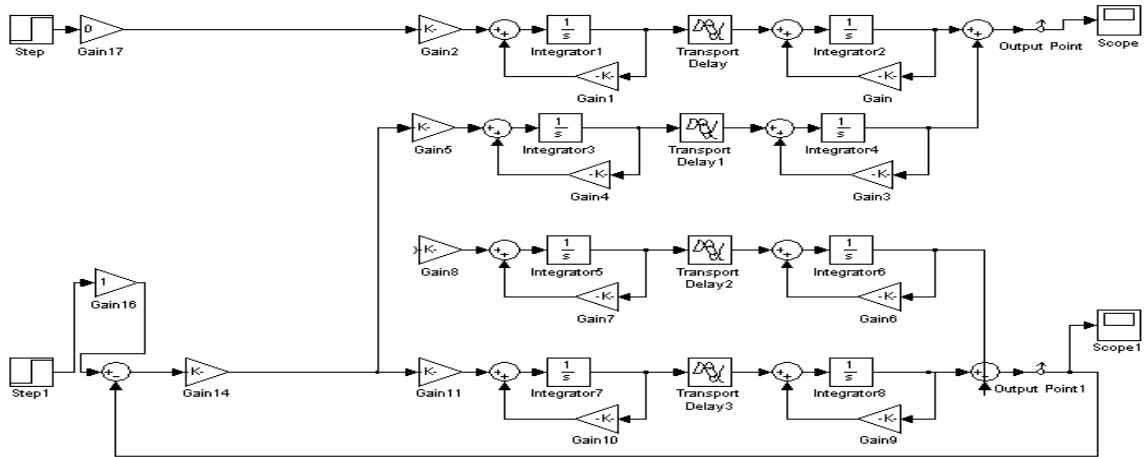| Method	P-Controller		PI-Controller		PID-Controller	
	Gain margin	*Phase margin*	*Gain margin*	*Phase margin*	*Gain margin*	*Phase margin*
Ziegler-Nichols	6.02	10.5	-4.7	-4.2	21.0	18.8
Cohen-Coon	6.02	10.8	-41.4	-51.5	-47.5	-56.7

4.5.1.Case I.d *Closed loop2 with feedback controller G_{C2} and open loop1*

Zeigler-Nichols method and Cohen-Coon methods are used to find the controller parameters for G_{C2}. The result of the controller parameters are given in table 4-7

Table 4-7 *Computed parameters for G_{C2} depending on open-loop frequency response*

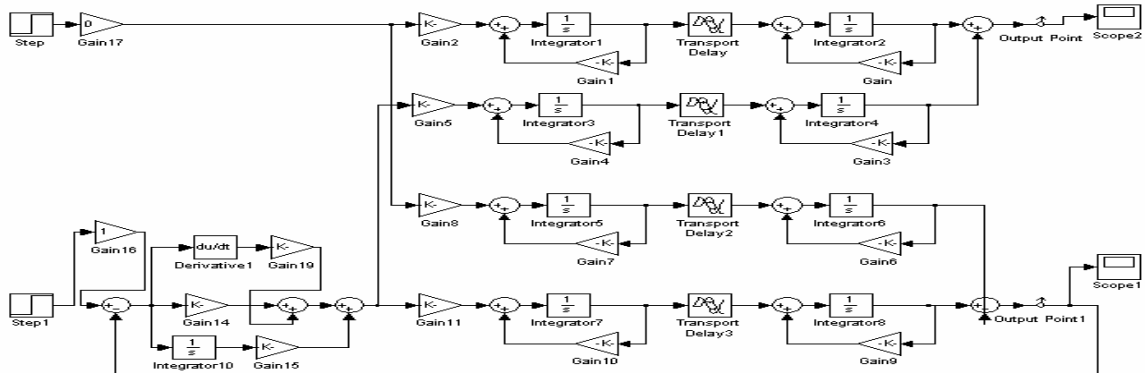| Method	P-Controller	PI-Controller		PID-Controller		
	K_C	K_C	$_I(s)$	K_C	$_I(s)$	$_D(s)$
Ziegler-Nichols	-61.097	-54.988	26.351	-73.317	15.811	3.953
Cohen-Coon	-61.098	-54.727	3.199	-81.229	2.441	0.362

The characteristic equation of this system is $1+G_{c2} G_{22}=0$, we take the same procedure to derive the equations *(4.5)* and *(4.6)* for the system (for loop1 is closed with feedback controller G_{c1} and loop2 is open)

Figure 4.23 *Block diagram for closed-loop2 with P-Controller*
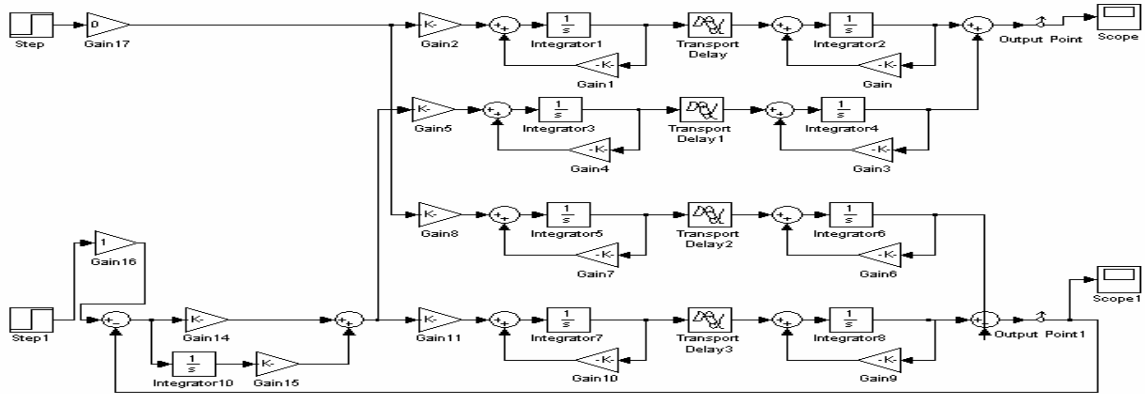
Figure 4.24 *Block diagram for closed-loop2 with PI-Controller*

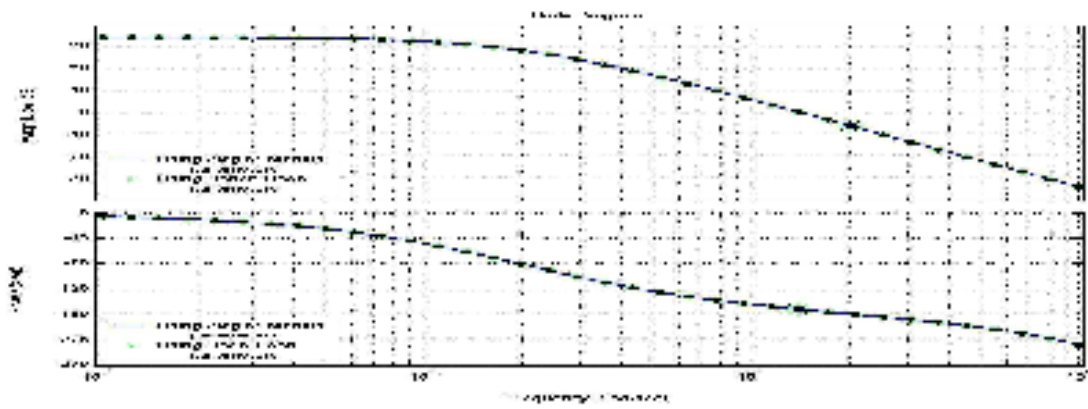**Figure 4.25** *Block diagram for closed-loop2 with PID-Controller*

Figure 4.26 *The frequency response of the open-loop2 system with P-controller*
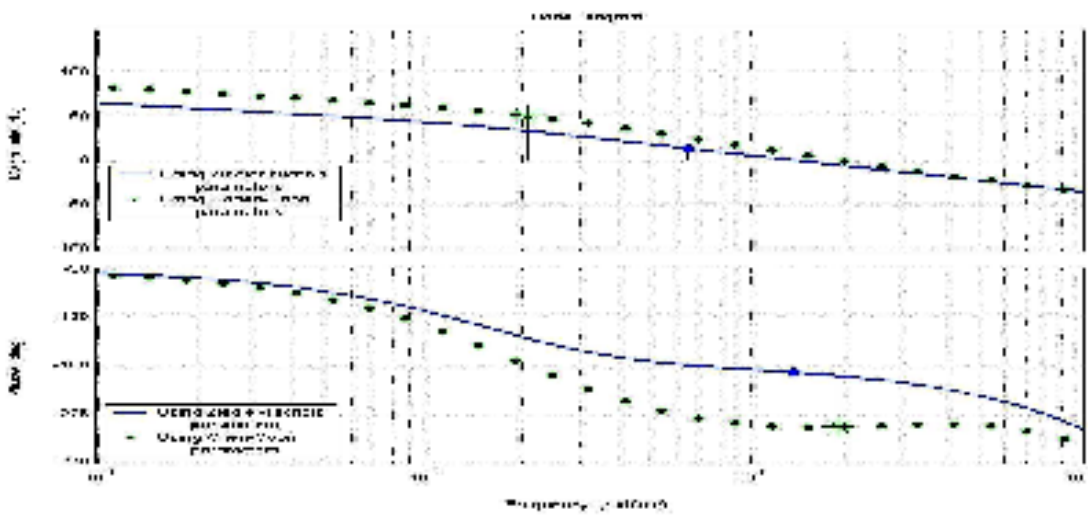

Figure 4.27 *The frequency response of the open-loop2 system with PD-controller*
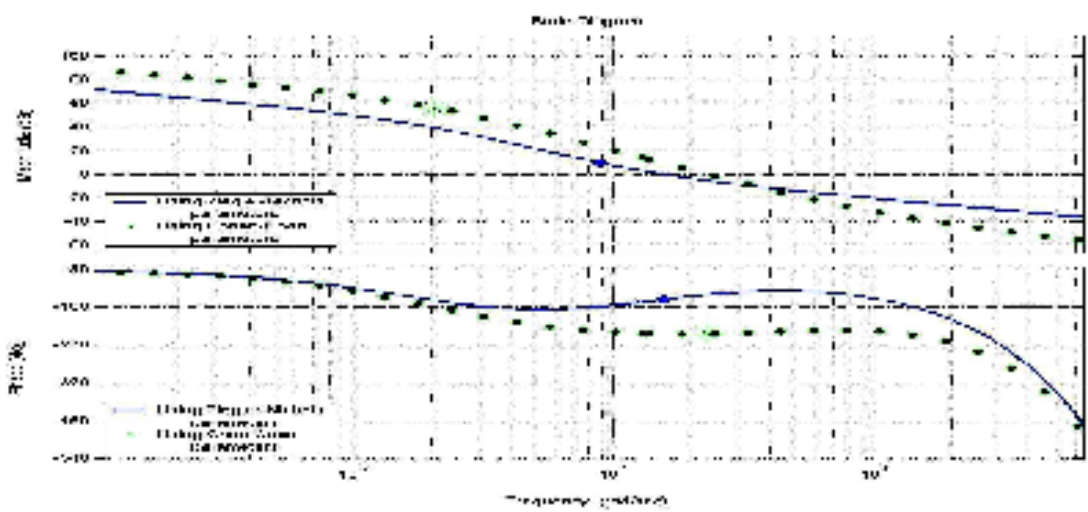

Figure 4.28 *The frequency response of the open-loop2 system with PID-controller*

From figure 4.26, 4.27, and 4.28, the stability of the system will be changed according to the type of controller, as explained previously. Gain margin and phase margin are given in table 4-8

Table 4-8 *Gain margin and phase margin if closed loop2 with feedback controller*

Method	P-Controller		PI-Controller		PID-Controller	
	Gain margin	*Phase margin*	*Gain margin*	*Phase margin*	*Gain margin*	*Phase margin*
Ziegler-Nichols	6.02	8.12	-13.3	-6.75	-9.91	17.2
Cohen-Coon	6.14	8.28	-50.3	-57.8	-56.4	-62.9

4.5.1.Case II *Both loops closed*

As shown in figure 4.12; where, the process at steady state with both outputs at their desired values. Consider a change in the set point $x_{D,sp}$ only, and keep the set point of loop2 the same (i.e $x_{B,sp}=0$) then the following results

(a) The controller of loop1 will change the value of L in such away as to bring the output x_D to the new set point value which gives the direct effect of L on x_D through loop1 and this is shown schematically by the dashed line in figure 4.12.a.

(b) The control action of L will not only attempt to bring x_D to the new set point, but it will also disturb x_B from its steady state value. Then the controller of loop2 attempt to compensate for the variation in x_B by changing appropriately the value of the manipulated variable V but a change in V, in turn, will affects on the output x_D and that is indirect effect of L on x_D, through loop2, as shown schematically by the dashed line in figure 4.12.b. [56]

By substituting equations *(4.3)* and *(4.4)* into equations *(4.1)* and *(4.2)* to get

73

$$(1 + G_{11}\, G_{C1})\, x_D(s) + (G_{12}\, G_{C2})\, x_B(s) = G_{11}\, G_{C1}\, x_{D,sp}(s) + G_{12}\, G_{C2}\, x_{B,sp}(s) \qquad \dots (4.7)$$

$$(G_{21}\, G_{C1})\, x_D(s) + (1 + G_{22}\, G_{C2})\, x_B(s) = G_{21}\, G_{C1}\, x_{D,sp}(s) + G_{22}\, G_{C2}\, x_{B,sp}(s) \qquad \dots (4.8)$$

After solving equations *(4.7)* and *(4.8)* with respect to the controlled output $x_{D,}\ x_B$ and take the following closed-loop input-output relationships

$$x_D(s) = T_{11}(s)\, x_{D,sp} + T_{12}(s)\, x_{B,sp} \qquad \dots (4.9)$$

$$x_B(s) = T_{21}(s)\, x_{D,sp} + T_{22}(s)\, x_{B,sp} \qquad \dots (4.10)$$

Where
$$T_{11}(s) = \frac{G_{11}\, G_{C1} + G_{C1}\, G_{C2}\, (G_{11}\, G_{22} - G_{12}\, G_{21})}{Q(s)}$$

$$T_{12}(s) = \frac{G_{12}\, G_{C2}}{Q(s)}$$

$$T_{21}(s) = \frac{G_{21}\, G_{C1}}{Q(s)}$$

$$T_{22}(s) = \frac{G_{22}\, G_{C2} + G_{C1}\, G_{C2}\, (G_{11}\, G_{22} - G_{12}\, G_{21})}{Q(s)}$$

and
$$Q(s) = (1 + G_{11}\, G_{C1})(1 + G_{22}\, G_{C2}) - (G_{21} G_{12} G_{C1} G_{C2}) \qquad \dots (4.11)$$

$T_{11}(s)$, $T_{12}(s)$, $T_{21}(s)$, and $T_{22}(s)$ are calculated by MATLAB$_{6.5}$ programs.

Equation *(4.11)* is representing the characteristic equation.

That gives the following:-

1. Equations *(4.9)* and *(4.10)* describe the response of outputs x_D and x_B when both loops are closed (i.e. they have accounted for the interaction between the two loops).

2. When $G_{12} = G_{21} = 0$, there is no interaction between the two control loops.The closed-loop outputs are given by the following equations:

$$x_D(s) = \frac{G_{11}G_{C1}}{1+G_{11}G_{C1}} x_{D,sp}(s) \qquad \text{... (4.12)}$$

$$x_B(s) = \frac{G_{22}G_{C2}}{1+G_{22}G_{C2}} x_{B,sp}(s) \qquad \text{... (4.13)}$$

The closed–loop stability at the two noninteracting loop depends on the roots of their characteristic equations. Thus if the roots of the two equations

$$1+G_{11}G_{C1} = 0 \quad , \quad 1+G_{22}G_{C2} = 0 \qquad \text{... (4.14)}$$

have negative real parts, then the two non-interacting loops are stable.

3. The stability of the closed-loop output for the two interacting loops is determined by the roots of the characteristic equation. Thus if the roots of equation *(4.11)* have negative real parts, then the two interacting loops are stable.
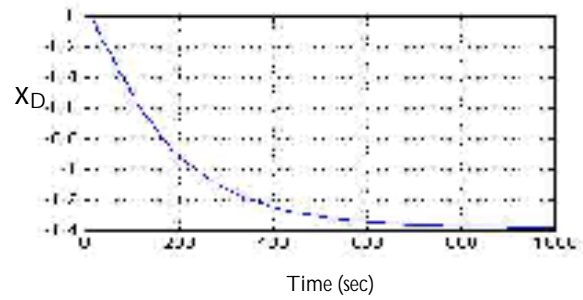
4.5.1.Case II.a *Both loops are closed (without controllers)*

The roots of the system in the present work are shown in figure 4.30, by applying equation *(4.11)* by using computer simulation programs.
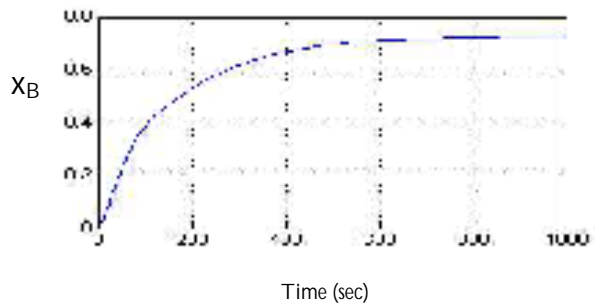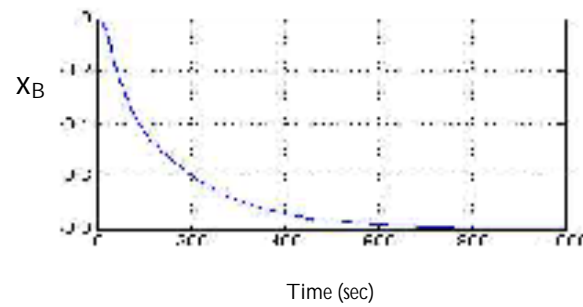

(a)
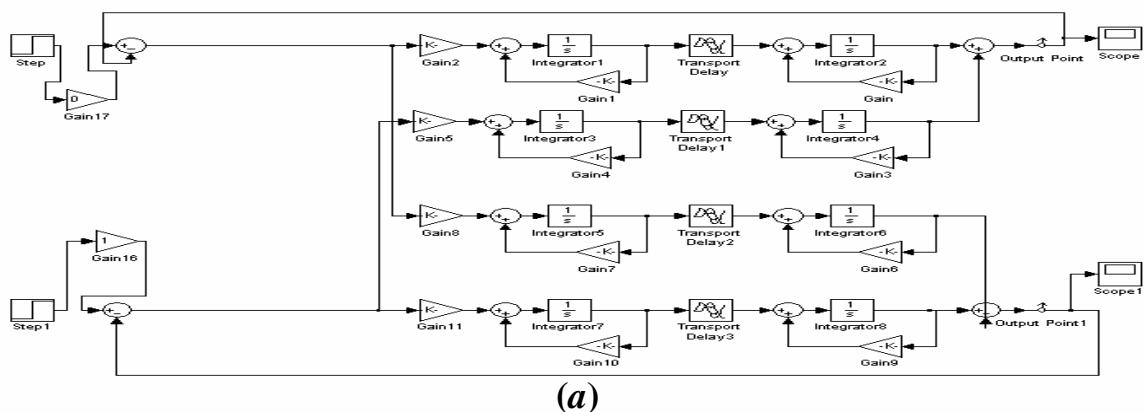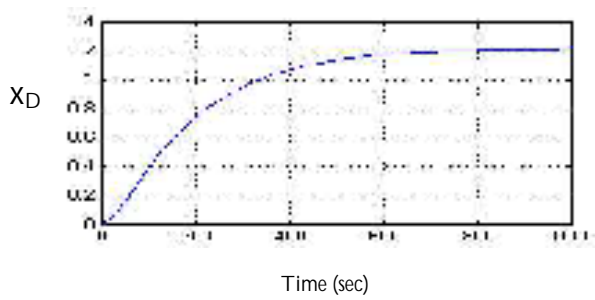
(*b.1*)

(*b.2*)

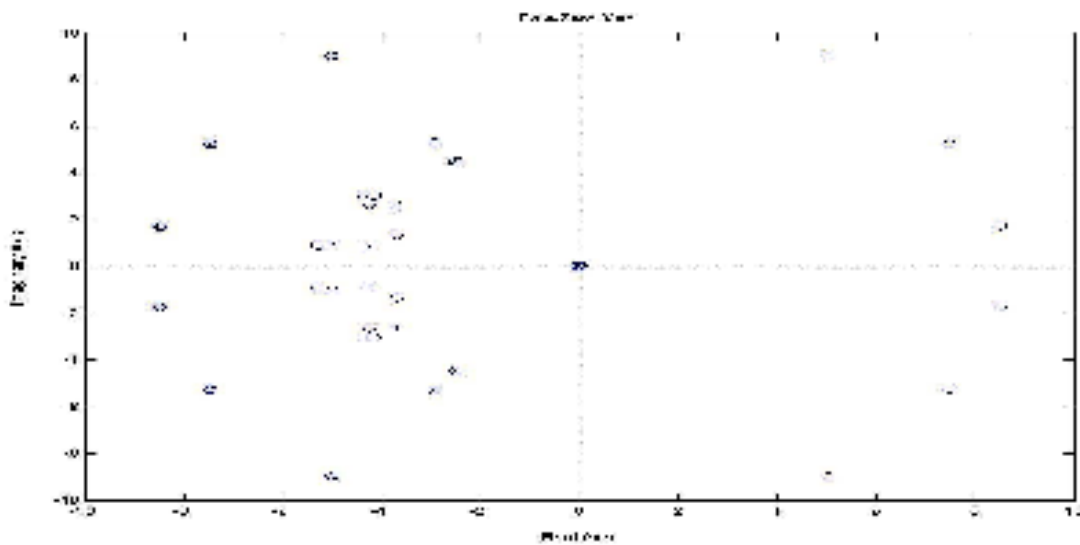(*b.3*)

(*b.4*)

Figure 5.29 (a) **Block diagram for the two closed-loops without controllers**
  (b) **The compositions response for closed-loop process.**
    (*b.1*) **The change of** x_D **with the change of** L.
    (*b.2*) **The change of** x_D **with the change of** V.
    (*b.3*) **The change of** x_B **with the change of** L.
    (*b.4*) **The change of** x_B **with the change of** V.

Figure 4.30 *The poles and zeros of the system without feedback closed loops*

From these results we find that the system with two feedback loops is stable, because all roots of the characteristic equation have negative real parts.

4.5.1.Case II.b *Both loops are closed (with controllers)*

In this section we use *P, PI,* and *PID*-controller in order to show the effect of these controllers on the dynamic system. The controller parameters, which are used in this section, are same in section 4.5.1.Case I.c. The roots of the system are shown in figures 4.32, 4.34, and 4.36 also in appendix B.2 after applying equation (*4.11*) and using computer simulation programs.
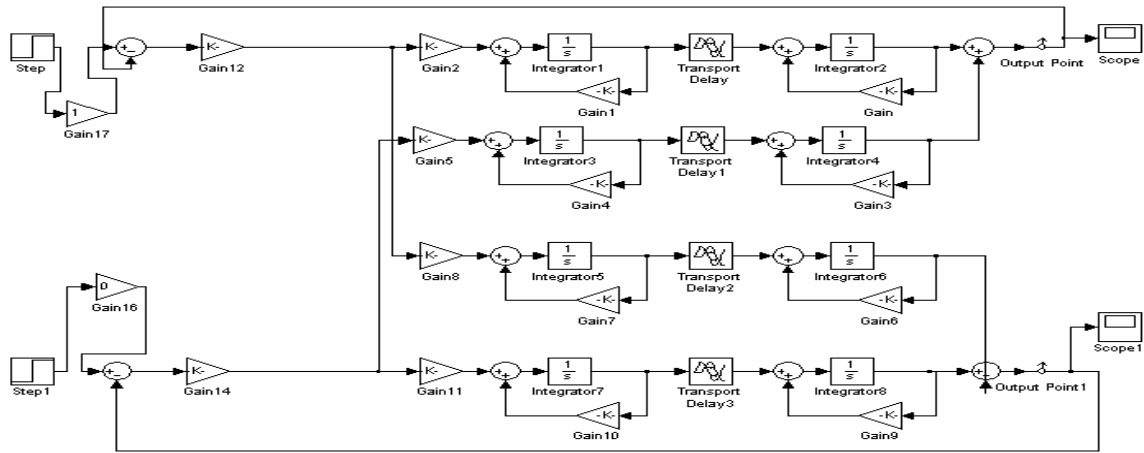

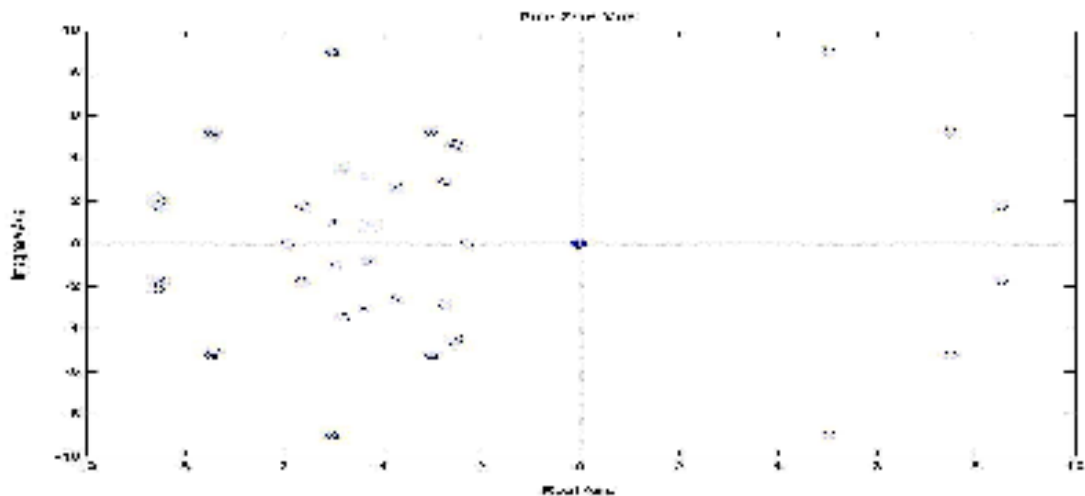**Figure 4.31** *Block diagram for the two closed-loop system with P-controllers*

Figure 4.32 *The poles and zeros of the characteristic equation for the system with two P-controllers*
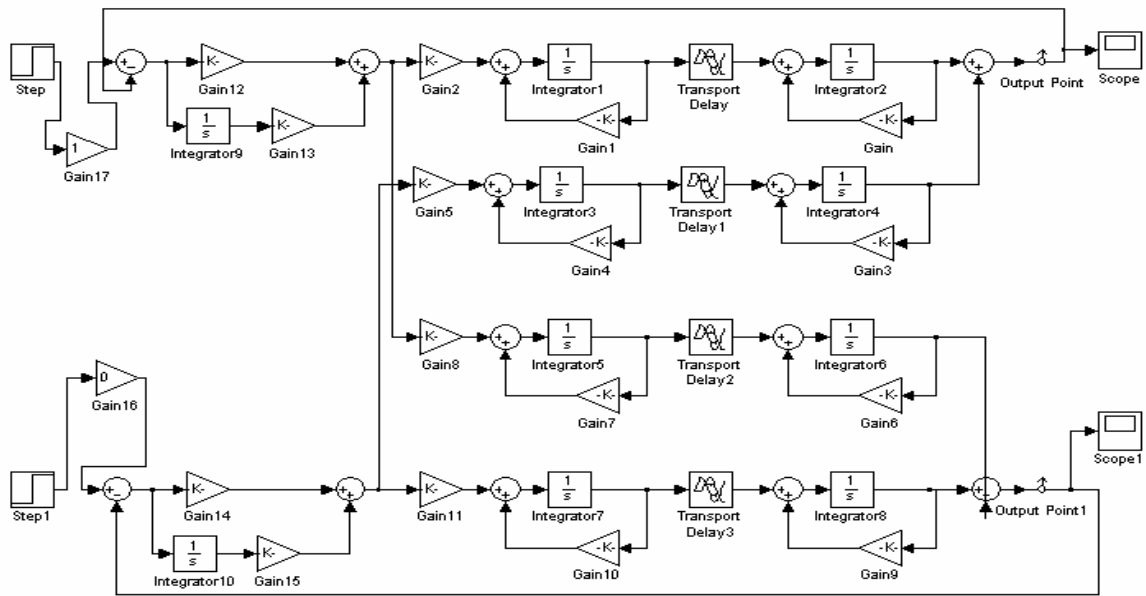
Figure 4.33 *Block diagram for the two closed-loop system with PI-controllers*
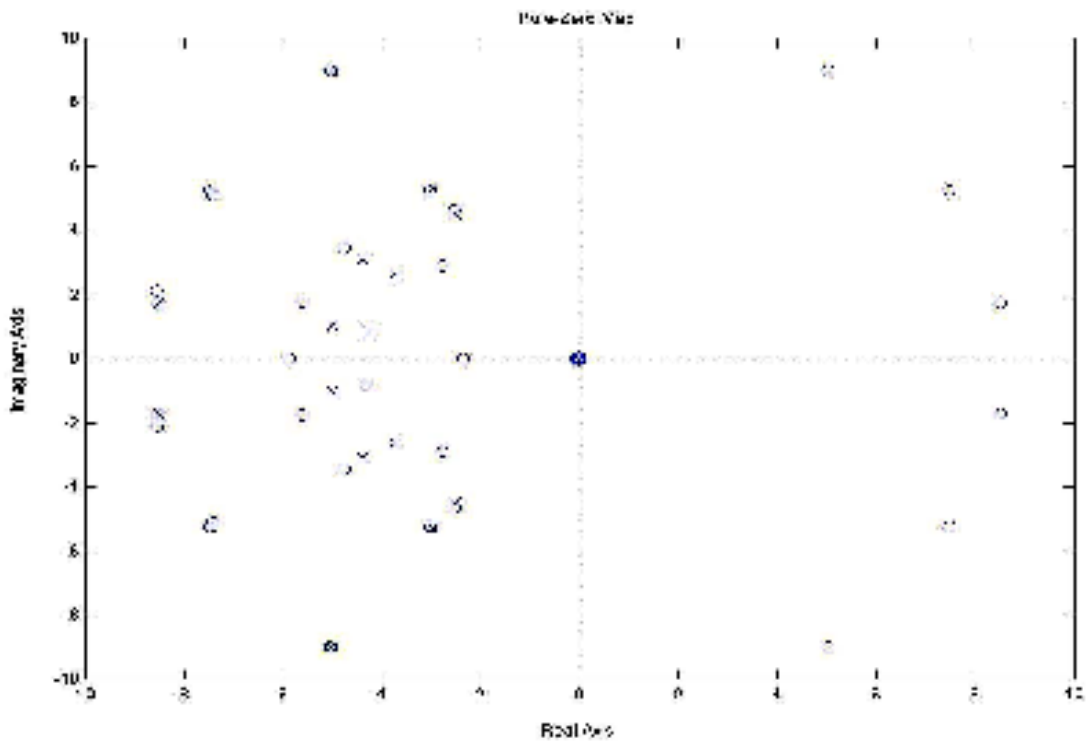

Figure 4.34 *Shows the poles and zeros of the characteristic equation for the system with two PI-controllers*
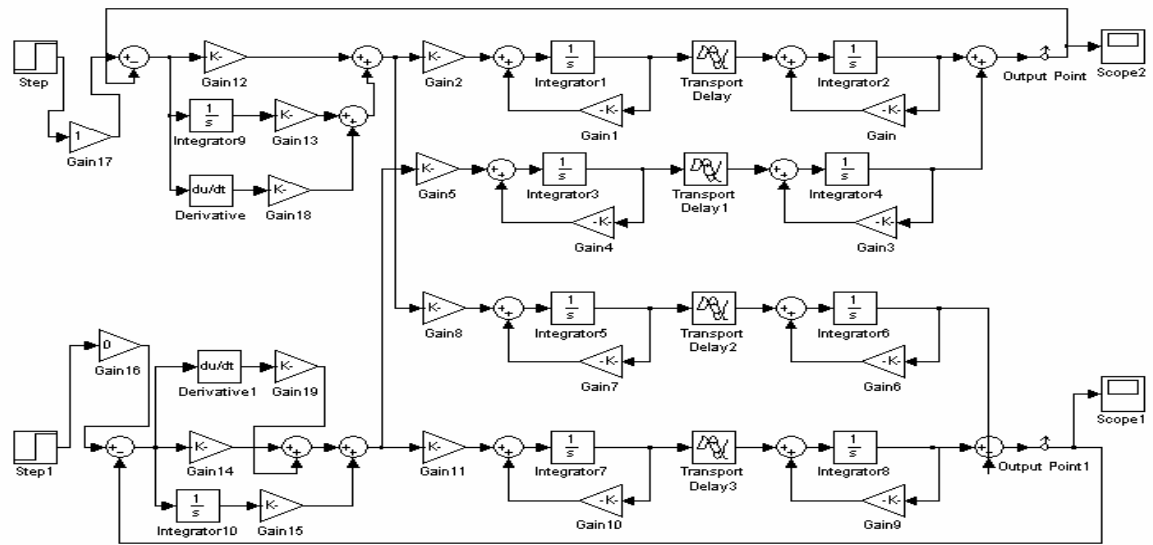
78

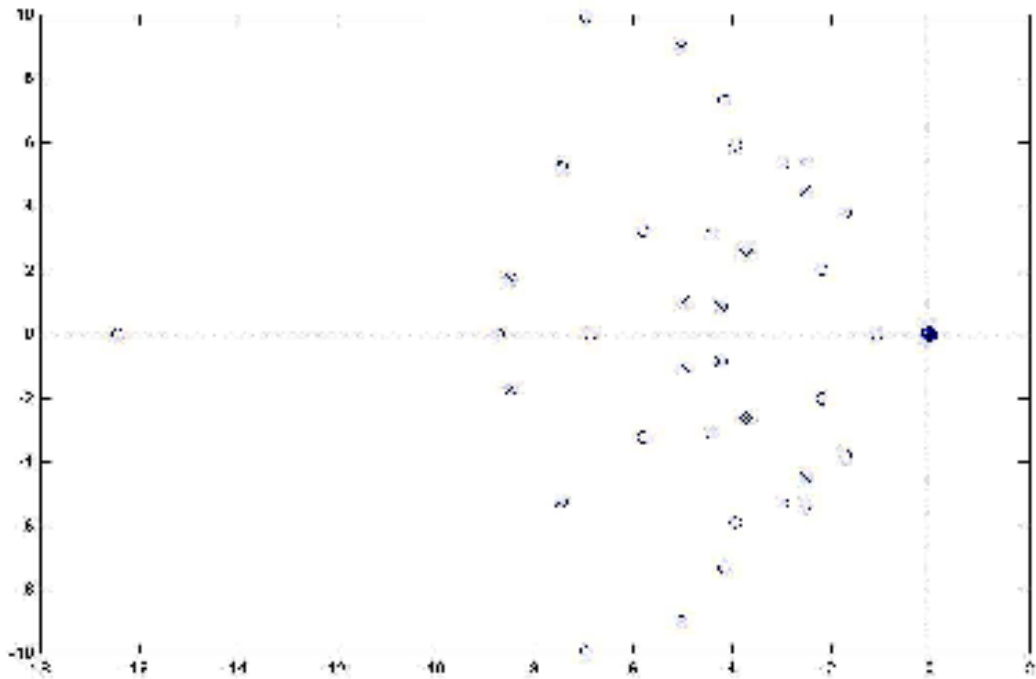**Figure 4.35** *Block diagram for the two closed-loop system with PID-controllers*

Figure 4.36 *The poles and zeros of the characteristic equation for the system with two*

PID-controllers

The poles of the overall system without controllers and with *P*, *PI,* and *PID*-controllers are shown in appendix B.2.

5.5.2 Relative Gain Array

The values of elements of relative gain array are:

$$\beta_{11} = \frac{1}{1 - \dfrac{K_{p12} K_{p21}}{K_{p11} K_{p22}}} \qquad \dots (4.14)$$

$$\beta_{11} = \frac{1}{1 - \dfrac{(-0.495 * 0.749)}{(0.471 * -0.832)}} = 18.557$$

then the rest of elements was found from (the sum of the elements in each row is 1 and the sum of elements in each column is also 1. this property holds for any RGA, so in the 2*2 case only have to calculate one element such as in this work)

$$\beta_{12} = 1 - \beta_{11} = 1 - 18.557 = -17.557 \qquad \dots (4.15)$$

$$\beta_{21} = 1 - \beta_{11} = 1 - 18.557 = -17.557 \qquad \dots (4.16)$$

and

$$\beta_{22} = 1 - \beta_{12} = 1 - (-17.557) = 18.557 \qquad \dots (4.17)$$

then

$$RGA = \begin{bmatrix} \beta_{11} & \beta_{12} \\ \beta_{21} & \beta_{22} \end{bmatrix} = \begin{bmatrix} 18.557 & -17.557 \\ -17.557 & 18.557 \end{bmatrix} \qquad \dots (4.18)$$

From this result we notice there are interactions between loops.

4.5.3 Design and Analysis of Non-Interacting Control Loops (Decoupling System)

In our system, ideal decoupling was used; it is shown in figure 4.37.
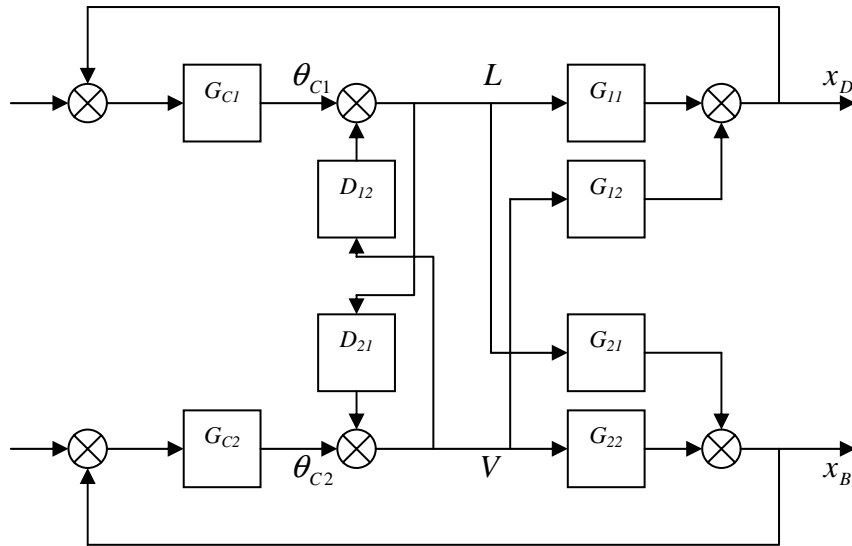
(*a*)
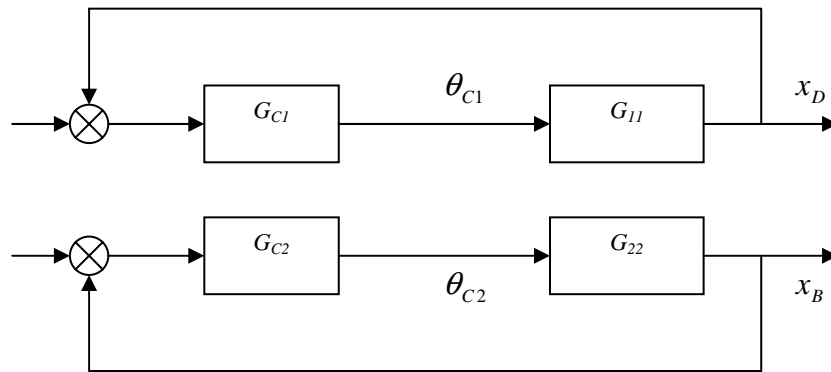
(*b*)

Figure 4.37   (*a*)   *Decoupling system*
                  (*b*)   *Resulting distillate and bottom loops*

From table 2-6 we find the transfer function of decouplers D_{ij} for ideal decoupling system.

Figure 4.37b is equivalent to figure 4.37a then the frequency response analysis can be explained in figures 4.38 and 4.39 for the two loops. Using *P, PI, and PID*-controllers to make a comparison between the effects of the controllers on the system. The controller parameters are the same as we calculated in section (4.5.1.Case I.c).
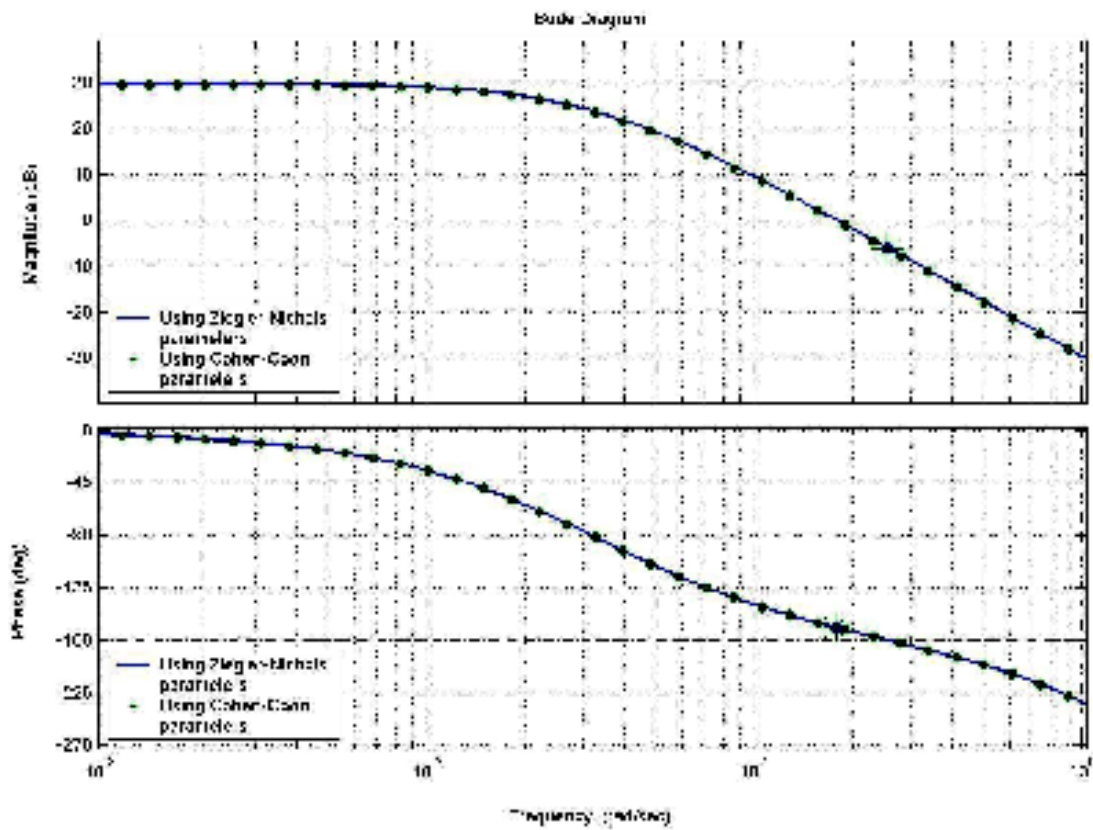
(a)
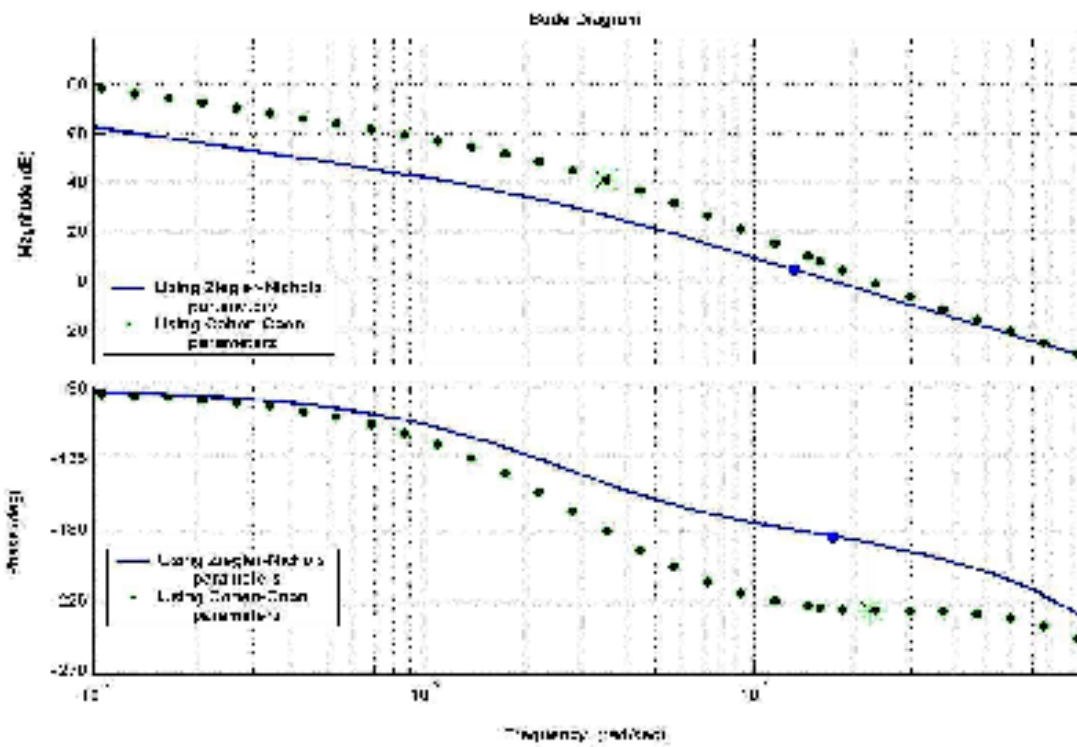
(b)
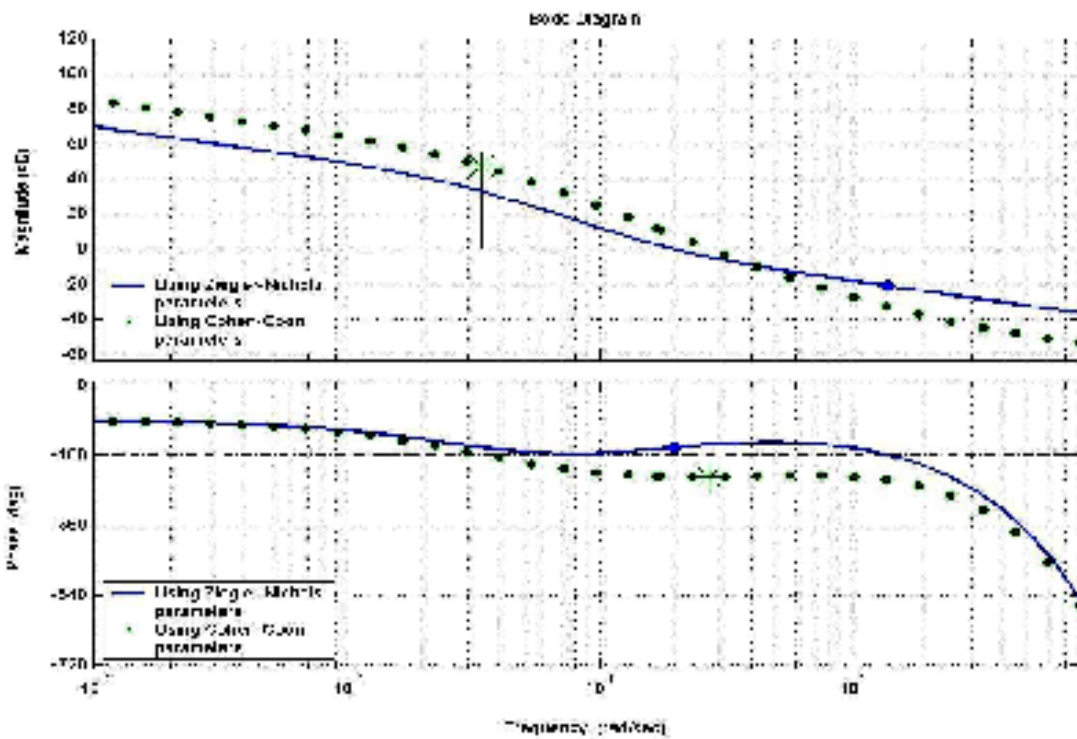
(c)

Figure 4.38 *The frequency response for distillate loop with P, PI, PID-Controller respectively*
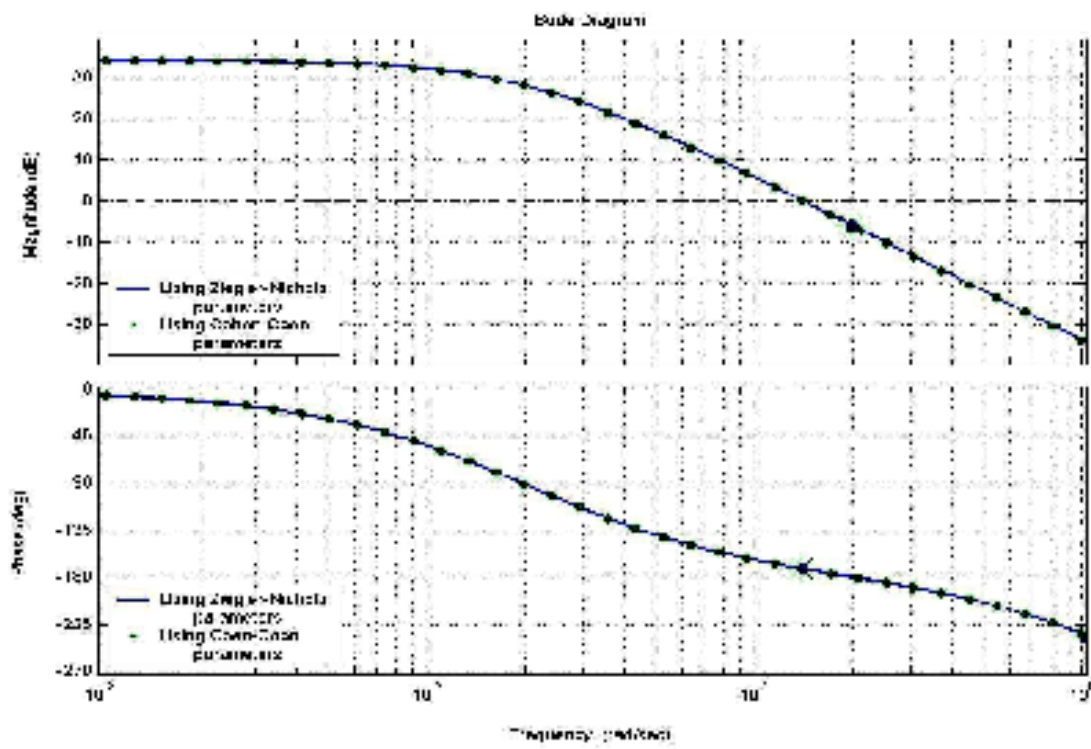
(a)
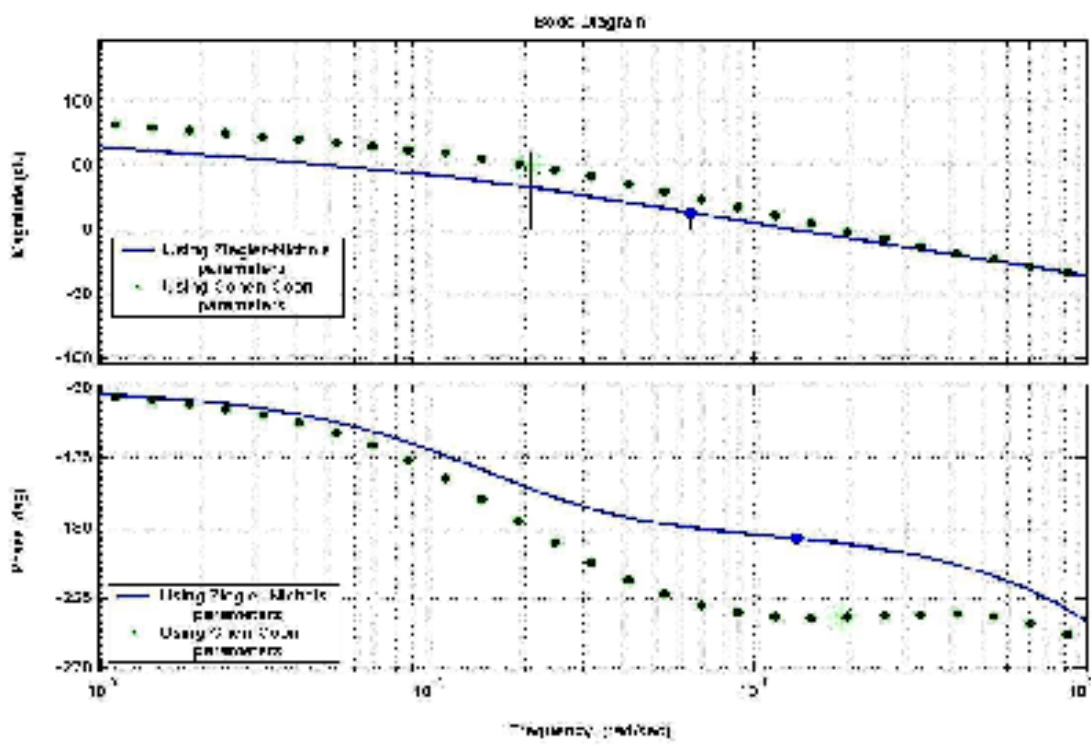
(b)
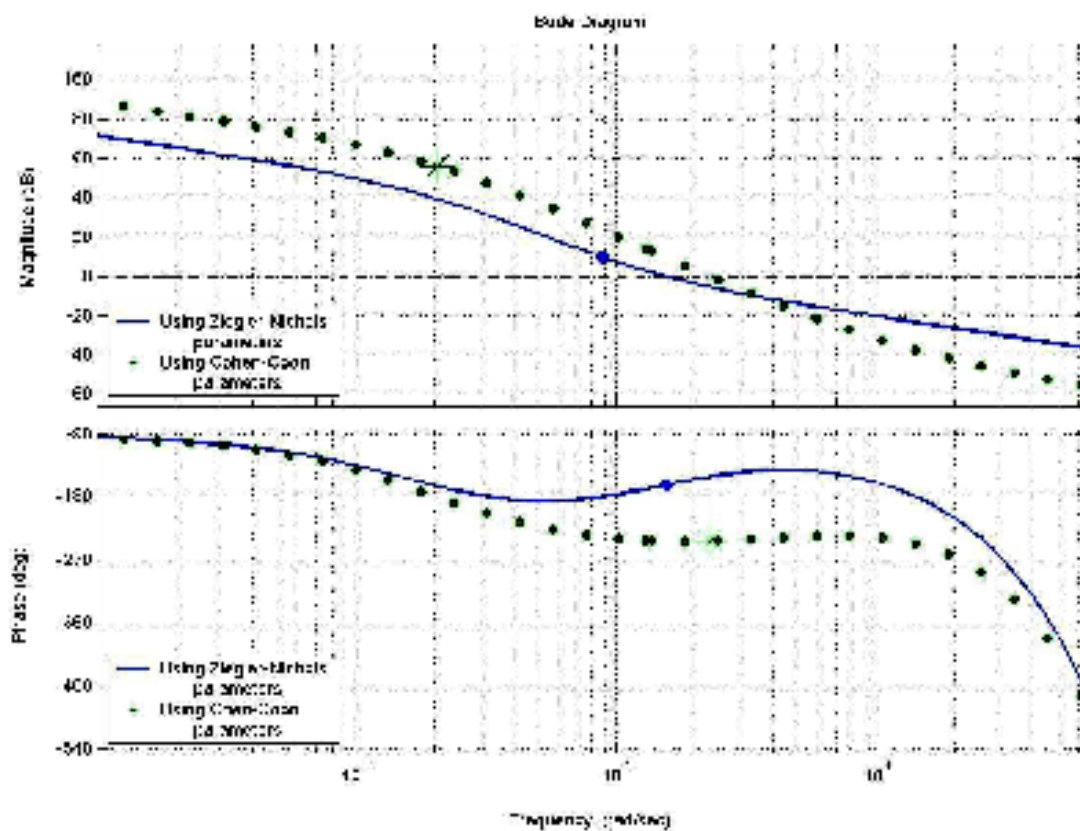
(c)

Figure 4.39 *The frequency response for bottom loop with P, PI, PID-Controller respectively*

From figures 4.38 and 4.39 the characteristics of the system (gain margin and phase margin) are shown in table 4-9.

Table 4-9 *Gain margin and phase margin if decoupling system with feedback controller and using Ziegler-Nichols parameters*

	P-Controller		PI-Controller		PID-Controller	
	Gain margin	Phase margin	Gain margin	Phase margin	Gain margin	Phase margin
Distillate Loop	6.02	10.5	-4.7	-4.2	21.0	18.8
Bottom Loop	6.02	8.12	-13.3	-6.7	9.9	17.2

Table 4-10 *Gain margin and phase margin if decoupling system with feedback controller and using Cohen-Coon parameters*

	P-Controller		PI-Controller		PID-Controller	
	Gain margin	Phase margin	Gain margin	Phase margin	Gain margin	Phase margin
Distillate Loop	6.2	10.8	-41.4	-51.4	-47.5	-56.7
Bottom Loop	6.1	8.3	-50.5	-57.8	56.4	-62.9

From tables (4-9) and (4-10) we find that Ziegler-Nichols parameters are more appropriate from Cohen-Coon parameters because the system with *PID*-controllers and Ziegler-Nichols parameters is stable while with Cohen-Coon parameters is unstable.

4.6 RELATIONSHIPS FOR FREQUENCY RESPONSE ANALYSIS

4.6.1 Relation Between Closed-Loop Transient and Closed-Loop Frequency Response.

4.6.1.1 *Damping ratio and closed-loop frequency response*

By plotting the resonant peak magnitude versus the percent overshoot the result is shown in figure 4.40
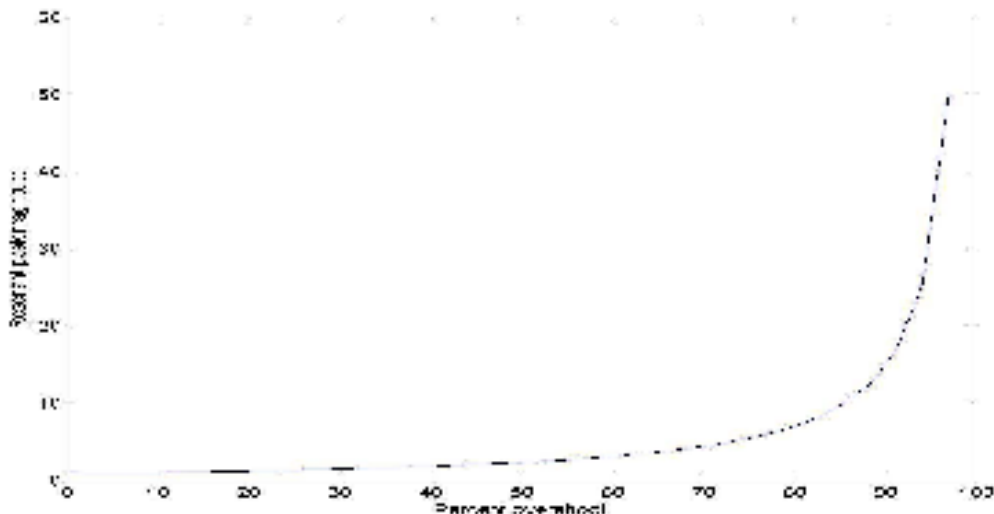
Figure 4.40 *Closed-loop frequency response peak vs. percent overshoot for a two pole system*

The transfer function of closed-loops for the distillation column are drawn as in figure 4.41, 4.42, 4.43, and 4.44 by using Bode plots by computer program.
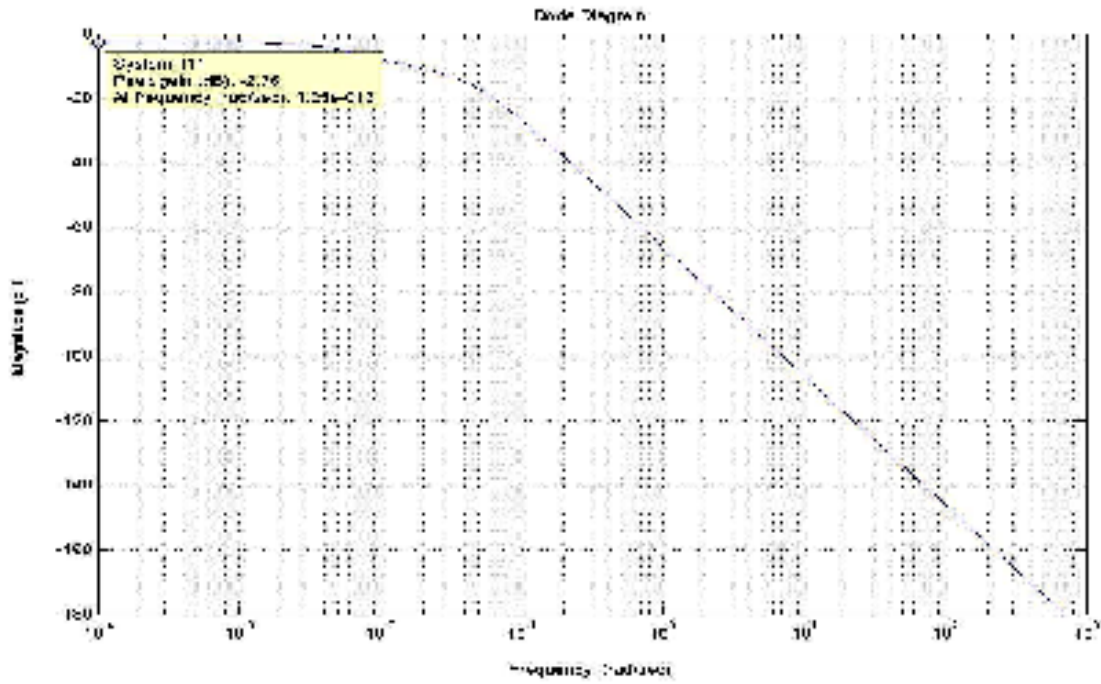
Figure 4.41 *The resonant peak magnitudes for the transfer function of overhead composition to reflux flow*
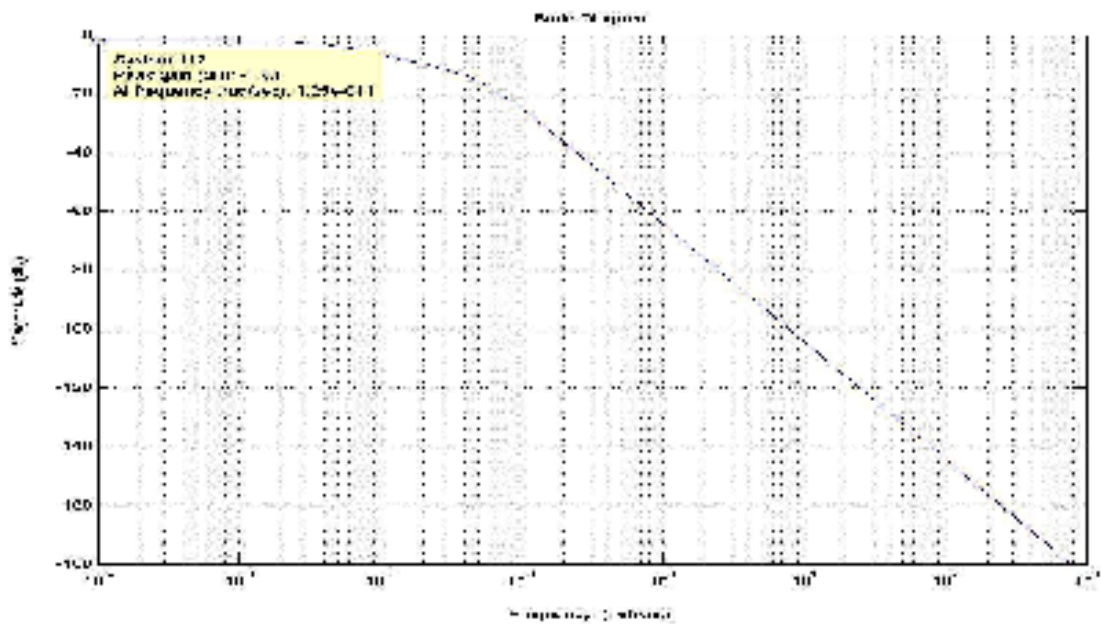
Figure 4.42 *The resonant peak magnitudes for the transfer function of overhead composition to vapor flow rate*
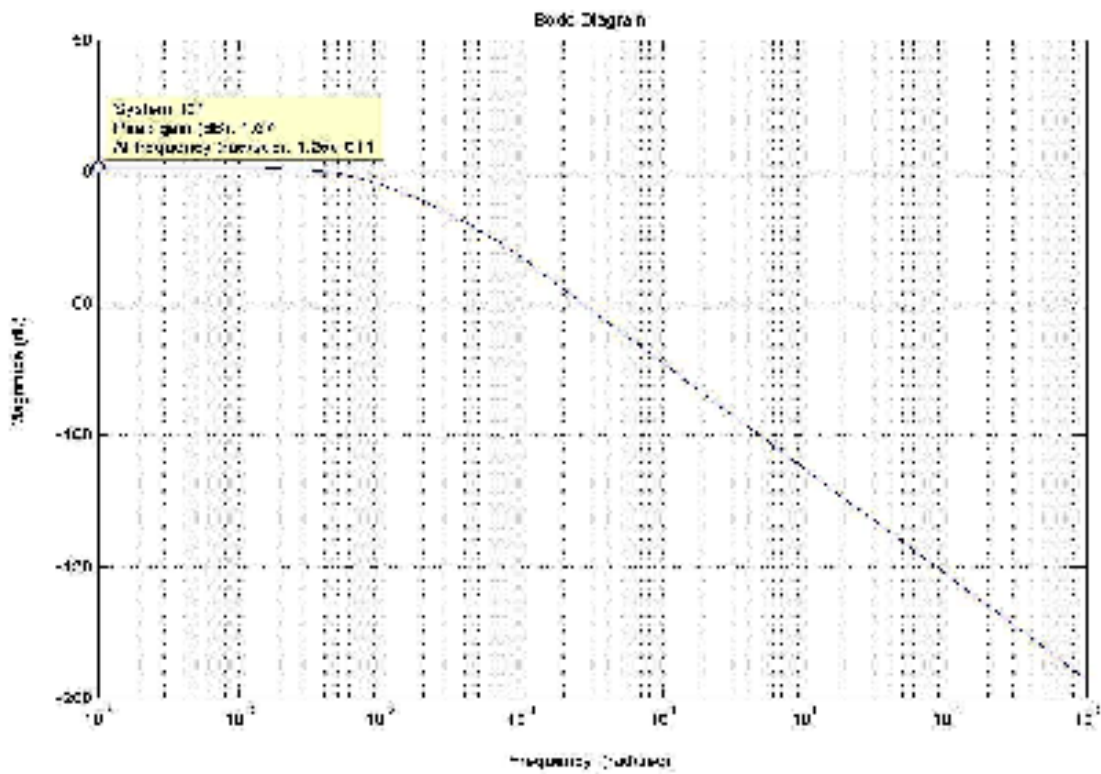
Figure 4.43 *The resonant peak magnitudes for the transfer function of bottom composition to reflux flow*
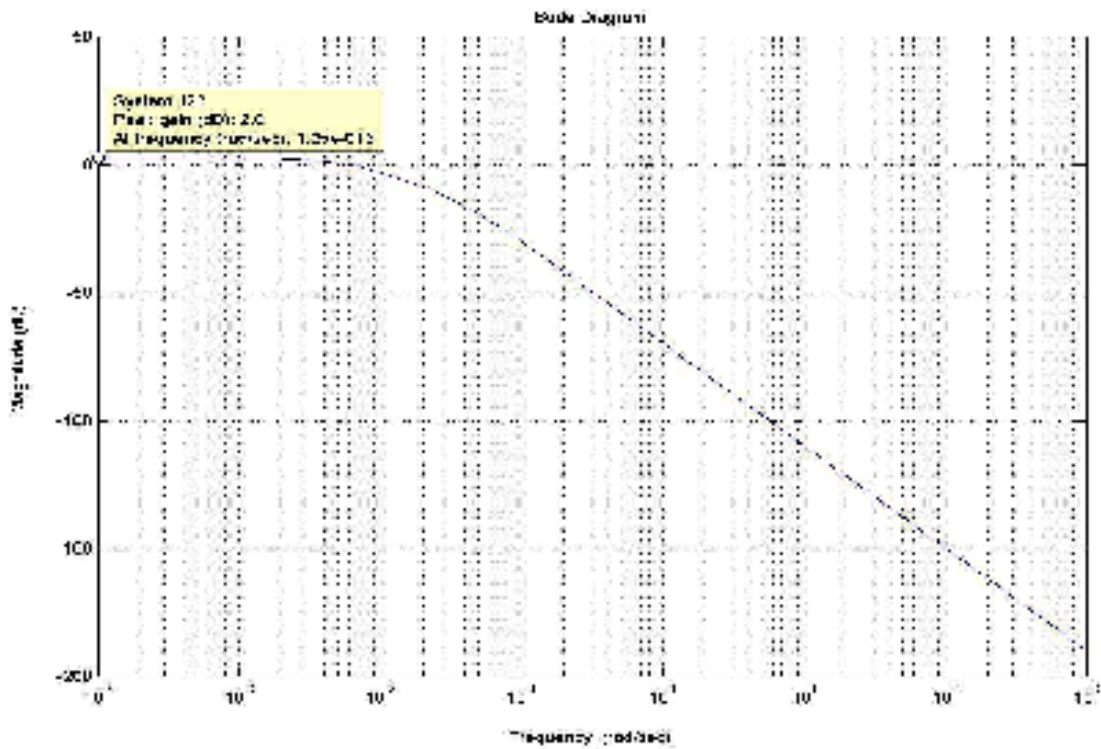
Figure 4.44 *The resonant peak magnitudes for the transfer function of bottom composition to vapor flow rate*

Figures 4.41 to 4.44 show the resonant peak magnitudes for the transfer functions of two feedback closed-loops system. (T_{11}, T_{12}, T_{21}, and T_{22} respectively). The resonant peak magnitudes are determined from these figures. By finding the percent overshoots from figure 4.40 then we calculate the damping ratio using equation 2.63.

From figures 4.41 to 4.44 we note that the system doesn't have a resonant peak magnitudes then it doesn't have a percent overshoot. From these results the damping ratio will be greater than 0.707 for all the transfer functions of the system.

4.6.1.2 *Response speed and closed-loop frequency response*

In this section, we calculate the bandwidth by plotting the equations *(2.66)* and *(2.67)* versus the damping ratio.
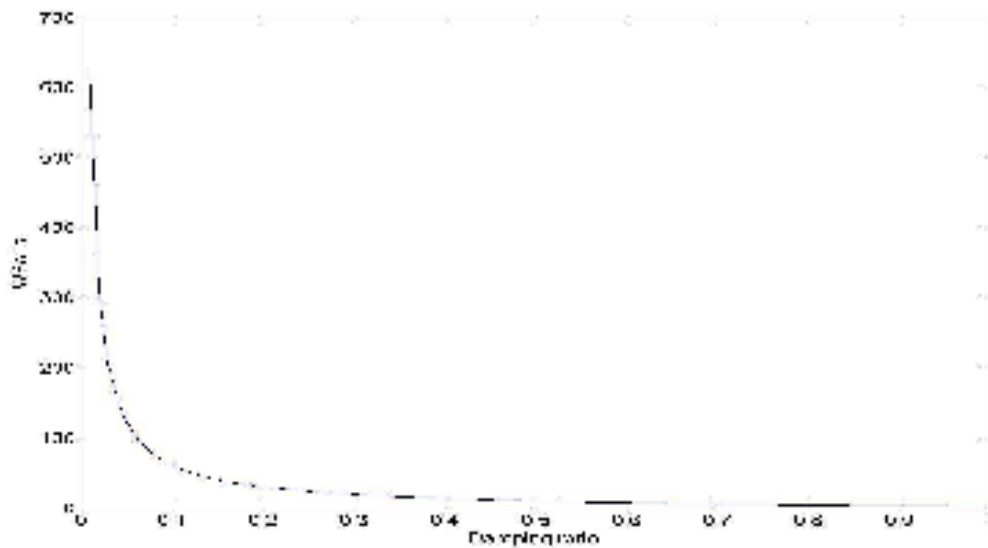
Figure 4.45 *The relation between settling time*band width frequency and damming ratio*
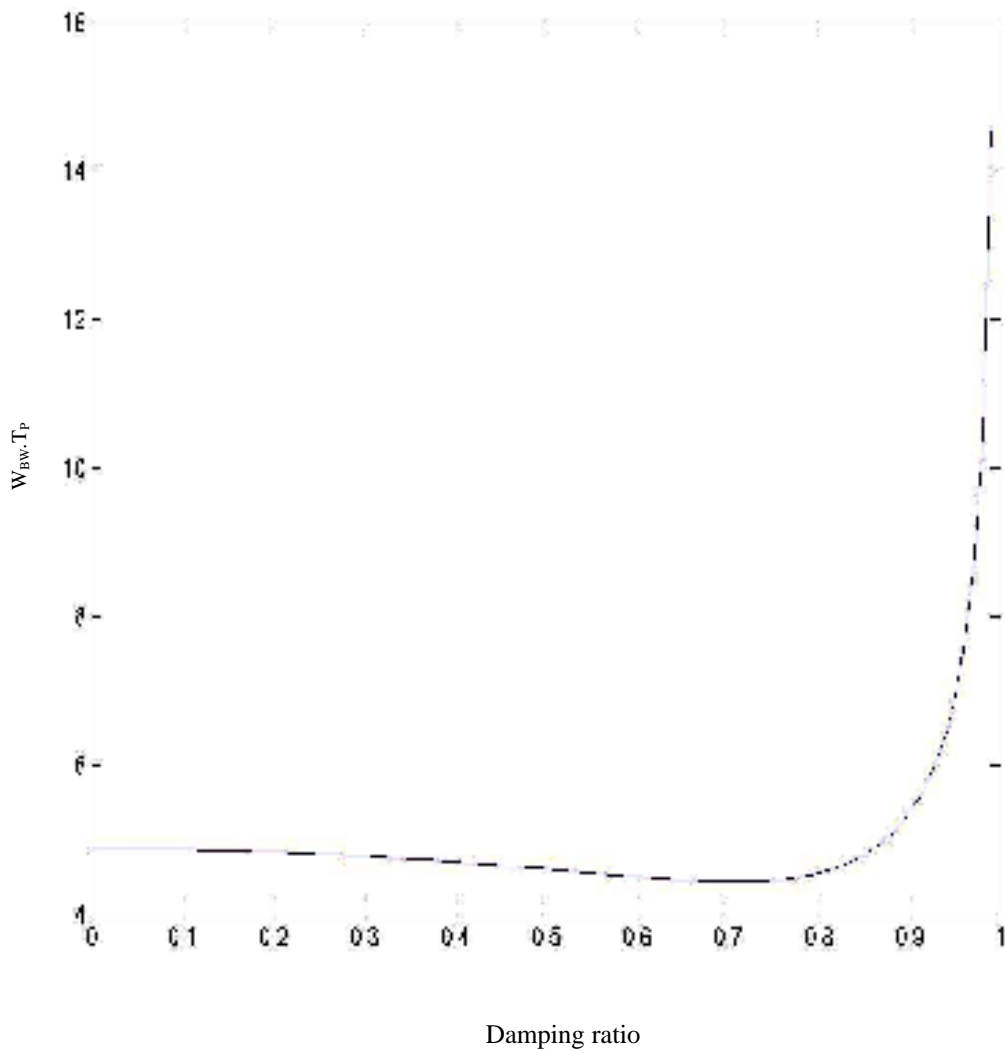
Figure 4.46 *The relation between peak time*Bandwidth frequency and damming ratio*

Because of the damping ratio is greater than 0.707 as shown in previous section, so this system doesn't have a bandwidth frequency

4.6.2 <u>Relation Between Closed and Open-Loop Frequency Response</u>

Nichols chart representing relationship between closed and open-loop frequency response and it is plotted for the open-loop transfer functions for distillation column.
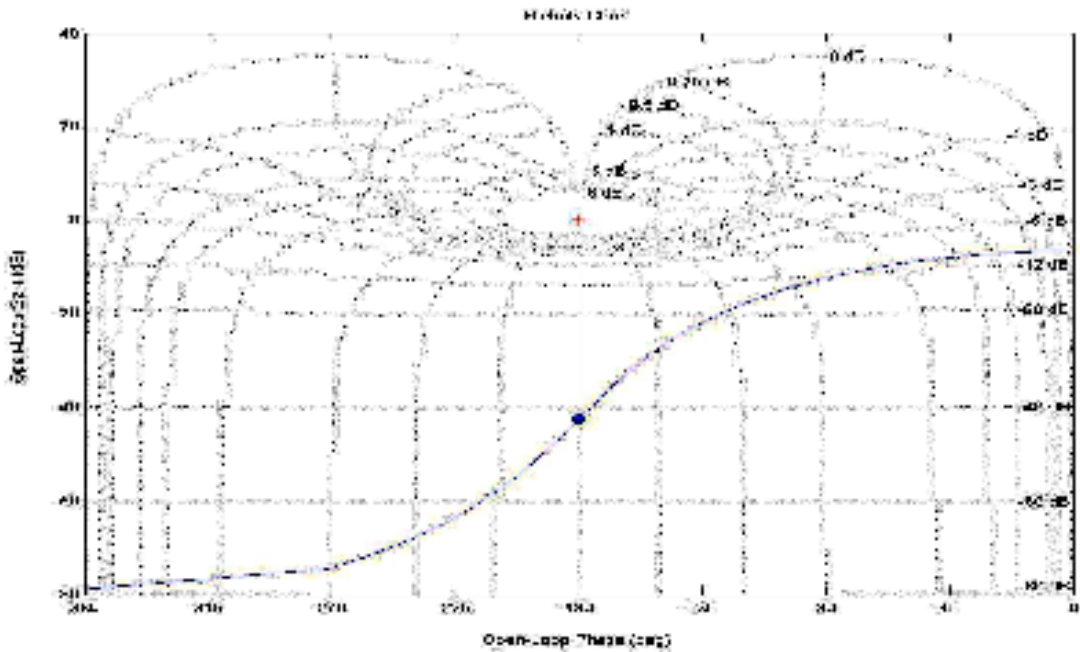
Figure 4.48 *The Nichols chart of overhead composition to reflux flow*
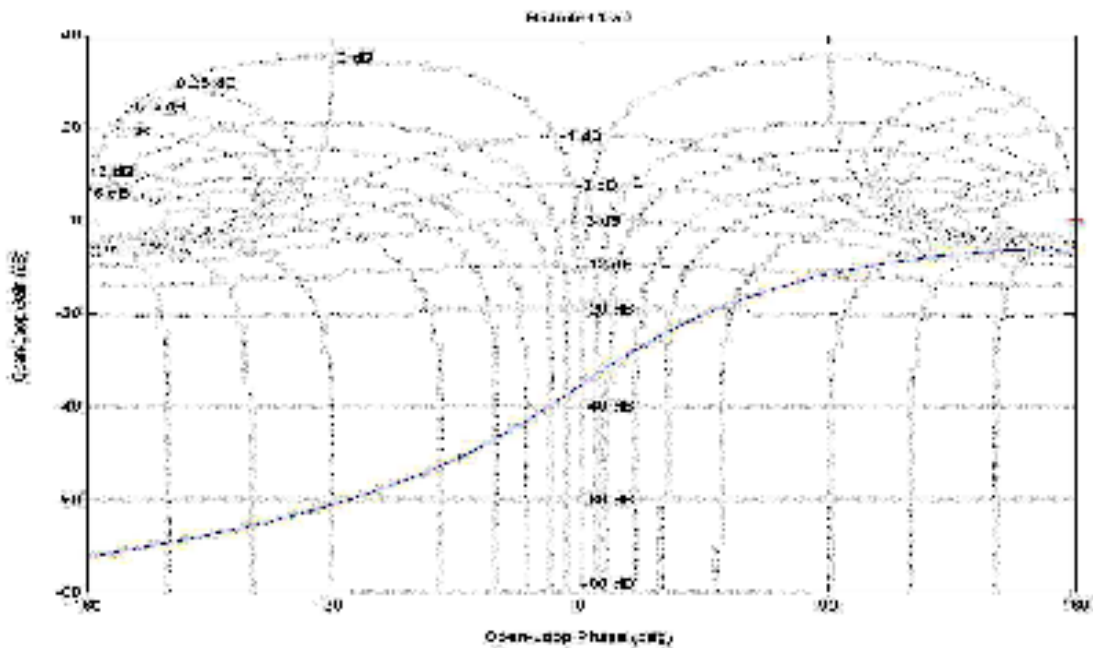
Figure 4.49 *The Nichols chart of overhead composition to vapor flow rate*
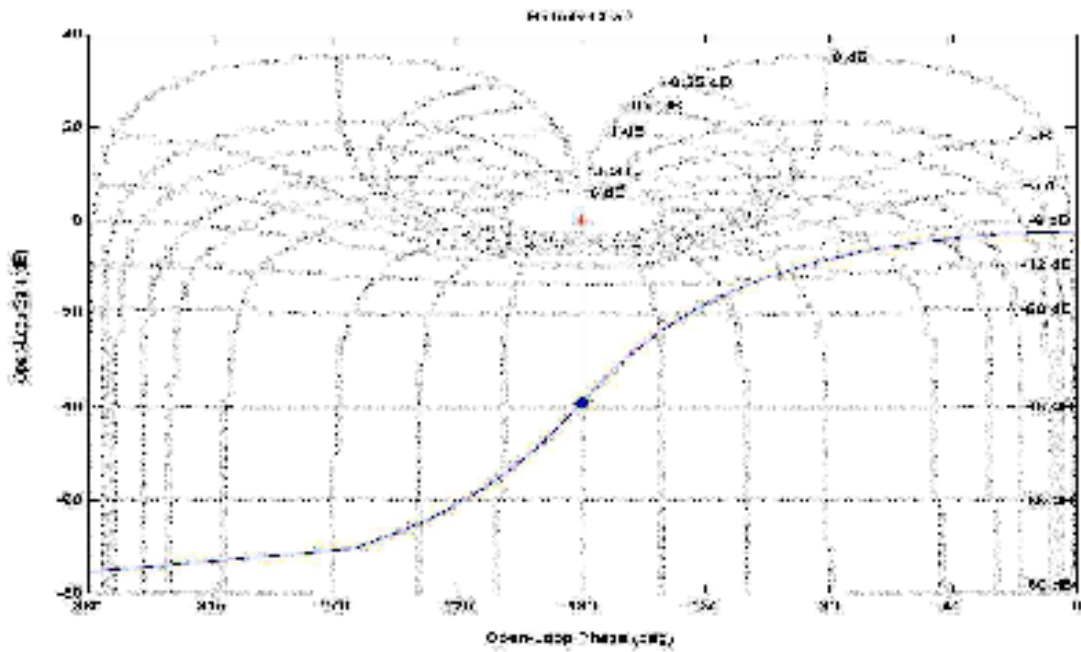
Figure 4.50 *The Nichols chart of bottom composition to reflux flow*
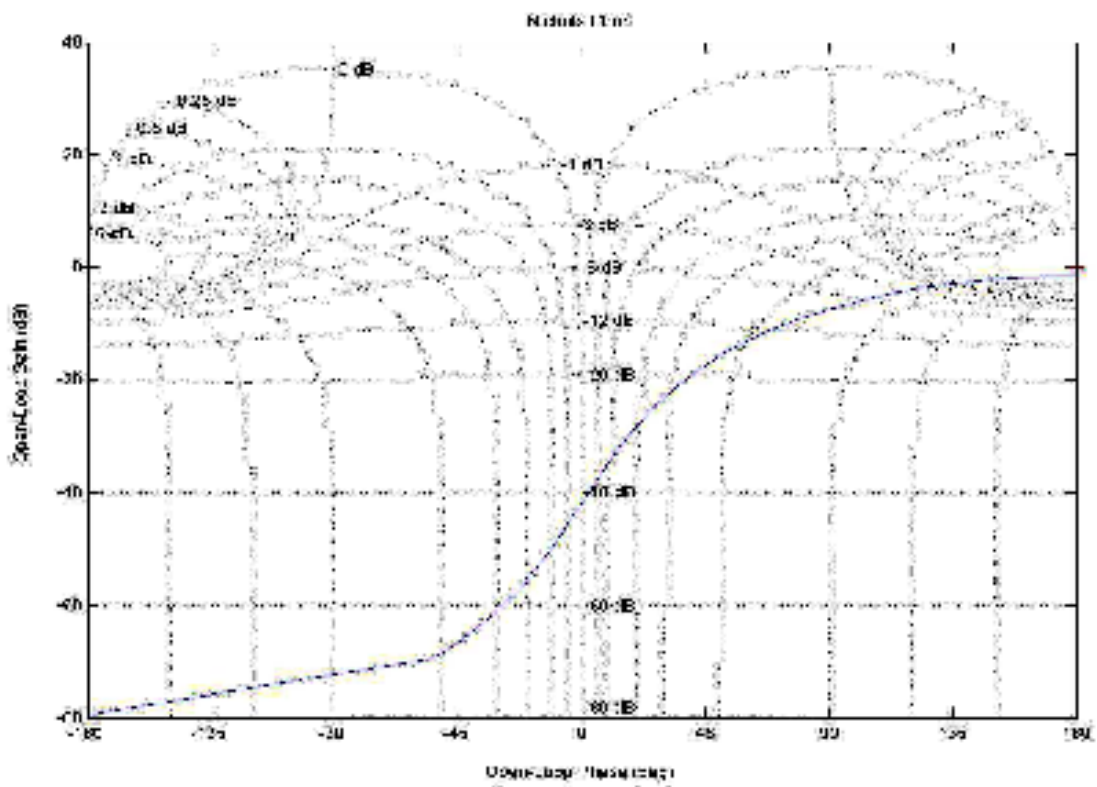
Figure 4.51 *The Nichols chart of bottom composition to vapor flow rate*

Figures from 4.48 to 4.51 show the Nichols chart for the transfer functions of the open-loop system. (G_{11}, G_{12}, G_{21}, and G_{22} respectively)

4.6.3 Relation Between Closed-Loop Transient and Open-Loop Frequency Response

4.6.3.1 *Damping ratio from phase Margin*

By this relation we can find the damping ratio from the open-loop transfer function by using equation *(2.73)*. Then the damping ratio versus phase margin is drawn by using MATLAB$_{6.5}$ program.
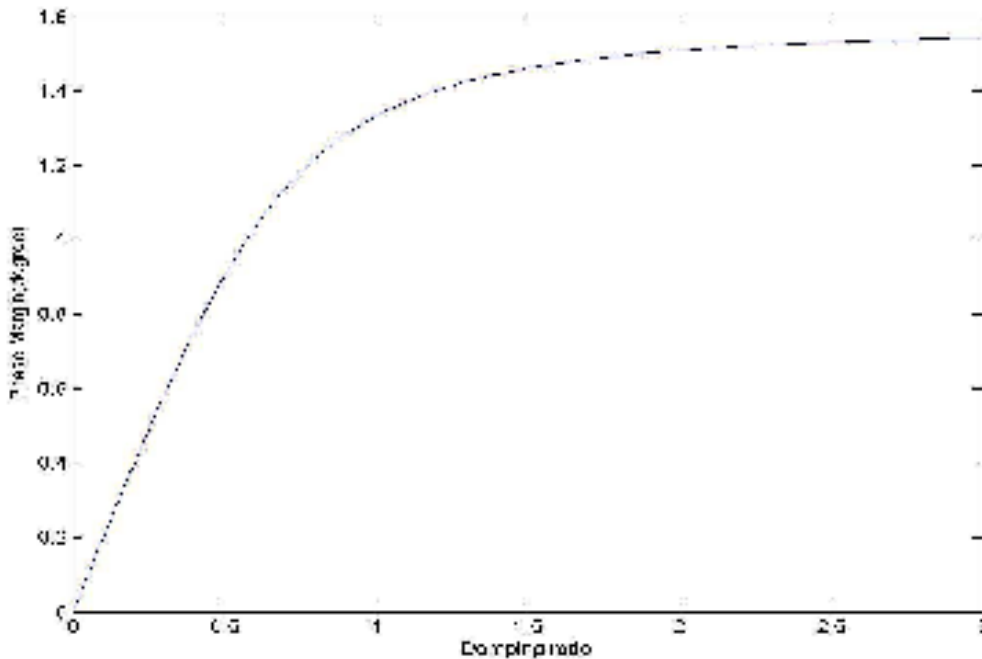
Figure 4.52 *The relation between damping ratio and phase margin*

From equation *(2.62)* we notice that there is no peak frequency, if the damping ratio equal (or greater than) to 0.707. There is no peak to the closed-loop magnitude frequency response. Thus from figure 4.52 a phase margin of 65.52º (damping ratio=0.707) or greater is required from the open-loop

frequency response. Then from above we notice that the damping ratio of all transfer functions of a system in this work greater than 0.707.

4.6.3.2 *Response speed from open-loop frequency response*

In order to find the response speed from open-loop frequency response using Figures (From 5.3 to 5.6) and equation 2.66 and 2.77 to find settling time, and peak time.

From section 5.6.3.1 the damping ratio of all transfer functions is greater than 0.707 then each transfer function have not a bandwidth then this relation can not be applied for this system.

4.7 STEADY-STATE ERROR CHARACTERISTICS

In order to find the values of the static error constants for equivalent unity feedback system: k_p for a type 0 system, k_v for a type 1 system, k_a for a type 2 system. The type of the system in this work is 0 system, the result can be obtained using figures (from 4.3 to 4.6) and equation (*4.19*).

$$e_{ss} = \frac{1}{1+k_p} [3] \qquad\qquad \dots (4.19)$$

This equation was used for 0 systems.

Table 4-13 *The steady-state error characteristics of the system*

	$\|G\| = 20*\log(k_P)$ (dB)	k_P	e_{ss}
Overhead composition to reflux flow	-6.539	0.471	0.679
Overhead composition to vapor flow rate	-6.108	0.495	0.668
Bottom composition to reflux flow	-2.510	0.749	0.572
Bottom composition to vapor flow rate	-1.597	0.832	0.546

4.8 Systems with Time Delay

Time delay caused by the difference in relative stability of the systems as shown in figures 4.53, 4.54, 4.55, and 4.56:
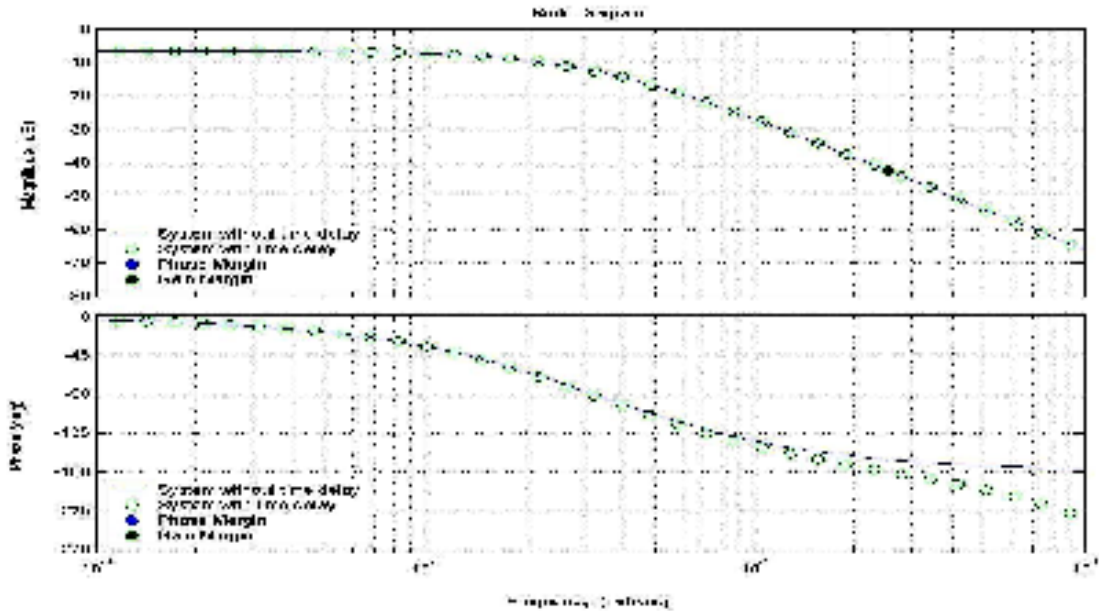
Figure 4.53 *The difference between the system with and without time delay of overhead composition to reflux flow*
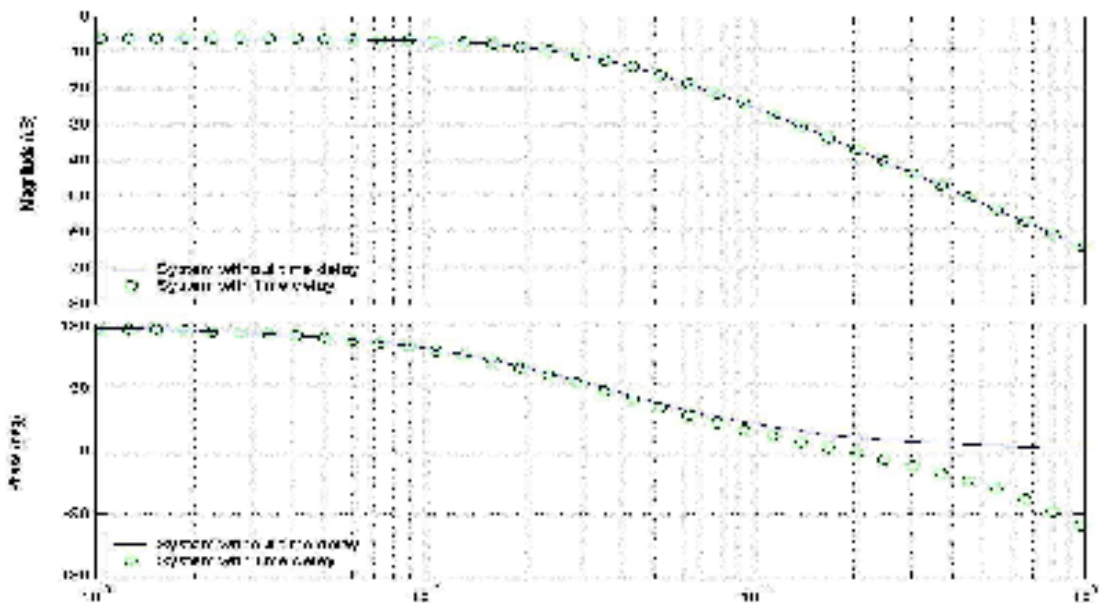
Figure 4.54 *The difference between the system with and without time delay of overhead composition to vapor flowrate*
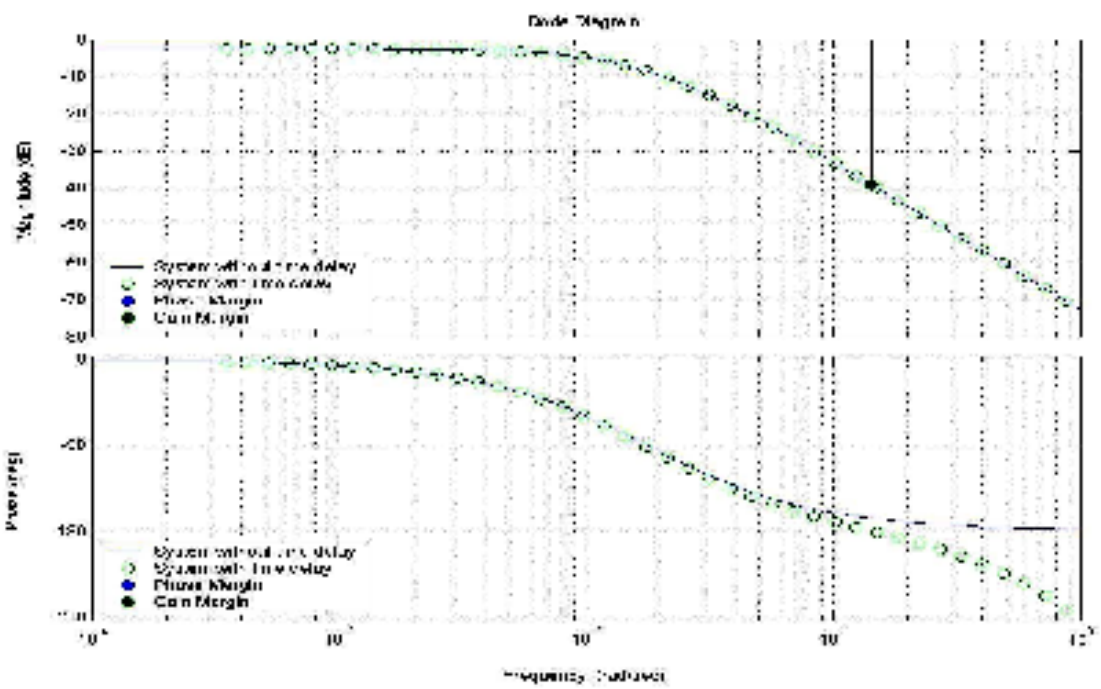
Figure 4.55 *The difference between the system with and without time delay of bottom composition to reflux flow*
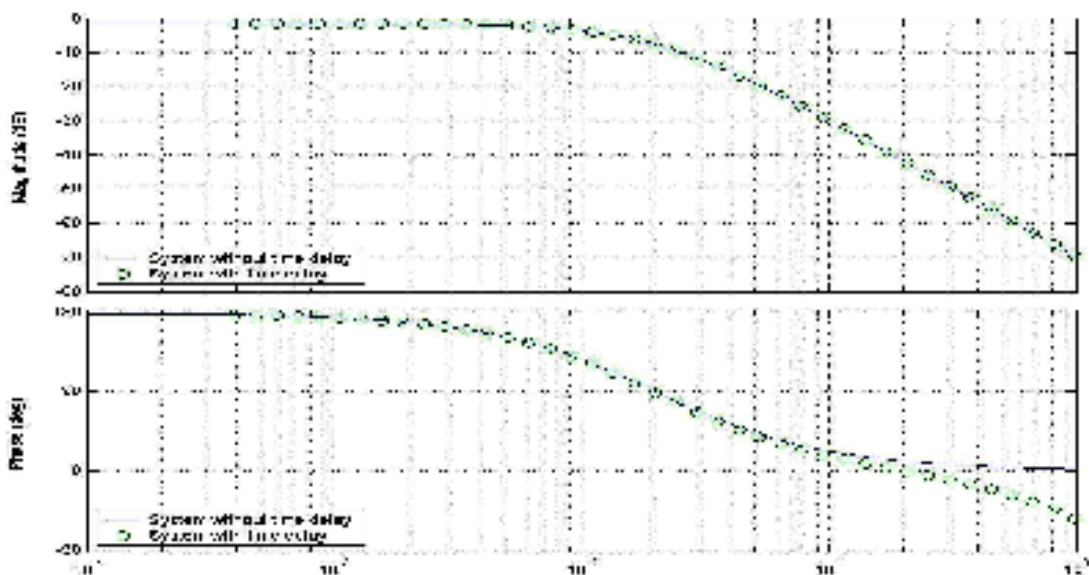
Figure 4.56 *The difference between the system with and without time delay of bottom composition to vapor flow rate*

Figures from 5.53 to 5.56 show the difference between the system with and without time delay. Then from these Figures we note that the system without time delay is more appropriate for stability than with time delay.

CONCLUSIONS AND SUGGESTIONS FOR FUTUR WORK

5.1 <u>CONCLUSIONS</u>

The present work was carried out to study the frequency response of a distillation column and process control implemented for different control strategies.

1- From table (4.5) and (4.8) the Ziegler-Nichols tuning parameters are more appropriate from the Cohen-Coon tuning parameters because the system with Ziegler-Nichols tuning parameters is stable while with Cohen-Coon tuning parameters is unstable.

2- From table (4.1) the response of distillation column with open loops is stable because of the overall individual loops are stable, if we have one closed loop of distillation column (top or bottom loop) with or without controllers then the system will be stable, and with both closed loops with or without controllers also will be stable.

3- The relative gain array method was used to find the interactions between the two loops of distillation column. So we use ideal decoupling in order to eliminate the interaction between loops and to make the system stable.

4- By using the existing relation between closed loop transient response and closed loop frequency response we notice that the system have no resonant peak magnitude and bandwidth frequency response as result to the value of damping ratio greater than 0.707.

5- The system without time delay is more appropriate for stability of the system than with system having time delay

5.2 <u>RECOMMENDATIONS FOR FUTURE WORK</u>

1- Application of interface control on distillation column, by using personal computer and interface units *IFRA*:- input (*ADC*) and output (*DAC*) interfacing.

2- Another study could be done by using the same software *IFRA*, (e.g. Heat Exchanger, Evaporator, … etc.)

3- The same procedure of this work is useful for another distillation column different in distillation specifications or using the same procedure for other controlled and manipulated variables.

REFERENCES

1- Nyquist, H., "Regeneration Theory", Bell System Tech. J., 11, pp. 126-47, 1932.

2- Bode, H. W., "Network Analysis and Feedback Design". New York: Van Nostrand Reinhold, 1945.

3- Ogata K;" Modern Control Engineering", Prentice Hall, Inc, New Jersey, 1997.

4- Pollard A.;" Process Control", Biddles Ltd, Guildford and King's lynn, 1981.

5- Norman S. N; "Control System Engineering", 3rd edition, John Wiley and Sons, Inc, 2000.

6- Kuba I.;"The Analysis and Design of Multivariable Control Systems by a Simplified Frequency Response Method", M.Sc., Thesis, University of Technology, Iraq, 1976.

7- Raymond T. S, Bahram, Shahian, Clement J. Savant, Jr. and Gene H. H; "Design of Feedback Control System", 4th edition, Oxford University press, New York, 2002.

8- Coughanowr D. R. and Koppel L. B.; "Process System Analysis and Control", McGraw-Hill, Inc, 1965.

9- Ziad T. A.;"Dynamics and Control of Continuous Stirred Tank Fermenter Using Matrix Laboratory (Matlab) Programming", M. Sc., Thesis, University of Technology, Iraq, 2002.

10- Tobia I. F.,"On-Line Control of Multicomponent Distillation Column", Ph. D, Thesis, University of Technology, Iraq, 2001.

11- Richard C. D. and Robert H. B; "Modern Control Systems", 9th Edition, Prentice-Hall, Inc., New Jersey, 2001.

12- Ross S. M., 1996, "Simulation", 2nd Edition, Academic press, Orlando.

13- Thomas F. E, "Process Engineering in the 21st Century: The Impact of Information Technology", Prentice-Hall, Inc., New Jersey, 1999.

14- David I. S,"An Introduction to Programming Using Visual Basic 4.0", 2nd Edition, prentice-Hall, Inc., New Jersey, 1997.

15- Lapidus L. and Amundson N. R., Ind. Eng. Chem., 42, 1071, 1950.

16- Rose A., Johnson R. C. and William T. J., Ind. Eng. Chem., 43, 2459, 1951.

17- Armstrong W. D and Wood R. M., Trans. Inst. Chem. Eng., 39,65,1961.

18- Morris G. G. and Sevreck S., Canad. J. Chem. Eng., 59, 382, 1981.

19- Thomas P. T., Ind. Eng. Proc. Des. Dev., 20, 166, 1981.

20- Berber R., Chemica Acta, Turcica, 13, 521, 1985.

21- Berber R. and Ates A., Chemica. Acta, Turica, 14, 130, 1986.

22- Chimowitz E. H., macchietto S. and Anderson T. F., Chem. Eng. Sci., 40, 10, 1974-1978, 1985.

23- Gani R., Ruiz G. A. and Cameron I. T., Comp. Chem. Eng., 10, 3, 181, 1986.

24- Ranzi E., Rovaglio M., Faravelli T., Dominichini R. and Biardi G., I. Chem. Eng. Symp. Series, 104, A-87, 1987.

25- Ranzi E. , Rovaglio M., Faravelli T. and Biardi G., Comp. Chem. . Eng., 12 , 8, 283, 1988.

26- Hu Y. C. and Fredramirez W., AICHE J., 18, 3, 479, 1972.

27- Luyben W. L., Ind. Eng. Chem. Proc. Des. Dev., 25, 654, 1986.

28- AL-Elg A. H. and Palazoglu, Comp. Chem. Eng., 13, 10, 1183, 1989.

29- Anderson H. W., Kummel M., Hansen A. N. and Nielsen K., Chem. Eng. Sci., 44, 3, 619, 1989.

30- Shinskey, F. G.; "Distillation Control"; McGraw-Hill: New York, 1977 a.

31- Luyben, W. L. Ind. Eng. Chem. Fundam., 18, 269, 1975.

32- Shinskey, F. G.; "The stability of Interacting Control Loops with and without Decoupling"; Proc. IFAC Multivariable Technological Systems conf., Univ. of New Brunswick,P 21, 1977 b.

33- Luyben W. L, AICHE J., 16, 2, 198, March 1970.

34- Wood, R. K. and Berry M. W, Chem. Eng. Sci. 28, 1707, 1973.

35- Ryskamp, C. J. "Explicit versus Implicit Decoupling in Distillation Control"Press: New York; P 69, 1974.

36- Waller K. V. T., AICHE J., 20, 3, 592, 1974.

37- Schwanke, C. D.; Edgar, T.F.; Hougen, J.O. ISA Trans., 16, 69, 1977.

38- Jafarey, A.; McAvoy, T. J., Ind. Eng. Chem. Process Des. Dev. 17, 485, 1978.

39- McAvoy, T. J. Ind. Eng. Chem. Fundam. 18, 269, 1979.

40- Weischedel K. and Mc Avoy T. J., Ind. Eng. Chem. Fund, 19, 379, 1980.

41- Fagervik, K. V.; Hammarstrom, L. G. "One-Way and Two_Way Decoupling in Distillation", ABO AKADEMI Report 81-3, 1981.

42- Frey R. M., Doherty M. F., Douglas J. M. and Malone M.F., Ind. Chem. Eng. Proc. Des. Dev., 23, 3, July 1984.

43-Arkun Y. and Mogan C. O., Comp. Chem. Eng., 12, 4, 303, 1988.

44- Frankelin , G ; Powell .J. D., and Emami-Naeini A.;" Feedback control of dynamic systems " , 2nd edition , Addison-Welsley, 1991.

45- Wayne B. B, "Process Dynamics modeling, Analysis, and Simulation", Prentic–Hall Ptr, Inc, 1998.

46- Luyben M. L. and Lnybem W. L.;"Essentials of process control" , McGraw Hill, New York, 1997.

47- Luyben, W. L.;"Process Modelling, Simulation and control for chemical engineering ", 2nd edition, McGraw-Hill, NewYork, 1990.

48- Charles L. and Cooney C.;"The principle Applications and Regulations of Bio Technology in Industry", vol. 2, pergamon press. Ltd, 1985.

49- Bristol, E. H. IEEE Trans. Autom. Cntrol 1966, AC-11, 1966.

50- Shinskey; "Process Control Systems", McGraw-Hill, New York, 1967.

51- McAvoy, 1983; "Interaction Analysis", Instr. Soc. America.

52- Yamman Arkan, billy Manous /Outhakis, and Ahmed palazolglu, Ind. Eng. Chem. process .Des. Der., 23, 93-101, 1984.

53- Law, A. M., and Kelto, W. D.; "Simulation Modeling and Analysis", McGraw Hill Co., Third edition, 2000

54- Duana H. and Bruce little; "The Student Edition of Matlab", Version 5, Math work, Inc, 1997.

55- Kirshna K. S. and Gayatri A G; "System Design through Matlab, Control Toolbox and Simuling", spring, 2001.

56- Stephanopoules G.; "Chemical Process Control: an Introduction to Theory and practice", Prentice Hall International, Ind, 1984.

57- Doyle III F. J.; "Process control Modules: A software laboratory for control Design; "Prentic Hall PTR, New Jersey, 2000.

RELATION BETWEEN TRANSIENT RESPONSE AND FREQUENCY RESPONE

A.1 *Derivation of the Closed-Loop System*

Open-loop transfer function assumes:

$$G(s) = \frac{1}{s(\tau^2 s + 2\zeta\tau s)} \qquad \text{... (A.1)}$$

Then closed-loop transfers function with unity feedback system:

$$T(s) = \frac{G(s)}{G(s) + 1} \qquad \text{... (A.2)}$$

$$T(s) = \frac{\frac{1}{s(\tau^2 s + 2\zeta\tau s)}}{\frac{1}{s(\tau^2 s + 2\zeta\tau s)} + 1} = \frac{1}{\tau^2 s^2 + 2\zeta\tau s + 1} \qquad \text{... (A.3)}$$

Substitute *s* with *jw* in equation *(A.3)*

$$T(jw) = \frac{1}{1 - w^2\tau^2 + 2\zeta\tau jw} \qquad \text{... (A.4)}$$

$$T(jw) = \frac{1}{1 - w^2\tau^2 + 2\zeta\tau jw} * \frac{1 - w^2\tau^2 - 2\zeta\tau jw}{1 - w^2\tau^2 - 2\zeta\tau jw}$$

$$= \frac{(1 - w^2\tau^2) - 2\zeta\tau jw}{(1 - w^2\tau^2) + 4\zeta^2\tau^2 w^2} \qquad \text{... (A.5)}$$

and the magnitude (*M*) of the closed-loop system is equal to

$$M = |T(jw)| = \sqrt{(\text{Re}al\ Part)^2 + (\text{Im}aginary\ Part)^2}\ [3] \qquad \text{... (A.6)}$$

Substitute equation *(A.5)* into equation *(A.6)*

$$M = |T(jw)| = \frac{1}{\sqrt{(1 - w^2\tau^2)^2 + 4\zeta^2\tau^2 w^2}} \qquad \text{... (A.7)}$$

A.2 *Derivation of the Resonant Peak Magnitude (M$_P$)*

Squaring equation *(A.7)*

$$M^2 = \frac{1}{\tau^4 w^4 - 2\tau^2 w^2 + 1 + 4\zeta^2 \tau^2 w^2} \qquad \dots (A.8)$$

and differentiating equation *(A.8)* with respect to w^2, and setting the derivative equal to 0.

$$\frac{\partial M^2}{\partial w^2} = \frac{2\tau^4 w^4 - 2\tau^2 + 4\zeta^2 \tau^2}{\tau^4 w^4 - 2\tau^2 w^2 + 4\zeta^2 \tau^2 w^2 + 1} = 0 \qquad \dots (A.9)$$

$$2\tau^2 w^2 - 2\tau^2 + 4\zeta^2 \tau^2 = 0 \qquad \dots (A.10)$$

Rearranging equation *(A.10)*

$$w^2 = \frac{1}{\tau^2}\left(1 - 2\zeta^2\right) \qquad \dots (A.11)$$

Then

$$w_P = \frac{1}{\tau}\sqrt{1 - 2\zeta^2} \qquad \dots (A.12)$$

Substitute equation *(A.12)* into equation *(A.7)*

$$M = \frac{1}{\sqrt{(1 - \tau^2 \frac{1}{\tau^2}\sqrt{1 - 2\zeta^2})^2 + 4\zeta^2 \tau^2 \frac{1}{\tau^2}\sqrt{1 - 2\zeta^2}}} \qquad \dots (A.13)$$

Then, the resonant peak magnitude is

$$M_P = \frac{1}{2\zeta\sqrt{1 - \zeta^2}} \qquad \dots (A.14)$$

A.3 *Derivation of the Relations between Response Speed and Closed-Loop System*

The bandwidth can be found by finding that frequency for which $M = 1/\sqrt{2}$ (i.e., -3 dB) in equation *(A.7)*.

$$M = \frac{1}{\sqrt{(1 - w^2\tau^2)^2 + 4\zeta^2\tau^2w^2}} = \frac{1}{\sqrt{2}} \qquad \dots (A.15)$$

Squaring equation *(A.15)*

$$M^2 = \frac{1}{(1 - w^2\tau^2)^2 + 4\zeta^2\tau^2w^2} = \frac{1}{2} \qquad \dots (A.16)$$

$$2 = (1 - w^2\tau^2)^2 + 4\zeta^2\tau^2w^2 \qquad \dots (A.17)$$

Rearranging equation *(A.17)* and solving by constitution law

$$\tau^4 w^4 - 2\tau^2 w^2 + 4\zeta^2\tau^2 w^2 - 1 = 0 \qquad \dots (A.18)$$

$$\tau^4 w^4 - (2\tau^2 + 4\zeta^2\tau^2)w^2 - 1 = 0 \qquad \dots (A.19)$$

Then

$$w_{Bw} = \frac{1}{\tau}\sqrt{(1 - 2\zeta^2) + \sqrt{4\zeta^4 - 4\zeta^2 + 2}} \qquad \dots (A.20)$$

and from [5]

$$T_S = \frac{4\tau}{\zeta} \qquad \dots (A.21)$$

$$T_P = \frac{\pi\tau}{(1 - \zeta^2)} \qquad \dots (A.22)$$

To relate w_{Bw} to settling time and peak time we substitute equations *(A.21)* and *(A.22)* into equation *(A.20)*

$$w_{Bw}T_S = \frac{4}{\zeta}\sqrt{(1 - 2\zeta^2) + \sqrt{4\zeta^4 - 4\zeta^2 + 2}} \qquad \dots (A.23)$$

$$w_{Bw}T_P = \frac{\pi}{1 - \zeta^2}\sqrt{(1 - 2\zeta^2) + \sqrt{4\zeta^4 - 4\zeta^2 + 2}} \qquad \dots (A.24)$$

A.4 _Derivation of the Relation between Closed-Loop Transient and Open-Loop Frequency Response to Find the Damping Ratio from Phase Margin_

Open-loop transfer function assumes:

$$G(s) = \frac{1}{s(\tau^2 s + 2\zeta\tau s)} \qquad \qquad ...\ (A.1)$$

Substitute s with jw in equation $(A.1)$

$$G(jw) = \frac{1}{-w^2\tau^2 + 2\zeta\tau jw} \qquad \qquad ...\ (A.25)$$

$$G(jw) = \frac{1}{-w^2\tau^2 + 2\zeta\tau jw} * \frac{-w^2\tau^2 - 2\zeta\tau jw}{-w^2\tau^2 - 2\zeta\tau jw}$$

$$= \frac{(-w^2\tau^2) - 2\zeta\tau jw}{(-w^2\tau^2) + 4\zeta^2\tau^2 w^2} \qquad \qquad ...\ (A.26)$$

and the magnitude of the open-loop system is equal to

$$|G(jw)| = \sqrt{(\text{Re}al\ Part)^2 + (\text{Im}aginary\ Part)^2} \qquad \qquad ...\ (A.27)$$

Substitute equation $(A.26)$ into equation $(A.27)$

$$|G(jw)| = \frac{1}{\sqrt{(-w^2\tau^2)^2 + 4\zeta^2\tau^2 w^2}} \qquad \qquad ...\ (A.28)$$

In order to evaluate the phase margin, we first find the frequency w_1 for which $|G(jw)| = 1$. Hence

$$|G(jw)| = \frac{1}{\sqrt{(-w^2\tau^2)^2 + 4\zeta^2\tau^2 w^2}} = 1 \qquad \qquad ...\ (A.29)$$

Rearranging equation $(A.29)$ and solving by constitution law

$$\tau^4 w^4 + 4\zeta^2\tau^2 w^2 - 1 = 0 \qquad \qquad ...\ (A.30)$$

$$\tau^4 w^4 + (4\zeta^2\tau^2)w^2 - 1 = 0 \qquad \qquad ...\ (A.31)$$

Then

$$w_1 = \frac{1}{\tau}\sqrt{-2\zeta^2 + \sqrt{1 + 4\zeta^4}} \qquad \qquad ...\ (A.32)$$

The phase angle of *G(jw)* at open-loop system [3]

$$\angle G(jw) = -Tan^{-1}\left(\frac{Imaginary\,Part}{Real\,Part}\right) \qquad \dots (A.33)$$

Then, the phase angle at frequency w_1 is

$$\angle G(jw) = -Tan^{-1}\left(\frac{-2\zeta\tau jw_1^{2}}{-w_1^{2}\tau^{2}}\right) \qquad \dots (A.34)$$

Substitute equation *(A.32)* into equation *(A.34)*

$$\angle G(jw) = -Tan^{-1}\left(\frac{2\zeta}{\sqrt{-2\zeta^{2}+\sqrt{1+4\zeta^{4}}}}\right) \qquad \dots (A.35)$$

From [5] phase margin is

$$P_m = 180 + \angle G(jw) \qquad \dots (A.36)$$

By substituting equation *(A.35)* into equation *(A.36)* the relation between damping ratio and phase margin can be found.

$$P_m = 180 - Tan^{-1}\left(\frac{2\zeta}{\sqrt{-2\zeta^{2}+\sqrt{1+4\zeta^{4}}}}\right) \qquad \dots (A.37)$$

B.1 *Ziegler-Nichols and Cohen-Coon method*

Two classical algorithms for *P, PI, PID*-controller s tuning are the Cohen-Coon and the Ziegler-Nichols methods.

Cohen-Coon method requires an open-loop first-order-plus-time-delay transfer function model of the process. This can be obtained from a process reaction curve. From the identified effective gain, time constant and dead time (K, , t_d), and one can computed controller using the rules which are summarized in table B-1; [57]

Table B-1 Computing parameters by Cohen-Coon method

Controller Type	Controller gain	Reset time	Derivative time constant
P	$K_c = (\dfrac{1}{K})(\dfrac{\tau}{t_d})(1+\dfrac{t_d}{3\tau})$		
PI	$K_c = (\dfrac{1}{K})(\dfrac{\tau}{t_d})(\dfrac{9}{10}+\dfrac{t_d}{12\tau})$	$\tau_I = t_d(\dfrac{30+3t_d/\tau}{9+20t_d/\tau})$	
PID	$K_c = (\dfrac{1}{K})(\dfrac{\tau}{t_d})(\dfrac{4}{3}+\dfrac{t_d}{4\tau})$	$\tau_I = \tau_d(\dfrac{30+3\tau_d/\tau}{9+20\tau_d/\tau})$	$\tau_D = t_d(\dfrac{4}{11+2t_d/\tau})$

The Ziegler-Nichols tuning method requires two key process parameters are the period of oscillation is defined as ultimate period (P_u) and the controller gain is referred to an ultimate gain (K_u). The rules for controller computing are summarized in table B-2 [57]

Table B-2 Computing parameters by Ziegler-Nichols method

Controller type	Controller gain	Reset time	Derivative time constant
P	$K_c = 0.5 K_u$		
PI	$K_c = 0.45 K_u$	$\tau_I = \dfrac{P_u}{12}$	
PID	$K_c = 0.6 K_u$	$\tau_I = \dfrac{P_u}{2}$	$\tau_D = \dfrac{P_u}{8}$

B.2 *Poles for the System with two feedback closed-loops*

Table B-3 Poles for the system

System without controller	System with-*P*-controller	System with-*PI*-controller	System with-*PID*-controller
-5.0319+8.9853i	-5.0319+8.9853i	-5.0319+8.9853i	-5.0319+8.9853i
-5.0319-8.9853i	-5.0319-8.9853i	-5.0319-8.9853i	-5.0319-8.9853i
-7.4714+5.2525i	-7.4714+5.2525i	-7.4714+5.2525i	-7.4714+5.2525i
-7.4714-5.2525i	-7.4714-5.2525i	-7.4714-5.2525i	-7.4714-5.2525i
-8.4967+1.7350i	-8.4967+1.7350i	-8.4967+1.7350i	-8.4967+1.7350i
-8.4967-1.7350i	-8.4967-1.7350i	-8.4967-1.7350i	-8.4967-1.7350i
-0.0326	-0.0326	-0.0326	-0.0326
-0.0326	-0.0326	-0.0326	-0.0326
-5.0319+8.9853i	-5.0319+8.9853i	0	0
-5.0319-8.9853i	-5.0319-8.9853i	-5.0319+8.9853i	-5.0319+8.9853i
-7.4714+5.2525i	-7.4714+5.2525i	-5.0319-8.9853i	-5.0319-8.9853i
-7.4714-5.2525i	-7.4714-5.2525i	-7.4714+5.2525i	-7.4714+5.2525i
-8.4967+1.7350i	-8.4967+1.7350i	-7.4714-5.2525i	-7.4714-5.2525i
-8.4967-1.7350i	-8.4967-1.7350i	-8.4967+1.7350i	-8.4967+1.7350i
-0.0198	-0.0198	-8.4967-1.7350i	-8.4967-1.7350i
-0.0198	-0.0198	-0.0198	-0.0198
-2.5159+4.4927i	-2.5159+4.4927i	-0.0198	-0.0198
-2.5159-4.4927i	-2.5159-4.4927i	0	0
-3.7357+2.6263i	-3.7357+2.6263i	-2.5159+4.4927i	-2.5159+4.4927i
-3.7357-2.6263i	-3.7357-2.6263i	-2.5159-4.4927i	-2.5159-4.4927i
-4.4284+0.8675i	-4.4284+0.8675i	-3.7357+2.6263i	-3.7357+2.6263i
-4.4284-0.8675i	-4.4284-0.8675i	-3.7357-2.6263i	-3.7357-2.6263i
-0.0351	-0.0351	-4.4284+0.8675i	-4.4284+0.8675i
-0.0351	-0.0351	-4.4284-0.8675i	-4.4284-0.8675i
-2.9599+5.2855i	-2.9599+5.2855i	-0.0351	-0.0351
-2.9599-5.2855i	-2.9599-5.2855i	-0.0351	-0.0351
-4.3950+3.0897i	-4.3950+3.0897i	0	0
-4.3950-3.0897i	-4.3950-3.0897i	0	0
-4.9981+1.0206i	-4.9981+1.0206i	-2.9599+5.2855i	-2.9599+5.2855i
-4.9981-1.0206i	-4.9981-1.0206i	-2.9599-5.2855i	-2.9599-5.2855i
-0.0175	-0.0175	-4.3950+3.0897i	-4.3950+3.0897i
-0.0175	-0.0175	-4.3950-3.0897i	-4.3950-3.0897i
		-4.9981+1.0206i	-4.9981+1.0206i
		-4.9981-1.0206i	-4.9981-1.0206i
		-0.0175	-0.0175
		-0.0175	-0.0175

.

.

.

Transient response

Gain margin phase margin.

Bode plots .

interface transient response

IFRA (*Interface Frequency Response Analysis*)

VISUAL BASIC$_{6.0}$ MATLAB$_{6.5}$

Bode plots

.

(*P,PI,PID*)

.

transient response

.(Nichols Chart)

.

relative gain array

.   Decouplers

Time delay   Time delay

.

Ø   Ø

Ø

Ø

(éççè   )

èëéì

éççë